

THE ROLE OF HYDROGEN AND FUEL CELLS FOR ULTRA LOW CARBON VEHICLES

Jinlei Shang

A thesis submitted to
The University of Birmingham for the degree of

Doctor of Philosophy



Chemical Engineering
University of Birmingham
April 2013

UNIVERSITY OF
BIRMINGHAM

University of Birmingham Research Archive

e-theses repository

This unpublished thesis/dissertation is copyright of the author and/or third parties. The intellectual property rights of the author or third parties in respect of this work are as defined by The Copyright Designs and Patents Act 1988 or as modified by any successor legislation.

Any use made of information contained in this thesis/dissertation must be in accordance with that legislation and must be properly acknowledged. Further distribution or reproduction in any format is prohibited without the permission of the copyright holder.

"The day it arrives, it will arrive. It could be today or 50 years later.

The only sure thing is that it will arrive."

----- Ayrton Senna

To my spiritual inspirer, Ayrton Senna, this thesis is dedicated.

For honouring his memory and fascinating character as the greatest racer in history.

Acknowledgments

This thesis is by far the most significant academic and personal accomplishment in my life; it would never have been completed without people who supported me and believed in me, to only some of whom it is possible to give particular mention here.

My greatest debt is to my supervisors Professor Kevin Kendall and Professor Robert Steinberger-Wilckens, for their unflagging faith in me and their ceaseless encouragement, support and inspiration, their extraordinary proficiency in fuel cell related field have given me treasurable experience in the journey to the completion of this thesis. I offer my profound gratitude to my former supervisor Professor Bruno G. Pollet for his supervision and stimulation from the very early stage of this research as well as his on-going stimulation and guidance.

I wish to express sincere appreciation to the University of Birmingham for their generous funds and the recognition of me without which I could never devote myself to my research physically and psychologically.

Special thanks must also be delivered to someone exceptional, for his depth of generosity to support my research and his unreserved sharing of his ideas, especially his surreal expertise on Excel. His extraordinary talent and competence had strangely stirred me and spurred me to polish up my work and research. I cherish the friendship I had with him, to Dr. Iain Staffell, my truthful friend and my mentor.

It has been my pleasure to work with all my colleagues in the Department of Chemical Engineering for their extended long-term assistance to Dr Waldek Bujalski, Dr Aman Dhir, John Hooper, Lynn Draper, Dr Shangfeng Du, Philip Hamilton, Dr. Artur Majewski, Bob Sharpe, Raj Sanni and especially to Peter Fisher for his valuable discussions, technical support and hands-on help in many aspects of this research program.

I would like to extend my sincere thanks to Stella Chen, John Jostins, Jay Gohil, John Turner, and Dustin McLarty for all the support and motivation in all my efforts during the course of my work.

Finally, my deepest gratitude is sent to my family for their unconditional love, fidelity, endurance, and blessing, which bring belief and hope into my life.

Though my name happens to be printed on the cover page, I did nothing more than depict all contributions of my advisors and collaborators in this thesis. However, errors and limitations remaining in this work are all mine.

Abstract

The problems of transport technology were analysed; present vehicles are polluting, inefficient and run largely on unsustainable fossil fuels with average CO₂ emission around 154 gCO₂/km.

The theory proposed here is that a hydrogen fuel cell battery hybrid system is the best for future vehicles; zero emission, twice as efficient compared with diesel van in campus drive cycle and running on renewable hydrogen from biomass, wind or solar.

Early testing compared a crude Micro-cab prototype (compressed hydrogen, Ballard fuel cell, lead acid batteries and an electric motor) with a hydrogen combustion dual fuel van to assess the technical demands of the proposed technology.

Then a battery scooter was modified and tested to show that a plug-in hydrogen battery hybrid with hydride store could have benefits which were quantifiable. A computer model was developed to predict the performance of this system. Reducing dissipation by removing DC converters was shown to be beneficial.

A prototype Micro-cab was analysed and tested to show how improved drive-train components could increase the vehicle efficiency.

The main part of the project was to use these ideas to build an urban car driven by a plug-in hydrogen fuel cell lithium ion battery hybrid with efficient motors, belt/pulley drive, and no DC/DC converter. The results showed that with a 2kg pressurised hydrogen store at 350bar, such a vehicle had good urban performance and a range of more than 150miles.

The conclusion was that the overall design concepts were correct and that costs and hydrogen infrastructure were the main future difficulties of future application.

Five publications have been submitted/published on these studies [1-5].

Table of Contents

Acknowledgments.....	ii
Abstract	iii
Table of Contents	iv
Index of Figures	vi
Index of Tables	x
Nomenclature & Abbreviations	xii
1. Chapter One Introduction	1
1.1 Motivation for a ‘Greener’ Society –Great Achievements, Greater Challenges	2
1.2 Project Objectives	10
2. Chapter Two Background	15
2.1 Current Status of Low-Carbon Vehicle Technologies	16
2.2 Conventional IC Engines Vehicles.....	19
2.3 Battery Electric Vehicles (BEVs)	27
2.4 Hydrogen Fuel Cell Vehicles (HFCVs).....	30
2.5 Comparison	34
2.6 Conclusion	36
3. Chapter Three Hydrogen as Fuel for Transport	38
3.1 Introduction.....	39
3.2 Hydrogen Internal Combustion Engine Vehicles (H ₂ ICE).....	42
3.3 Hydrogen Fuel Cell Vehicle HFCVs.....	48
3.4 Key Problems for Hydrogen Fuel	49
3.5 Conclusions.....	59
4. Chapter Four Hydrogen and Fuel Cell Hybrid Scooter with Plug-In Feature - An Early Project	61
4.1 Introduction.....	62
4.2 Experimental Methods.....	63
4.3 Results and Discussion	69
4.4 Conclusions.....	73
5. Chapter Five Novel Hydrogen PEM Fuel Cell and Battery Hybrids without DC-DC Converters	75
5.1 Introduction.....	76
5.2 Experimental Methods.....	77

5.3	<i>Results and Discussion</i>	79
5.4	<i>Limitations</i>	87
5.5	<i>Conclusions</i>	87
6.	Chapter Six Study of Micro-Cab H4 Fuel Cell Hybrid Vehicles	90
6.1	<i>Introduction</i>	91
6.2	<i>Micro-cab H4</i>	93
6.3	<i>Main Components</i>	97
6.4	<i>Data Monitoring and Collection</i>	103
6.5	<i>Conclusions</i>	105
7.	Chapter Seven Testing of Micro-cab H4 Vehicles	106
7.1	<i>Introduction</i>	107
7.2	<i>Results</i>	108
7.3	<i>Postal Service</i>	129
7.4	<i>Discussion and Recommendations</i>	131
7.5	<i>Conclusions</i>	133
8.	Chapter Eight Drive Cycle Simulation of Various Vehicle Drive-trains	136
8.1	<i>Introduction</i>	137
8.2	<i>Methodology</i>	137
8.3	<i>Results</i>	144
8.4	<i>Conclusions</i>	149
9.	Chapter Nine Upgraded Version of H4 Micro-Cab	150
9.1	<i>Introduction</i>	151
9.2	<i>Experimental Method</i>	151
9.3	<i>Upgrades</i>	152
9.4	<i>Results</i>	162
9.5	<i>Conclusions</i>	175
10.	Chapter Ten Conclusions and Future Works	179
10.1	<i>Overview</i>	180
10.2	<i>Summary of Conclusions</i>	180
10.3	<i>Future Works</i>	183
	References	186

Index of Figures

<i>Figure 1.1 EU27 greenhouse gas emissions by sector and mode of transport, 2009 [11]</i>	3
<i>Figure 1.2 Roadmap of EU low carbon vehicle [34]</i>	7
<i>Figure 2.1 List of main low-carbon technologies for vehicles</i>	17
<i>Figure 2.2 Share of Fuel Type in EU New Passenger Vehicles (EU Commission, 2010) [57]</i>	18
<i>Figure 2.3 Schematic drawing of a) IC engines vehicle, b) BEV and c) FCEV</i>	19
<i>Figure 2.4 Typical IC engine Operation under NEDC Condition</i>	21
<i>Figure 2.5 Schematic drawing of a) Series hybrid vehicle, b) Parallel hybrid vehicle, c) Series Parallel hybrid vehicle and d) Complex hybrid vehicle</i>	25
<i>Figure 2.6 Overall efficiency of the vehicle system</i>	35
<i>Figure 3.1 Schematic of the H₂ fuelled vehicle concept. Patented by Isaac de Rivaz, 1807</i>	39
<i>Figure 3.2 Royal Mail Collaborated Hydrogen vehicle projects, Micro-Cab HFCV (left), H₂ICE Transit Van (right)</i>	41
<i>Figure 3.3 Diagrams of Petrol and Hydrogen with Mount of Air Mixture in IC engine</i>	43
<i>Figure 3.4 Modified IC engines for Hydrogen Fuel</i>	44
<i>Figure 3.5 Hydrogen Storage Tank Layouts and Position</i>	45
<i>Figure 3.6 Hydrogen Consumption (miles per bar drop)</i>	46
<i>Figure 3.7 University of Birmingham hydrogen dispenser</i>	53
<i>Figure 3.8 Cost of hydrogen from a 150,000kg/d central plant (estimated)</i>	54
<i>Figure 4.1 Horizon Fuel Cell 500W PEMFC stack characteristics showing cell voltage and power vs. current</i>	65
<i>Figure 4.2 12V lead-acid discharge characteristics showing voltage vs., discharge at various amperages and at 25°C [155]</i>	66
<i>Figure 4.3 Component diagram of the HFCHS showing all components</i>	67
<i>Figure 4.4 Photo of the HFCHS</i>	67
<i>Figure 4.5 Mathematical Performance of modelling</i>	68
<i>Figure 4.6 Performance of HFCHS when the batteries are low [SoC = 20%]</i>	69
<i>Figure 4.7 Performance of HFCHS when the batteries are fully charged [SoC = 100%]</i>	70
<i>Figure 4.8 Scooter built for Royal Institute Lecture</i>	73
<i>Figure 5.1 Configuration of the FC and batteries hybrid system</i>	78

<i>Figure 5.2 Fuel cell stack output against electric load when hybrid with 4 x 12V lead acid batteries.....</i>	<i>80</i>
<i>Figure 5.3 Change of battery power distribution against electric load with 4 x 12V lead acid batteries.....</i>	<i>81</i>
<i>Figure 5.4 Fuel cells stack output against electric load when hybrid with 16 x 3.4V Li-Ion batteries.....</i>	<i>83</i>
<i>Figure 5.5 Fuel cell stack output against electric load when hybrid with 15x 3.4V Li-Ion batteries.....</i>	<i>85</i>
<i>Figure 6.1 Development timeline of Micro-cab (courtesy Micro-cab).....</i>	<i>91</i>
<i>Figure 6.2 Five H4 series Micro-Cab HFCVs in Campus University of Birmingham</i>	<i>93</i>
<i>Figure 6.3 Design of frame showing the layout of the fuel cell, hydrogen tank and motor (courtesy Micro-cab).....</i>	<i>95</i>
<i>Figure 6.4 Schematic of H4 Configuration.....</i>	<i>97</i>
<i>Figure 6.5 Ballard Nexa™ fuel cell efficiency curve[172].....</i>	<i>99</i>
<i>Figure 6.6 Hydrogen fuelling station in University of Birmingham with nozzle zoomed in ...</i>	<i>101</i>
<i>Figure 6.7 Traction and auxiliary batteries located under the vehicle floor.....</i>	<i>102</i>
<i>Figure 6.8 Driver interface on Micro-Cab H4.....</i>	<i>103</i>
<i>Figure 7.1 Postal service route[176].....</i>	<i>108</i>
<i>Figure 7.2 Temperature change before and after the hydrogen refuelling process</i>	<i>110</i>
<i>Figure 7.3 Time of refilling process.....</i>	<i>111</i>
<i>Figure 7.4 Combined fuel consumption of each vehicle under campus drive cycle</i>	<i>112</i>
<i>Figure 7.5 I-V curve for the fuel cell stacks measured in each vehicle in comparison to manufacturer rated specification[162]</i>	<i>114</i>
<i>Figure 7.6 Hydrogen consumption rate (SLPM) against fuel cell stack current in typical 'Postal duty cycle'.....</i>	<i>115</i>
<i>Figure 7.7 Cell temperature behaviour in a typical postal duty cycle</i>	<i>116</i>
<i>Figure 7.8 Gross and net efficiency of the red vehicle's fuel cell stack for a representative drive cycle.....</i>	<i>117</i>

<i>Figure 7.9 Net efficiency for the fuel cell stacks measured in each vehicle against instantaneous power output. The colour intensity of each data point indicates how frequently the stack operated at that point.....</i>	<i>118</i>
<i>Figure 7.10 The efficiency and usage profile of the main DC converters averaged across all four vehicles.....</i>	<i>120</i>
<i>Figure 7.11 Efficiency of the auxiliary DC converters in all four vehicles over their operating range.....</i>	<i>121</i>
<i>Figure 7.12 Available battery capacities as a function of discharge power, showing the Peukert effect.....</i>	<i>122</i>
<i>Figure 7.13 State of charge and energy transfer to/from the battery pack during the course of a typical drive.....</i>	<i>123</i>
<i>Figure 7.14 Swollen Batteries of Micro-cab H4</i>	<i>124</i>
<i>Figure 7.15 Motor efficiency plotted against power input and the corresponding vehicle speed, overlaid with a histogram showing how frequently the motors were operated at each power level.....</i>	<i>126</i>
<i>Figure 7.16 Motor controller input power and net motor power comparison.....</i>	<i>126</i>
<i>Figure 7.17 The combined efficiency of the fuel cell and main DC converter. For the fuel cell and DC converter, the three lines show the average efficiency plus and minus one standard deviation.</i>	<i>128</i>
<i>Figure 7.18 Academic drive cycle.....</i>	<i>129</i>
<i>Figure 7.19 Results for both Ford Connect diesel vehicle and Micro-cab H4 hydrogen fuel cell vehicle.....</i>	<i>130</i>
<i>Figure 8.1 New European Driving Cycle.....</i>	<i>140</i>
<i>Figure 8.2 ARTEMIS (Assessment and reliability of transport emission models and inventory systems) driving cycle</i>	<i>141</i>
<i>Figure 8.3 Illustration of FTP 72.....</i>	<i>142</i>
<i>Figure 8.4 WLTC Class 3 drive cycle</i>	<i>143</i>
<i>Figure 8.5 Fuel consumption of different power train under different drive cycles</i>	<i>145</i>
<i>Figure 8.6 Degree of sensitivity of power train to drive cycles (ratio of different drive cycles)</i>	<i>146</i>

<i>Figure 8.7 Power train Tank to Wheel (TTW) energy efficiency of different power train under different drive cycles.....</i>	<i>147</i>
<i>Figure 8.8 Power train fuel consumption sensitivity ratio for 150 kg, 350 kg and 511 kg payload.</i>	<i>148</i>
<i>Figure 9.1 The performance of Agni 95-R motor at 48V[188].....</i>	<i>153</i>
<i>Figure 9.2 Illustration of in-wheel hub motors</i>	<i>154</i>
<i>Figure 9.3 Horizon 3 kW PEM fuel cell at front to supply the traction power.....</i>	<i>155</i>
<i>Figure 9.4 Upgraded power train configuration</i>	<i>158</i>
<i>Figure 9.5 Comparisons of passenger/driver side motor current output.....</i>	<i>160</i>
<i>Figure 9.6 Characteristics of ECE 15 drive cycle</i>	<i>161</i>
<i>Figure 9.7 Testing track with speed indication of ECE drive cycle.....</i>	<i>162</i>
<i>Figure 9.8 ECE 15 drive cycle test without passenger</i>	<i>164</i>
<i>Figure 9.9 Details of energy recovery during the test</i>	<i>167</i>
<i>Figure 9.10 Energy split between each power sources of ECE 15 drive cycle test without passenger.....</i>	<i>168</i>
<i>Figure 9.11 ECE 15 drive cycle test with 1 passenger.....</i>	<i>169</i>
<i>Figure 9.12Energy split between each power sources of ECE 15 drive cycle tests with 1 passenger.....</i>	<i>170</i>
<i>Figure 9.13 Vehicle top speed test.....</i>	<i>171</i>
<i>Figure 9.14 Power split between each power sources at vehicle speed of 80 km/h</i>	<i>173</i>
<i>Figure 9.15 Energy split between each power sources of top speed test.....</i>	<i>173</i>
<i>Figure 9.16 Comparisons of energy contribution from different power source between ECE 15 test and Top Speed test</i>	<i>175</i>
<i>Figure 10.1 New Micro-cab H₂EV (courtesy Coventry University).....</i>	<i>185</i>

Index of Tables

<i>Table 2.1 List of technologies for IC engine improvements [57]</i>	22
<i>Table 2.2 Comparison of vehicle technologies from a consumers' perspective.</i>	34
<i>Table 3.1 Densities of hydrogen in conventional fuels under different conditions</i>	49
<i>Table 3.2 Cost of hydrogen produced from various feedstock [136]</i>	54
<i>Table 4.1 Parameters used to build modelling</i>	68
<i>Table 4.2 Summary of fuel cell hybrid, battery and petrol powered scooters characteristics.</i>	71
<i>Table 4.3 Well-to-wheel carbon Footprint from different energy sources.</i>	72
<i>Table 5.1 Bench test components and specifications</i>	78
<i>Table 5.2 Results from FC stack hybrid with 4 x 12V PbA batteries at 20% SoC, 50% SoC, 80% SoC and 100% SoC</i>	80
<i>Table 5.3 Results from FC stack hybrid with 16 x 3.4V LPB at 5% SoC, 20% SoC, 50% SoC, 80% SoC and 100% SoC</i>	84
<i>Table 5.4 Results from FC stack hybrid with 15 x 3.4V LPB at 20% SoC, 50% SoC and 80% SoC</i>	85
<i>Table 6.1 Specifications of Ballard Nexa™ 1.2kW PEMFC stack</i>	98
<i>Table 6.2 Traction and auxiliary batteries specifications</i>	102
<i>Table 6.3 Specification of motor used in H4</i>	103
<i>Table 7.1 Summary usage of each vehicle</i>	108
<i>Table 7.2 hydrogen refuelling record and fuel economy of each vehicle</i>	109
<i>Table 7.3 Average and peak efficiencies of each component in the Micro-cab power-train</i> .	128
<i>Table 8.1 Parameters of glider, data based on VW MK VI Golf hatchback</i>	137
<i>Table 8.2 Parameters of simulation models under NEDC</i>	138
<i>Table 8.3 Characteristic of different drive cycles</i>	139
<i>Table 8.4 Fuel consumption with different weight under combined drive cycle</i>	148
<i>Table 9.1 The specifications of Agni Lynch pancake shape light weight permanent magnet DC motors</i>	153
<i>Table 9.2 Specifications of Horizon 3kW PEM fuel cell</i>	156
<i>Table 9.3 Data logger settings</i>	159

<i>Table 9.4 Preference of ECE 15 drive cycle</i>	<i>161</i>
<i>Table 9.5 Readings difference before and after ECE 15 testing without passenger</i>	<i>163</i>
<i>Table 9.6 Performance of other components at motor peak power output</i>	<i>166</i>
<i>Table 9.7 Readings difference before and after ECE 15 testing with 1 passenger</i>	<i>170</i>
<i>Table 9.8 Performance of other components at vehicle speed of 80 km/h.....</i>	<i>172</i>
<i>Table 9.9 Parameters change between testing.....</i>	<i>174</i>

Nomenclature & Abbreviations

The abbreviations and terminology are defined in the following tables:

Abbreviation	Actual
GHG	- Green House Gases
LPG	- Liquefied Petroleum Gas
NG	- Natural Gas
SMR	- Steam Methane Reforming
CCS	- Carbon Capture and Storage
VOC	- Volatile Organic Compound
TtW	- Tank to Wheel
WtW	- Well to Wheel
DI	- Direct Injection
VVT-i	- Variable Valve Timing with intelligence
GRP	- Glass Reinforced Plastic
FPGA	- Field Programmable Gate Array
EV	- Electric Vehicle
BEV	- Battery Electric Vehicle
FCV	- Fuel Cell Vehicle
HFCV	- Hydrogen Fuel Cell Vehicle
HFCEV	- Hydrogen Fuel Cell Electric Vehicle
HEV	- Hybrid Electric Vehicle
H₂IC ENGINESS	- Hydrogen Internal Combustion Engine
PHEV	- Plug-in Hybrid Electric Vehicle
HFCHS	- Hydrogen Fuel Cell Hybrid Scooter
H4	- Micro-Cab 2 nd generation hydrogen fuel cell hybrid vehicle
H₂EV	- Micro-Cab 3 rd generation hydrogen fuel cell hybrid vehicle
AFV	- Alternative Fuel Vehicle
BMS	- Battery Managing System
PbA	- Lead Acid Battery
LPB	- Lithium ion Phosphate Battery
LiFePO₄	- Lithium ion Phosphate Battery
VRLA	- Valve Regulated Lead Acid Battery
CS	- Charge Sustaining
CD	- Charge Depleting
PPS	- Peak Power Source
SoC	- State of Charge
DoD	- Depth of Discharge
PHCA	- Pulse Hot Cranking Ampere
HCA	- Hot Cranking Ampere
CCA	- Cold Cranking Ampere
PEMFC	- Proton Exchange Membrane Fuel Cell
PEM	- Proton Exchange Membrane or
FC	- Fuel Cell

IPCC	- Intergovernmental Panel on Climate Change
IEA	- International Energy Agency
EPRI	- Electric Power Research Institute
CARB	- California Air Resources Board
BERR	- The Department for Business, Enterprise & Regulatory Reform
DfT	- Department for Transport, UK
TUV NEL	- National Engineering Laboratory
DoE	- Department of Energy (US)
ANL	- Argonne National Laboratory
NREL	- National Renewable Energy Laboratory
AWM	- Advance West Midlands
DVLA	- UK Driver and Vehicle Licensing Agency
CENEX	- Centre of Excellence for low carbon and fuel cell technologies
BRICS	- Brazil Russia India China and South Africa
EPA	- US Environmental Protection Agency
SME	- Small and Medium Enterprise
LHV	- Lower Heating Value
HHV	- Higher Heating Value
NL	- Normal Litre
STP	- Standard Temperature and Pressure
SLPM	- Standard Litre per Minute
gge	- Gasoline Gallon Equivalent
ppb	- Parts per billion
psi	- Pounds per Square Inch
RPM	- Revolution per Minute
DC	- Direct Current
AC	- Alternative Current
MPG	- Mile Per Gallon
NEDC	- New European Drive Cycle
ARTEMIS	- Assessment and Reliability of Transport Emission Models and Inventory Systems
CADC	- Common ARTEMIS Driving Cycle
UDDS	- Urban Dynameters Driving Scheme
FTP	- Federal Test Procedure
ECE 15	- Economic Commission for Europe, vehicle emission regulation 15
UDC	- Urban Drive Cycle
MVEG	- Motor Vehicle Emission Group
WLTC	- Worldwide harmonized Light-duty driving Test Cycle

1. Chapter One

Introduction

1.1 Motivation for a 'Greener' Society –Great Achievements, Greater Challenges

1.1.1 Achievements

The development of internal combustion (IC) engines, especially those used in passenger vehicles, is one of the greatest achievements of modern technology [6]. Since Henry Ford fine-tuned the mass production of his revolutionary Model-T 100 years ago [7], the world drove off into the era of affordable transportation—forever altering our notions of place, distance, and community. Society built roads, bridges and tunnels to satisfy many of the needs for mobility in everyday life [6]. By the end of the 20th century, motorists were travelling in the region of 16,000 kilometres a year in most developed countries [8]. In the future, along with global development, road transport will further expand, and bring more benefits to our society.

The number of vehicles in operation worldwide surpassed the 1 billion mark in 2010 according to Ward's research [9] and is estimated to increase to 2.5 billion by 2050 with the industrialization process of BRICS (Brazil, Russia, India, China and South Africa) [10]. The automotive industry is therefore one of the largest economic forces globally, employing nearly 10 million people and generating a value chain in excess of USD 3 trillion a year [11], even more than the total GDP of the United Kingdom which was worth USD 2.4 trillion in 2011, according to a report published by the World Bank [12].

1.1.2 Challenges

As a consequence of this colossal industry, the large number of automobiles in use worldwide has caused and would continue to cause a series of major challenges in our

society [1, 9]. Greenhouse gases (GHG) and other emissions from vehicles' tailpipes affect not only the climate but also humans, especially the particulate emissions from the increasing numbers of diesel vehicles on the road [13-17]. In addition, rapid oil depletion, issues with energy security, dependency on foreign sources and population growth make the challenges posed by automobiles even greater [18-20]:

- **Greenhouse gas (GHG) emissions** – the transportation sector contributes in the region of 24.2% of GHG emissions in Europe as shown in Figure 1.1, with more than two thirds from road transport [21]. While greenhouse gas emissions from other sectors are generally falling, decreasing 24% between 1990 and 2009, those from transport have increased by 29% in the same period [22]. This increase has happened despite improved vehicle efficiency because the amount of personal and freight transport has increased sharply. Worldwide, around 13.1% of GHG emissions comes from transportation and a total 5 billion tonnes per year [21]. Hence reducing GHG emission in the automotive sectors has become a national and international priority.

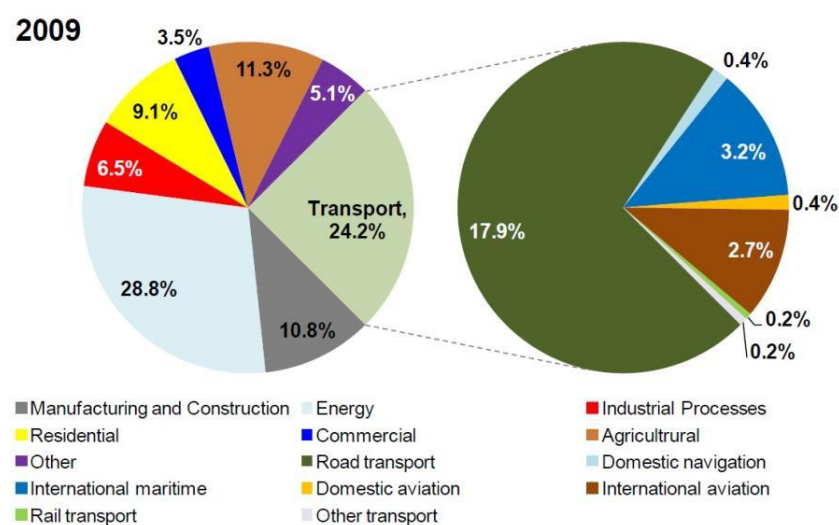


Figure 1.1 EU27 greenhouse gas emissions by sector and mode of transport, 2009 [11]

- **Air pollution** – vehicular (tailpipe) emissions are responsible for several debilitating respiratory conditions, such as asthma[23], as the use of fossil fuels in internal combustion engines produces harmful regulated air pollutants such as CO, SO_x, fine particulate matter (PM₁₀), volatile organic compounds (VOCs) and nitrogen oxides (NO_x) [24]. The increasing number of diesel vehicles on Europe's roads will further worsen air quality [25]. Also it is worth noting that when combusting the same amount of hydrocarbon fuel, the pollutants emitted from vehicles causes more damage when released in an urban area as opposed to upstream at a rural power station, due to the fact that greater numbers of people are affected [26].
- **Oil depletion** – According to a recent report in 2010, by 2023, oil reserves that provide liquid fuels today will only have the capacity to services just over half of business as usual demand [27]. Transport is already responsible for almost 70% of the EU's oil use and this figure continues to increase [28]. The crude oil prices has risen to a staggering USD 145 per barrel in July 2008, and it is projected to rise to around USD 185 per barrel in 2020 [29, 30]. Consequently, the petrol/diesel prices at the pump will be affected, and motorists will think again of the fuel efficiency and running cost when they purchase a vehicle.
- **Energy security** – Europe's dependency upon foreign oil is more than 80% and reserves of conventional oil are increasingly concentrated in politically unstable regions [28]. Dependency on fossil fuel for transportation therefore needs to be

reduced significantly. The transportation sector accounts for approximately half of the EU's EUR €300 billion annual oil import bill [28].

These challenges have been addressed and must be acted on immediately; many automotive manufacturers have now shifted their research effort to focus on high energy efficiency and renewable energy automobiles, especially on Hybrid Electric Vehicles (HEVs), Battery Electric Vehicles (BEVs) and Fuel Cell Electric Vehicles (FCEVs). One of the most representative examples is Ford, whose experience with FCEV technology began over ten years ago with the P2000 concept [31]. BEVs and FCEVs share many components and technologies, development on BEVs also can be used on FCEVs, or vices versa [32]. In principle, at least, BEVs and FCEVs could overcome those challenges [33]. This has also been recognised by government policy makers, for instance, in the US, where the transportation sector is responsible for about 67% of the oil consumed [34], government has provided significant levels of funding for research and development of alternative vehicles and fuels [35].

1.1.3 Governmental Commitments to Tackle Global Warming

1.1.3.1 EU 80% Decarbonisation Target by 2050

In October 2009, the European Council set an economy-wide greenhouse gas (GHG) abatement objective of 80–95% below 1990 levels by 2050 in order to keep climate under the safety level [36].

“The European Council calls upon all Parties to agree to global emission reductions of at least 50%, and aggregate developed country emission reductions of at least 80-95%. It supports an EU objective, in the context of necessary reductions according to the IPCC by developed countries as a group,

to reduce emissions by 80-95% by 2050 compared to 1990 levels.” Presidency Conclusions, Brussels European Council.

Even the lower target 80% decarbonisation overall by 2050 may require 95% decarbonisation of the road transport sector [10]. Yet 80% reduction in the transportation sector would be a huge challenge itself, but it is made even greater by the fact that overall road transport use is projected to increase by 28% between 2003 and 2025, and could double by 2050 [37]. Moreover, the ever increasing travel distance of personal vehicles and the nearly total dependency upon liquid hydrocarbons mean that emission reductions from this sector will be particularly difficult [38], perhaps not achievable through improvements to the traditional IC engines vehicles, although existing researches have proved the fuel consumption of IC engines could be reduced by certain methods, such as to heat engine oil directly with an exhaust gas heat exchanger [39]. However further engine efficiency improvements are limited and relatively costly and achieving 80-95% decarbonisation goal is not possible through IC engines efficiency improvement alone [40]. Bearing in mind that the IC engines vehicles may still stay dominant for the following few decades, low-carbon vehicles, from different levels of hybrid to battery electric and fuel cell electric, will gradually and eventually penetrate the automotive market and replace IC engines vehicles, in order to achieve the 80-95% decarbonisation in the transport sector by 2050 [41].

1.3.3.2 120 g/km CO₂ Emission by 2015

In 2009, the European Parliament finally agreed to limit the CO₂ emissions for new passenger vehicles sold in the European Union (EU) to an average of 130 g/km (vehicle tailpipe emission) by 2015 [42]. This regulation is one aspect of EU climate-energy package for Kyoto and post-Kyoto emissions reduction goals. In order to meet the EU 120 g/km

target, a further emission reduction of 10 g/km is to be provided by additional measures, such as the use of biofuels. 10% biofuel will be blended into the current fuel [42], make the overall CO₂ emission to 120 g/km. This policy's target date was originally set for 2012. But before it became legally-binding, the target was postponed to 2015 for the objective was said to be too aggressive [43]. By the end of 2010 Toyota, Peugeot-Citroen and Fiat had already achieved their targets for 2015 [44]. To enforce achievement, manufacturers who miss their average CO₂ targets will be subject to a penalty up to 95 Euro/kilogram CO₂ [42]. These CO₂ emissions are measured over the New European Drive Cycle (NEDC) test cycle, so the emission in the real life drive condition may vary. Also it should be noticed that this regulation covers only CO₂ emissions, with other greenhouse gases and tailpipe pollutants not regulated [42].

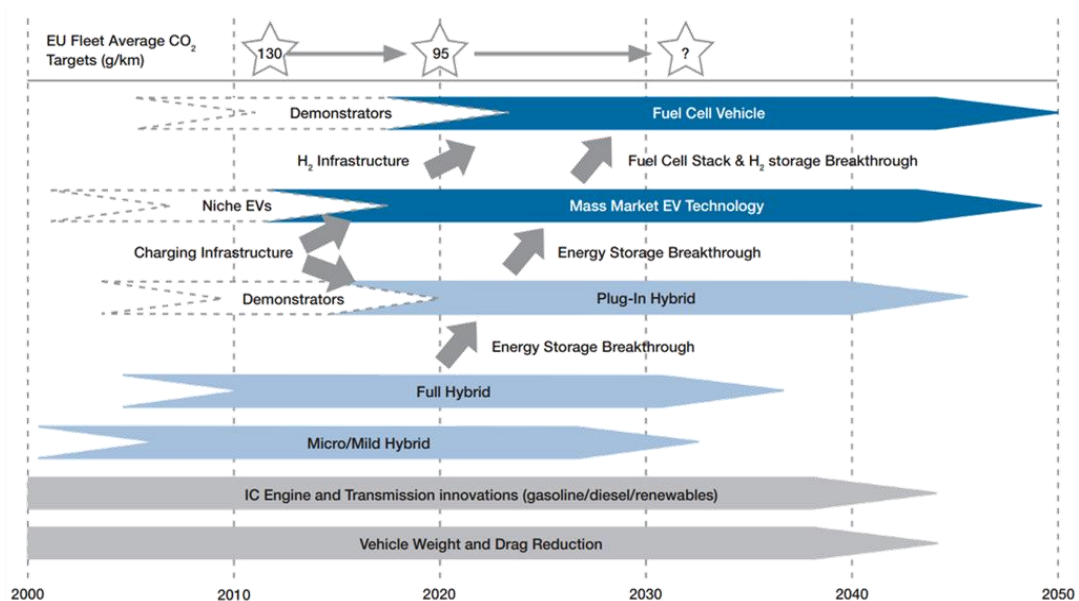


Figure 1.2 Roadmap of EU low carbon vehicle [34]

Furthermore, a probable longer-term CO₂ emissions target of 95 gCO₂/km is specified for 2020 but will be limited at this stage due to the cost of further improvement. However even

95 gCO₂/km is still far away from 95% decarbonisation, hence BEV and FCEV powered by sustainable energy source must be deployed as depicted in the EU roadmap for low carbon vehicle of Figure 1.2 [45].

1.1.3.3 Government Incentives

An auto vehicle is probably the most important purchase for a household, so consumers are likely to consider numerous factors before their decision is made. Safety, comfort, fuel consumption, exterior and interior design are compared but all within a predetermined budget range of course. In fact, price is the top priority. The new low carbon vehicles generally are more expensive than conventional vehicles due to the new technologies, design, components and production rate. Government incentives are to be rolled out in order to encourage the consumers' decision and stimulate the low carbon vehicles market.

In the UK, the government confirmed that consumers will receive up to £5,000 towards the cost of an ultra-low carbon vehicle from January 2011. The grant will reduce the up-front cost of eligible vehicles by 25% (capped at GBP 5,000), and is available across the UK and open to both private and business fleet buyers [46, 47]. Low carbon vehicles are also exempt from road tax, and free of congestion charge in cities like London. Spain, Portugal, France and other EU nations have similar incentives [48].

In Denmark, electric vehicles weighing less than 2,000 kg are exempt from the registration tax. The registration tax is based on the price of the vehicle. It is calculated as follows: (105% multiply vehicle price up to DKK 79,000, around EUR 10,600 in April 2012) + (180% multiply vehicle price above DKK 79,000) [48].

In China, the government announced a trial program to provide incentives up to 60,000 CNY (~EUR 7,200 in April 2012) for private purchase of new battery electric vehicles and 50,000 CNY (~EUR 6,000 in April 2012) for plug-in hybrids in five cities. The subsidies are paid directly to automakers rather than consumers. The amount of the subsidy will be reduced once 50,000 units are sold. In addition to the subsidy, the Chinese government is also introducing an exemption from annual taxes for pure electric, fuel-cell, and plug-in hybrid vehicles. Hybrid vehicles will be eligible for a 50% reduction only [28, 49].

The various incentives from different countries not only stimulate the motorist to purchase ultra-low carbon vehicles by offsetting the higher upfront costs, but will also be stimulation for vehicle makers who are behind much of the push for ultra-low carbon vehicle introduction.

1.1.4 New Automotive Revolution

It has become clear that, in the longer term, road transport will need to be emission free. The automotive industry is changing with an ever increasing speed and the current economic and environmental pressures mean that the vehicles of tomorrow will be very different to those we drive today; however, there is no single 'silver-bullet' i.e. a single clear solution, as shown in Figure 1.2. The automotive world is entering a period of great revolution in the drive-train, involving a lot of experimental and developmental at work. On the other hand, this revolution can be a catalyst for a new way of life, and a new generation of wealth, a huge opportunity for many people and organizations. Given the global automotive manufacturing industry generated total revenue of USD 1,185 billion in 2010, which is

expected to drive the industry to a value of USD 1,654 billion by the end of 2015 [50], even capturing a few percentage points would still be a considerable market.

Obviously there will be a significant demand for engineers and scientists with experience in designing and engineering alternative vehicles. Therefore there is no better time than now to do research on the most advanced vehicle technology—fuel cell hybrid electric vehicles.

1.2 Project Objectives

This PhD project aims to study, design, model and demonstrate advanced hydrogen fuel cell hybrid vehicles, with the focus on power train efficiency improvement, including the power train design and optimisation, computer modeling and road testing, based on the Micro-Cab HFCEV prototype [51]. At the same time, other low carbon vehicle technologies such as hybrid vehicles and battery electric vehicles, are also analysed and compared to conventional vehicles. Their power train efficiency, performance and Well-to-Wheel (WtW) CO₂ emission, are assessed and compare with that of hydrogen fuel cell vehicles in different drive cycles. A novel approach of fuel cell vehicle engineering design with plug-in features is also investigated. This thesis is organized as follows:

Chapter 1 describes the motivations and background behind this PhD study.

Chapter 2 is partially adapted from author's published paper "Current status of hybrid, battery and fuel cell electric vehicles: From electrochemistry to market prospects" in *Electrochimica Acta* [1], analysed the current status of low carbon vehicle technologies, including battery electric vehicle (BEV), different conventional hybrid electric vehicles (HEVs),

and hydrogen fuel cell vehicle (FCEV). This chapter also compares the history, current development and future development trend of the mentioned types of vehicles. Research shows most automakers consider hydrogen FCEV as the most promising long-term alternative, regardless of whether they are investing in HEVs or BEVs or not. However, it is broadly agreed that all currently viable technologies are likely to play a part in a future sustainable transport system.

Chapter 3 is developed from author's contributed chapter "Fuel-Cell (Hydrogen) Electric Hybrid Vehicles" of book "Alternative fuels and advanced vehicle technologies: Towards zero carbon transportation", by Woodhead Publishing [5]. This chapter assessed the benefits and disadvantages of hydrogen based transport by evaluating H₂ICE vehicles and hydrogen fuel cell hybrid vehicles (HFCHVs) from various aspects. It is clear that the key technical problems of hydrogen are infrastructure, storage, cost and safety.

Chapter 4 is based on the published paper "Hydrogen fuel cell hybrid scooter (HFCHS) with plug-in features on Birmingham campus" in International Journal of Hydrogen Energy [2]. In this study, a commercially available 'pure' lead-acid battery electric scooter (GOPED) was converted to a hydrogen fuel cell hybrid scooter (HFCHS) in views of investigating the effect of hybridisation on driving duty cycles, range, performance, recharging times, well-to-wheel CO₂ footprint and overall running costs.

Chapter 5 is on the basis of the published paper "Hybrid Hydrogen PEM Fuel Cell and Batteries without DC-DC Converter" in International Journal of Low-Carbon Technologies [3].

According to the study of the Micro-Cab HFCEV, nearly 20% of energy generated by the FC was lost through DC-DC converter, mainly caused by the fact that the DC-DC converter can only obtain its peak efficiency at full load, which is rarely achieved in real driving cycles, especially under urban drive cycles that involve many stops, where the fuel cell could only achieve maximum efficiency at partial load. To minimise the power loss in the DC-DC converter, this chapter investigates a fuel cell hybrid equipped with battery that is without voltage conversion, in a 48V system.

Chapter 6 studies the theory and experimental methodology on the early prototype Micro-cab H4 HFCHVs that were designed and manufactured by Micro-Cab at Coventry University. This was an innovative design owing to its light weight and economic components, more than 4000km having been done by those vehicles, with an enormous amount of data collected.

Chapter 7 analyses the results of the 2 year test of the Micro-cab. This includes the hydrogen refueling and consumption, fuel cell performance and efficiency, DC-DC converter behaviour, traction battery performance as well as the motor performance and efficiency. Those HFCVs are also compared to the diesel van under different duty cycles. The findings from this chapter have guided the development of an updated power train, as well as the Micro-cab Industries' next generation vehicle [52].

Chapter 8 uses ADVISOR to simulate the energy efficiency of the different vehicle power trains, including conventional petrol and diesel vehicles, with their hybrid electric power

train, battery electric vehicle and hydrogen fuel cell vehicle. The glider vehicle was designed based on the bestselling vehicle VW Golf MK6, simulated under 4 representative drive cycles: NEDC, ARTEMIS, UDDS (FTP 72) and WLTC. The simulation results then were compared on an equivalent basis.

Chapter 9 introduces the re-designed Micro-cab which was improved in terms of the performance and efficiency. In the new design, higher energy density lithium ion phosphate batteries replaced lead acid batteries; a 3 kW PEMFC without DC-DC converter was installed to prevent the energy from losing via power converters. Two individual Lynch pancake style permanent magnet DC motors powered each rear wheel through high-efficiency belt and pulley mechanism, controlled by two separate Kelly motor controllers, with re-generative braking also enabled in this design. Most of the components were rated at 48V DC to eliminate energy loss during voltage conversions. The tests have been done under ECE 15 drive cycle at Shakespeare Raceway. Results have been analysed with respect to the vehicle performance and energy efficiency, fuel cell consumption, power distribution and re-generative braking.

Chapter 10 concludes the findings and results, as well as proposing further research in future.

2. Chapter Two Background¹

¹Chapter 2 is partially adapted from author's published paper "Current status of hybrid, battery and fuel cell

2.1 Current Status of Low-Carbon Vehicle Technologies

The challenges posed by automobiles are large and urgent, and over the past decade, there has been rapid, on-going progress in the development of low carbon vehicle technology, and auto manufacturers have gradually brought models with improved fuel economy to market. On the positive side, most vehicles being sold in the EU now emit significantly less than the equivalent model sold ten years ago, despite a trend towards increased sales of larger and more powerful vehicles, and it also been observed that 0.6% improvement has been achieved per year on fuel efficiency [53]. On the negative side, 99% of those vehicles are still conventional IC engines vehicles and consume fossil oil, and the CO₂ emission figures are way from the EU 80% decarbonisation goal [54].

At the same time, alternative and sustainable low carbon vehicle solutions have been developed and demonstrated in worldwide, such as Nissan Leaf, Mitsubishi iMEV battery electric vehicles, Toyota Prius, Honda Insight hybrid vehicles and Honda FCX Charity, Toyota Highlander FCV fuel cell electric vehicles etc. [55]. There are many more potential solutions to eliminating these problems, see Figure 2.1. Whereas the electric power-train technologies are considered to be the most viable solutions, and are being adopted and developed by leading automotive manufacturers, as mentioned. Each of these technologies has its own advantages and disadvantages with regards to cost, range, performance, and infrastructure [18, 19, 46, 56], as listed in Table 2.2. Currently there is no clear answer as to which one could dominate the future low carbon vehicle market. McKinsey report [10] stated that many automobile companies have an equal interest in all four power-trains, including conventional IC engines, hybrids, BEVs and FCEVs [10]; In addition, most of the automakers

see hydrogen FCEVs as the most promising long-term alternative, regardless of whether they are investing in PHEVs or BEVs or not. However, it is broadly agreed that all currently viable technologies are likely to play a part in a future sustainable transport system [10].

Hybridisation	Alternative Propulsions	Alternative Fuels for ICE	Vehicle Technologies
<ul style="list-style-type: none"> •Micro hybrid •Mild hybrid •Full hybrid •Plug-in hybrid 	<ul style="list-style-type: none"> •Battery Vehicles •Fuel cells Vehicles •Air, Solar and others 	<ul style="list-style-type: none"> •Hydrogen •Bio-Fuel •Ethanol •Methanol •LPG, CNG, LNG, H₂ & CNG mixture 	<ul style="list-style-type: none"> •Engine down sizing •Adding the electric systems •Transmission improvement

Figure 2.1 List of main low-carbon technologies for vehicles

In other words, the future automotive market will be divided into specific segments, people purchasing a vehicle for more specific purposes, i.e. there will be a small size battery electric vehicle designed for urban city and medium-large size fuel cell electric vehicle for multipurpose, the era of IC engines vehicle will gradually phase out, and electric drive trains such as fuel cell vehicle will totally or partially replace other drive trains for passenger vehicles in a longer-term.

It is very important to note that the average efficiency of all kinds of vehicles is strongly related to the way they are used. Driving style, traffic situations (e.g. speed limits and congestion), and the percentage of urban, rural and highway driving all have an effect on a vehicle's energy consumption and the average power-train efficiency, and thus the carbon emission, refer to Chapter 8 for detailed results.

2.1.1 New Passenger Vehicle Trend

Figure 2.2 shows the trend for EU new passenger vehicles from the year 2000 [57]. A progressive dieselization process of the vehicles can be seen, along with the obvious trend of an increasing adoption rate (although small in share) for alternative fuel vehicles (AFV), namely Liquefied Petroleum Gas (LPG), Natural Gas (NG), Electricity, Hydrogen, and Dual Fuel (Gasoline-Bioethanol, Petrol-LPG, Gasoline-NG).

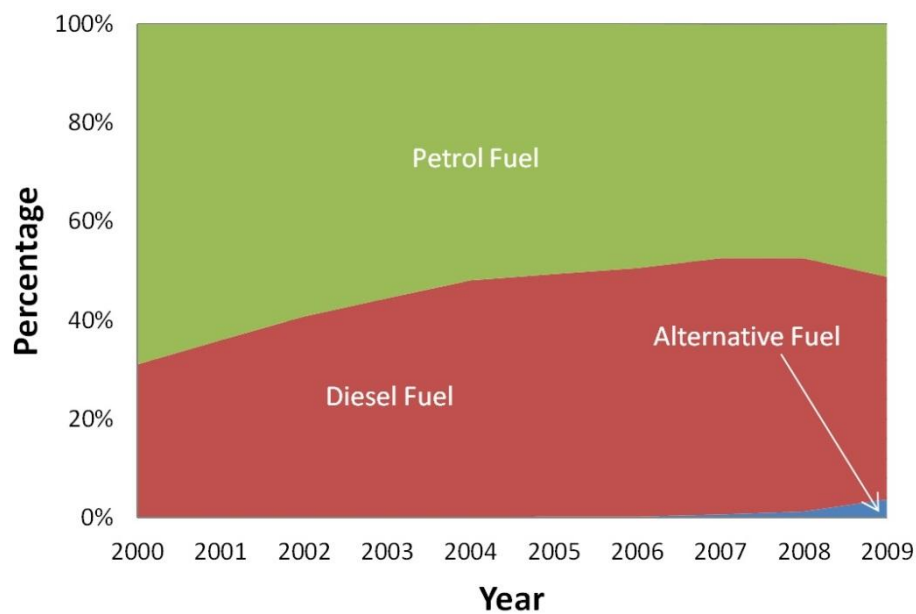


Figure 2.2 Share of Fuel Type in EU New Passenger Vehicles (EU Commission, 2010) [57]

Although diesel vehicles have better fuel efficiency than current petrol vehicles, more diesel vehicles on Europe's roads would further worsen air quality due to the diesel fumes leading to respiratory problems, asthma, bronchitis [58], and would also worsen energy security as Europe depends to a large extent on imports of diesel (while exporting petrol) [59]. Diesel vehicles are also likely to be driven more miles than petrol vehicles, for example, in 2005 the average diesel vehicle was driven 64% further in France than the average petrol vehicle [60]. This situation has changed since 2009; although alternative fuel vehicles sales increased by 3

times since the previous year, petrol vehicles returned to take a majority share of the new sales [57].

2.2 Conventional IC Engines Vehicles

2.2.1 History

The IC engines powered vehicle (Figure 2.3a) is one of the greatest achievements in human history; the design has been perfected over 150 years, overcoming many issues which made it noisy, smelly, cantankerous and unreliable, and finally beating steam engine vehicles and electric vehicles in the early 20th century [61]. The IC engine has now become the most popular power plant for vehicles and probably will remain the dominant technology in the coming decades under the business as usual scenario. This is because the IC engines vehicle had one dominant feature - it used petrol/diesel as a fuel, and so had a range that was far superior to other vehicles, for instance, battery vehicle (Figure 2.3b) and fuel cell electric vehicle (Figure 2.3c). This can be explained by the energy density of petrol/diesel fuel compared to batteries.

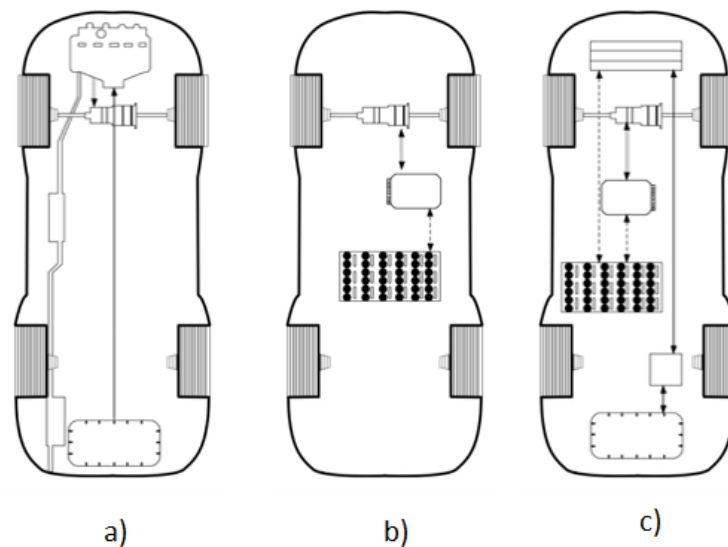


Figure 2.3 Schematic drawing of a) IC engines vehicle, b) BEV and c) FCEV

2.2.2 Current Status

The IC engines dominated and will continue to dominate automobile technology for many years, even in today's most advanced hybrid vehicles: the internal combustion engine is still the first choice as the main power supply. However the hybrid vehicle's IC engine is different from the conventional vehicle's IC engine: the engine in the hybrid vehicle is normally smaller and runs at its high efficiency point for longer periods of time, hence achieving better fuel economy. For instance, the Toyota Prius engine runs the Atkinson cycle with "Variable Valve Timing with intelligence" (VVT-i) rather than the conventional Otto cycle; the Atkinson features a longer power stroke than the compression stroke by keeping the intake valve open longer than normal. Although some of the fuel is pushed back through the intake, overall economy is increased [62].

The current status of the IC engines can be summarised as follows:

- 96% of passenger vehicles on the road are powered by IC engines [63];
- Most of time the engine runs way below its peak efficiency, especially when driving in urban conditions. Figure 2.4 illustrates a typical petrol engine efficiency map operating under the New European Driving Cycle (NEDC) using the ADVISOR simulation tool;
- The average cost for IC engines is around 25-35 USD/kW [64];
- The average engine power was 84kW in 2008 [65];
- The average engine capacity has remained constant at 1690 cc [65];
- The average specific CO₂ emissions in 2008 were 153.5 gCO₂/km [57].

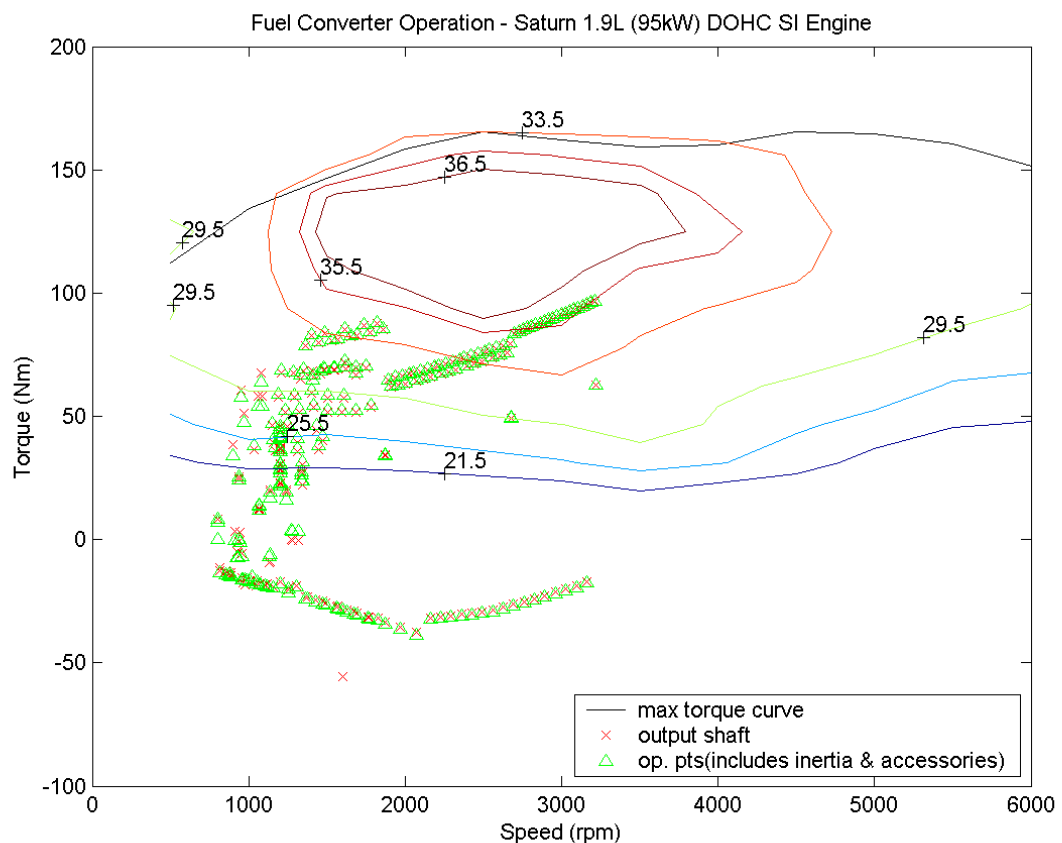


Figure 2.4 Typical IC engine Operation under NEDC Condition

2.2.3 Future Developments and Trends

2.2.3.1 Engine Improvement and Downsizing

Although modern engines achieve power levels that we could only dream about 20 years ago [66], most engines are still not equipped with the most efficient technologies such as turbochargers or variable valve timing, mainly because of the cost. Downsizing the engine with a turbocharger or mechanical supercharger is, however, one of the most effective ways of saving fuel without reducing performance or driving pleasure. Smaller engines with lower displacements would gain more efficiency due to the lighter weight and lower friction thereby reaching their maximum efficiency effectively.

More options to improve the efficiency of IC engines that are foreseen for the short to medium term future are listed in Table 2.1. It is important to note that the reduction potential cannot simply be added together to gain higher efficiency, as one improvement may reduce the potential of others.

Method	Reduction Potential
Reduced engine friction losses	3%
Variable valve timing	3%
Variable valve control	7%
Variable compression ratios	10%
Direct injection	3%-10%
Downsizing with turbo-charging/super-charger	10%-20%
Cylinder deactivation	8%-25%
Waste heat recovery	5%-30%

Table 2.1 List of technologies for IC engine improvements [57]

2.2.3.2 Stop/Start Sequences

Research shows vehicles are at a standstill for one-third of the time while in urban drive cycle [67]. Therefore it is better to turn the engine off, to avoid burning fuel unnecessarily. Stop-start systems operate by cutting the engine off when the driver comes to a complete standstill. The engine is then turned back on when the driver engages the clutch or releases the brake pedal. Such systems help reduce exhaust emissions therefore improving engine efficiency and urban air quality. Other low carbon power trains used in HEVs, BEVs, and HFCVs, which will be discussed in the following sections, however are not affected while the vehicle is at a standstill.

2.2.3.3 Vehicle Size Reduction

Reduction in vehicle size and weight can significantly reduce fuel consumption. Every 10% of weight reduced from the average new car or light truck can cut fuel consumption by around 6%-7% according to the ADVISOR simulations [63]. The three strategies to reduce weight are:

- Lightweight material substitution
- Vehicle design changes, i.e. smaller aero drag, bigger cabin space.
- Vehicle downsizing.

In addition, size reduction will benefit all types of future vehicles.

2.2.3.4 Hybrid Electric Vehicles (HEV)

The concept of hybrid vehicle is almost as old as the automotive itself [68], although the original purpose was not to lower the fuel consumption or emissions, but rather to assist IC engines to provide an acceptable level of performance.

Broadly speaking, a hybrid vehicle power-train can combine any two power sources. Possible combinations include but are not limited to petrol/diesel IC engines with a battery, capacitor or flywheel, or fuel cell with a battery or capacitor. Typically one component is for storage and the other is for the conversion of a fuel into useable energy.

The term Hybrid Electric Vehicle (HEV) usually refers to the combination of an IC engine and electric motor/generator. Currently the worldwide market for HEVs is dominated by Toyota (including Lexus), 4 million Toyota hybrid vehicles have been sold worldwide (April-2012) and the sales figure are still increasing dramatically. Hybrid vehicles have accounted for 15% of Toyota's global vehicle sales [69], followed by Honda, with remarkable sales that surpassed 800,000 units up to the end of December 2011 worldwide [70]. But other automakers such as Ford, General Motors and Nissan are also aggressively pursuing strategic campaigns to push hybrid sales.

2.2.4 Why Hybrid?

Conventional vehicles with IC engines provide good performance and long operating range by combusting liquid fuels, with the advantage of high energy density. However, conventional IC engines vehicles have the disadvantages of poor fuel economy and environmental pollutions. The main reasons for their poor fuel economy are:

- Mismatch of engine fuel efficiency characteristics with real-world driving conditions (as described in Figure 2.4).
- Waste of vehicle kinetic energy while braking, especially when driving in urban conditions.
- Energy wastage during engine idling and standby.
- Low efficiency of hydraulic transmission (automatic) in current vehicles under stop-and-go driving conditions.

Battery Electric Vehicles (BEVs), on the other hand, possess some advantages over conventional IC engines vehicles, such as high energy efficiency and zero tailpipe emissions. However, the limited range and long-time charging makes them far less competitive than IC engines vehicles. Furthermore, due to the much lower energy density of the batteries compared to liquid fuels, BEVs could hardly threaten the dominant position of IC engines vehicles in the current stage. HEVs combine the benefits of power sources by gaining the advantages of both IC engines vehicles and BEVs and overcoming their individual disadvantages. However, HEVs are more expensive than conventional vehicles because of the extra components and complexity required, but may be less expensive than BEVs because the batteries used in BEVs are of high cost at the moment.

There are five common design options: series, parallel, series-parallel, complex and plug-in hybrid [19]. In any IC engines based HEV, there are two forms of energy flowing through the drive train: mechanical energy and electrical energy. Adding two powers together or splitting one power into two at the power merging point always occurs with the same power type, that is, electric or mechanical [71].

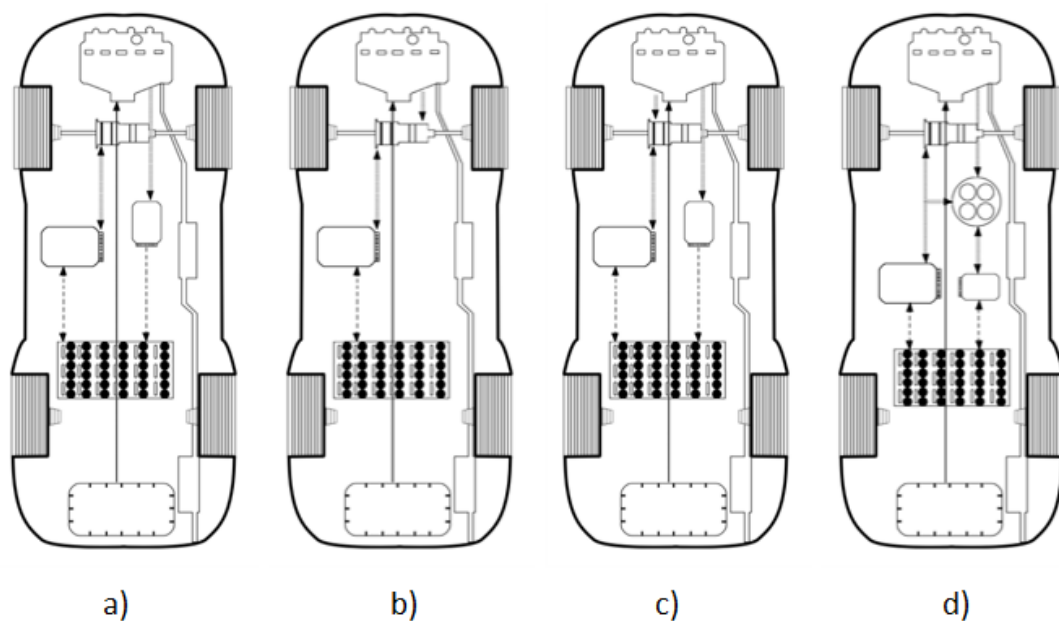


Figure 2.5 Schematic drawing of a) Series hybrid vehicle, b) Parallel hybrid vehicle, c) Series Parallel hybrid vehicle and d) Complex hybrid vehicle

- **Series Hybrid** – as shown by Figure 2.5a). This is the simplest model of HEVs (also named range extender hybrid). In this power train, the IC engines mechanical power is firstly converted into electrons using a generator; the converted electricity either charges the battery pack or supplies the electric motor directly for traction. Since there is no mechanical connection between the engine and the driven wheels, the IC engines can operate at the peak efficiency point continuously, therefore improving the engine thermal efficiency. The disadvantage is there are three propulsion devices,

which increases the total vehicle weight. One example of series hybrid vehicle is Chevrolet Volt (however it can also classify as Plug-in Hybrid) [72].

- **Parallel Hybrid** – as shown by Figure 2.5b). The parallel HEVs allow both the engine and the electric motor to deliver power in parallel to drive the traction wheels. The electric motor operates as a generator to charge the battery while braking, or when the IC engine output is greater than the required to drive the wheels. Compare to series hybrid, parallel hybrid needs less propulsion devices, and a downsized IC engine and a smaller motor can be used. A good example is Honda Insight [73].
- **Series-Parallel Hybrid** – as shown by Figure 2.5c), series–parallel hybrid incorporates the features of series and parallel HEVs. It consists of an additional mechanical link compared with the series hybrid and another generator compared with the parallel hybrid. Although the series–parallel HEV is more complicated and costly [74], with the advances in control and manufacturing technologies, some modern HEVs manufactures still prefer to adopt this system.
- **Complex Hybrid Systems** – as shown by Figure 2.5d), the generator and electric motor in series–parallel hybrids are both electric machinery. However, the key difference is between the bidirectional power flow of the electric motor in the complex hybrid and the unidirectional power flow of the generator in the series–parallel hybrid. The complex hybrid suffers from higher complexity and costliness.

However some newly introduced HEVs adopted this system, such as the dominating hybrid vehicle -Toyota Prius [75].

- **Plug-in Hybrid Systems** – By increase the size of the storage battery, the regular hybrid system could convert a plug-in hybrid system, however, plug-in hybrid vehicles (PHEVs) include but are not limited to the mentioned four IC engines based hybrid systems, they can also be plug-in hydrogen hybrid vehicles (discussed in Chapter 5). PHEVs have larger battery packs than standard HEVs, which provide an all-electric driving range of about 10 to 40 miles, referred to PHEV-miles, e.g. PHEV-10 or PHEV-40 [76]. On an empty battery, PHEVs perform like HEVs, consuming less fuel and producing fewer emissions than similar IC engines vehicles.

2.3 Battery Electric Vehicles (BEVs)

2.3.1 History

Battery Electric Vehicles (BEVs) simply use an electric motor for traction, and chemical batteries as energy sources. The first Battery Electric Vehicle (BEV) was built by Thomas Davenport in 1834 - a few decades earlier even than the IC engines vehicle [77]. The first vehicle to surpass the 100 km/h barrier was also a battery vehicle, namely the 'Jamais Contente' which was driven by Camille Jenatzy in 1899 [78]. Hence BEVs were not a new concept even 100 years ago. In comparison with early IC engines vehicles, BEVs were comfortable, quiet, and clean and did not need to be cranked. However, due to the limited energy storage capacity of the battery, the range was very limited, and at the same time internal combustion engine technologies improved dramatically. As a consequence, the BEV

almost vanished by the 1930s [79]. Several decades later, due to the energy crisis and oil shortage in the 1970s, automakers and policy makers started to reconsider improving BEVs, as they offered high energy efficiency and allowed the diversification of energy sources [80]. According to a 2007 analysis by the Natural Resources Defence Council and the Electric Power Research Institute, no matter how a plug-in hybrid gets its power - fully from coal power plants, from the national average fuel mix, or from renewable energy - it always has a smaller carbon footprint than an IC engine vehicle [81, 82].

2.3.2 Current Status

BEVs use an electric motor for traction instead of an IC engine, and use batteries for their energy source instead of liquid fuels. BEVs have many advantages over the conventional IC engines vehicles, such as no tailpipe emissions, which improves urban air quality, high Tank to Wheel (TtW) energy efficiency and independence from fossil fuels. The battery vehicle drive train consists of three major sub-systems [6]:

- Electric motor propulsion system—vehicle controller, power electronic converter, the electric motor, and transmission.
- Battery system—batteries, Battery Manage System (BMS), and charging unit.
- Auxiliary system—heating/cooling, electronic pumps, and other electronic auxiliaries.

The principle of the BEVs operation is very straight forward, based on the control inputs from the accelerator and brake pedals, the vehicle controller provides control signals to the electronic power convertor, which functions to regulate the power flow between the electric motor and battery. Then the electric motor provides traction to the wheels. The motor can also play the role of a generator, converting the braking energy to electrons and charging the battery, the energy management unit cooperates with the vehicle controller to control the

regenerative braking and its energy recovery. The electric motors produce a great amount of torque from rest to give amazing performance. In terms of acceleration and power, BEVs are superior to IC vehicles.

Although both BEVs and HEVs have a battery pack, the characteristics of the BEVs and HEVs battery packs are distinctly different. The BEVs battery pack has high specific energy while the HEVs battery pack has high specific power. Since the motor in a power-assist (grid-independent) HEV is used intermittently and must be capable of producing high power for short periods of time (e.g. during maximum acceleration), its battery pack should be optimized for high power. Whereas in BEVs, the motor needs to provide all of the traction power, hence the battery pack is relatively in a larger size, the battery not only needs to be capable of producing high power, but also needs to be capable of high energy to last. In this case, the high power factor will not be an issue due to the size of the battery pack.

2.3.3 Future Development

While significant progress has been made in developing automotive batteries, the following challenges remain:

- **Reduce cost**- Currently a Li-ion battery with 35 kWh storage capacity costs around £18,000 to manufacture, while a few organizations (ANL, IEA, EPRI, and CARB) project future price about 1/3 of this. Reducing the cost of battery pack therefore is the key challenge for BEVs development, according to BERR & DfT reports 2008 [83].
- **Improve safety**- Current nickel and cobalt-based oxide Li-ion cathode materials have potential issues with overcharging [84]; clearly, voltage control at cell, module and battery level is critical to prevent overcharging of automotive Li-ion batteries, but all

factors that will inevitably increase Li-ion battery cost further. Lithium iron phosphate cathodes offer a promising future but with less specific power density.

- **Prolong the life-span**- as an automotive battery, it should last at least 10 years or 150,000 miles under variety of conditions, whereas current average life of vehicles registered in the UK is 13.2 years [85].
- **Shorten the charging time** and better charging facility is needed.
- **Reduce size and weight** of battery pack.
- **Charging infrastructures** in both public and home.

2.4 Hydrogen Fuel Cell Vehicles (HFCVs)

2.4.1 Introduction

Fuel cell technology was introduced in 1839 when Sir William Grove discovered that it is possible to generate electricity by reversing the electrolysis of water [86]. More than 100 years later, in the 1960s, fuel cells were used in the Apollo space program as they are safe, compact, light and zero emission [87].

Recently, a number of automobile makers and government agencies have supported large R&D programmes for hydrogen fuel cell technology in transportation. Hydrogen Fuel Cell Vehicles (HFCEVs) share many of the same components as those used in BEVs, such as electric motors and power controller or inverters; however, the main energy sources are completely different. While BEVs use energy stored in the battery, HFCVs use a fuel cell. A fuel cell is an electrochemical device that converts stored energy into electricity by chemical reactions, similar to a battery, but superior to a battery in many ways relevant to

automobiles [88]. The major advantages are that fuel cells are lighter and smaller and can convert stored energy into electricity as long as fuel is supplied.

Due to the clear similarities between batteries and fuel cells, both of these technologies will coexist in the future, while the BEVs is suitable for short range and small vehicles, the HFCEV is suggested to be applied in medium-large and long range vehicles [2].

The PEM (Proton Exchange Membrane) fuel cell is probably the best choice for automobile use [89]. The principle of how Hydrogen Fuel Cell Vehicles (HFCEVs) work is simple, they use fuel cells to convert hydrogen into electricity; the electricity is then used either to drive the vehicle or to be stored in an energy storage device, such as batteries or ultra-capacitors. Since fuel cells generate electricity from chemical reactions, they do not combust fuel and therefore producing nil pollutants and much less heat compared to an IC engine. The by-product of a hydrogen fuel cell is merely pure water. Fuel cells have few moving parts nor irregular shapes, so they have the potential for high reliability and low manufacturing cost for automobiles [90].

Although HFCVs possess wide range of advantages, they also have certain limitations; these relate to the fuel cell stack itself and its fuel: hydrogen generation, cost, transportation, infrastructure, safety and storage.

2.4.2 PEM Fuel Cell Stack

The PEM fuel cell stack acts as the power generator as the engine does in a conventional vehicle, which is the most important part. Recently, PEM fuel cell technologies have been

developing rapidly [82]. However, two key limitations still remain: cost and durability. The cost for an IC engine power plant is about USD25-35 per kW. Current fuel cell systems are estimated to be about 5 times more expensive, even taking into account the cost savings that can be made with high-volume manufacturing [91]. This is because the direct costs of raw materials and manufacturing for catalysts, bipolar plates, membranes, and gas diffusion layers are currently extremely high. On the other hand, the fuel cell stack for an automotive engine is expected to be as durable and reliable as current automotive engines, i.e. 5,000 h lifespan or 150,000 miles equivalent under a range of operating conditions, including different temperatures and climates [92].

2.4.3 Hydrogen as Fuel for Fuel Cell Hybrid

Fuel cell performs better when operating in a consistent condition and could achieve their maximum efficiency at partial load. However, a vehicle requires a variety of power outputs according to the road and traffic conditions. Hybridization of a fuel cell with Peak Power Sources (PPS) could solve these problems, for instance, to use batteries or ultra-capacitors when the demand of power is large to reach higher speed or acceleration. PPS could also help the fuel cell to provide the boost while power demand is low, such as when deceleration or downhill. The extra energy can be replenished to PPS; this allows the fuel cell system to be operated more efficiently [93]. In addition, a smaller fuel cell can be used, for instance, to maintain a vehicle at 70 mph continuously requires 15 kW at the wheels, so a 20 kW fuel cell stack should be able to cope with this.

So a hybrid fuel cell with a Peak Power Source (PPS) could offer a viable solution for electric vehicles. This configuration will offer the following advantages compared to full fuel cells vehicles [6]:

- Smaller fuel cell means lower cost.
- Fuel cell could operate at partial load to achieve its optimum efficiency.
- Fuel cell life will be extended.
- The fuel cell designer will be able to optimize the cells for power and efficiency instead of cycle life.
- Eliminate deep discharging from the battery; therefore improving the batteries' life.
- Allows fast start-up of the fuel cell.
- Allows capture of regeneration energy.

The disadvantages of hybridization are the complexity of the vehicle system, weight increase, complexity of the control system, and extra battery cost.

2.4.4 Future Development

Based on the above discussion, further research should focus on:

- Reducing the cost of hydrogen—it has to be competitive with conventional fuels.
- Improving hydrogen storage technology—the low volumetric energy density of hydrogen makes storage a challenge. The storage needs to meet vehicle packaging, cost, and performance requirements.
- Reducing fuel cell cost and improving durability—the cost of fuel cell power systems has to be reduced and durability must be improved for fuel cells to compete with conventional technologies.

2.5 Comparison

Table 2.2 shows the different types of vehicles in terms of cost, performance to CO₂ emissions. The chosen model for each vehicle type is the representative of the most advanced technologies in its class.

Power Train	Petrol IC	Diesel IC	Petrol / Electric Hybrid	Hydrogen Fuel Cell	Battery Electric
Reference vehicle	Volkswagen Golf 1.4 TSI	Volkswagen Golf 1.6 TDI	Toyota Prius III	Honda FCX Clarity	Nissan Leaf
Top speed (mph)	125	118	112	100	90
Acceleration (0-60 mph, s)	9.5	11.3	10.4	10.0	7.0
Maximum range ^(a) (miles)	500	500	650	240	100
Number of seats / doors	5/5	5/5	5/4	4/4	5/5
Storage space (L) (rear seat unfolded/folded)	350/1305	350/1305	612L	371L	410L/680L
Purchase price (before subsidy)	\$21,400 ^(b)	\$21,740 ^(b)	\$24,000	\$50,000 (estimated)	\$35,200
Fuel cost – before tax (\$/miles)	\$0.097/\$0.046	\$0.059/\$0.028	\$0.073/\$0.03 5	N/A	N/A
– price after tax ^(c) US/UK(\$/mile)	\$0.11/\$0.14	\$0.07/\$0.9	\$0.082/\$0.10 3	\$0.067 ^(d)	\$0.041
Official fuel economy ^(a) (mpg, US)	38	62	50	60 ^(e)	99 ^(e)
CO ₂ emissions – tailpipe (g/km)	144	99	89	0	0
– estimated total WTW(g/km)	163	118	101	0 to 134 ^(f)	0 to 75.7 ^(g)

Table 2.2 Comparison of vehicle technologies from a consumers' perspective.

Notes:

- Based on the US EPA dynamometer drive cycles;
- Equivalent US price, as those model not available in US market, price was estimated based on the average ratio between UK and US retail price. Guided UK retail price is £18,395 [94].
- Ranges based on energy price and taxation levels in the US (low, average \$0.49 per US gallon, plus VAT) [95] and UK (high, £0.5795 per litre or £2.19 per US gallon, plus VAT) [96]. Electricity cost of \$0.12/ Kw-hr [97] and premium gasoline price of \$4.12 per gallon (Sep, 2012) [98], UK petrol cost £1.31/L (July 2012)[99], equal £3.3 per US gallon. And 1GBP=1.57USD
- Based on hydrogen price retail in California \$3.99/kg [100].
- Conversion 1 US gallon of gasoline=33.7 kW-hr and 1 kg of hydrogen is roughly equivalent to 1 US gallon of gasoline.
- Based on US hydrogen production CO₂ emission from centralised SMR plants, every 1 kg hydrogen production emit 13.7 kg CO₂ gas [101], however, 90% reduction can be achieved by CCS [102].
- Based on 2009 average US electricity generation CO₂ emission 508 g/kWh, data from IEA [103].

2.5.1 Vehicle Energy Efficiency (TtW)

The terms of Tank to Wheel (TtW) is a measure of the overall efficiency of the vehicle system, i.e. how efficiently the vehicle converts the fuel in its tank to energy to rotate its wheel and move the vehicle. Figure 2.6A illustrates the TtW energy efficiency of IC engines vehicles and shows that more than half of the energy is wasted as heat from the engine heat and exhaust. Moreover, the idle and standby cycles are responsible for around 17.2% loss of useful energy, with today's highly efficient gearbox, driveline and electronic device, another 7.8% energy is lost, with only 12.6% energy to overcome the aero drag, rolling resistance and inertia (braking) forces [104].

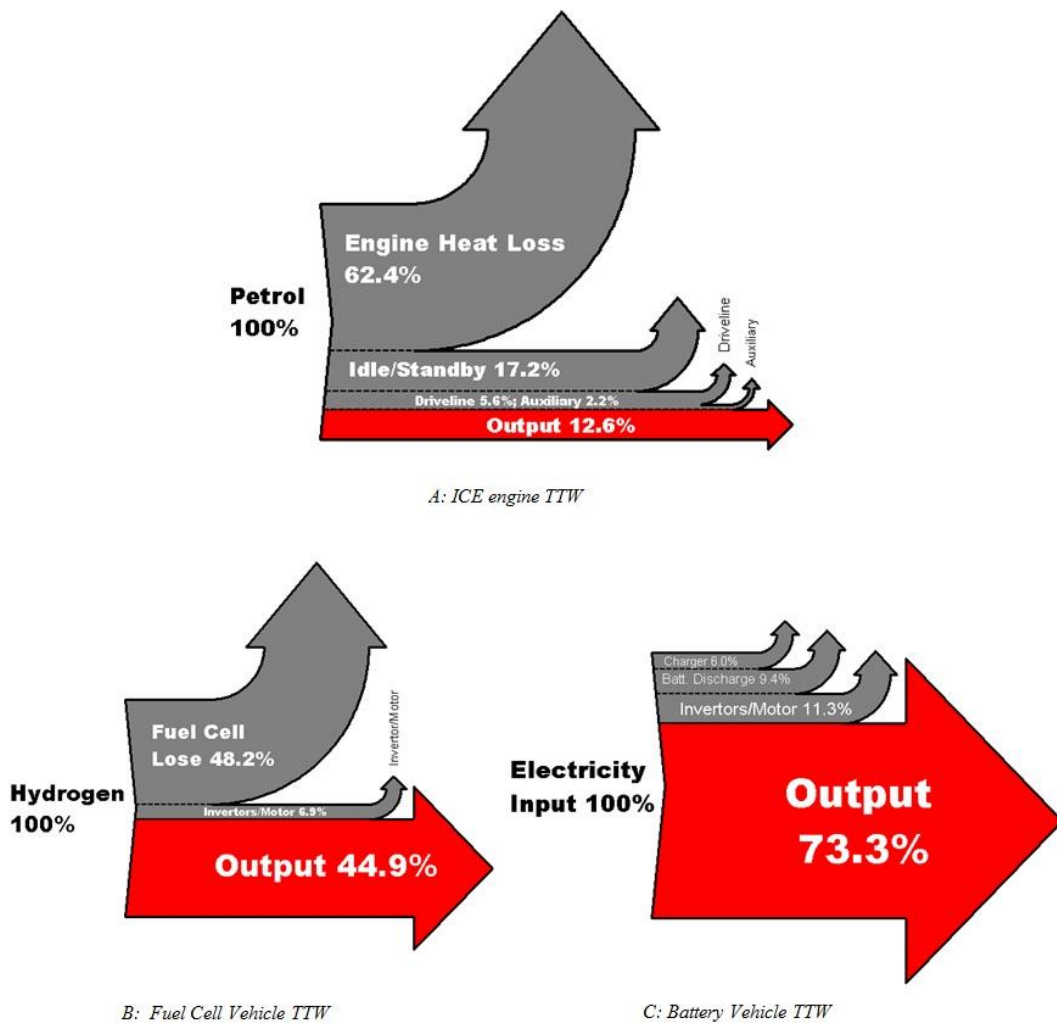


Figure 2.6 Overall efficiency of the vehicle system

Figure 2.6B and Figure 2.6C show the TTW efficiency of battery vehicle and fuel cell vehicle respectively. The figures show that they have common characteristics, for example, both generate electricity to drive the electric motors. Fuel cells derive their energy from hydrogen stored in the vehicle, while battery vehicles are powered solely from batteries charged via the electrical grid. Both hydrogen and electricity can be made from low and zero carbon sources such as solar, wind and biomass [105]. From the figures it can be seen that the net output of 73.3% for battery is much higher than 44.9% which was output by fuel cell. But the battery is limited by poor energy storage compared to hydrogen.

2.6 Conclusion

Hydrogen FCEVs present the most promising long-term alternative to current IC engines vehicles because they give improved efficiency, zero emissions and equivalent performance and range to conventional vehicles.

3. Chapter Three

Hydrogen as Fuel for Transport²

²Chapter 3 is developed from author's contributed chapter "Fuel-Cell (Hydrogen) Electric Hybrid Vehicles" of book "Alternative fuels and advanced vehicle technologies: Towards zero carbon transportation", by Woodhead Publishing.

3.1 Introduction

This chapter assesses the benefits and disadvantages of hydrogen based transport by evaluating hydrogen combustion vehicles and hydrogen fuel cell hybrid vehicles. It is clear that the key problems of hydrogen are infrastructure, storage, cost and safety. A theoretical model for comparing combustion and fuel cell hybrids is put forward to show that the hybrid gives the best results in most drive cycle tests. The extra efficiency of the HFCV hybrid reduces the storage problem significantly.

3.1.1 History of Hydrogen as Fuel

Historically, the first internal combustion engine was developed by François Isaac de Rivaz (from Switzerland) in 1806 who designed an engine to run upon mixtures of fuel of hydrogen and oxygen as shown in Figure 3.1 [106].

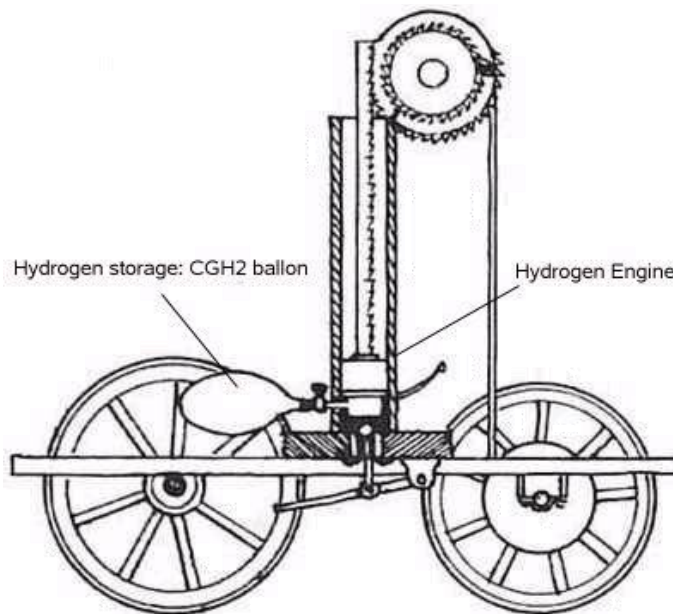


Figure 3.1 Schematic of the H_2 fuelled vehicle concept. Patented by Isaac de Rivaz, 1807

At that time, the hydrogen was stored on-board as compressed gas in a balloon which was only able to power the vehicle for about 100 metres. The hydrogen storage problem was evident two centuries ago, this is because hydrogen has the lowest atomic weight of any chemical compounds and hence has extremely low density in both forms of gaseous and liquid [107]. However, on the other hand, hydrogen has the potential to be the ideal fuel for transport. It is abundant in nature, and is efficient in providing power to automobiles. Since 1807, hydrogen has been used as a fuel in 456 applications in transports, including automobiles, ships, aeroplanes, and space shuttles. The use of hydrogen as a potential fuel can reduce dependency on foreign fossil oil, improve local air quality and eliminate carbon dioxide emissions from transport, regardless of how the hydrogen is used and its origin [108].

Hydrogen is acknowledged to be a long-term sustainable alternative fuel for fossil fuels in the transportation sector which is forecasted to be the single largest market [109]. It is considered as fuel with vertically unlimited supply and has been named as “forever fuel” by Hoffmann [110].

3.1.2 Ways to Use Hydrogen as Fuel in Transport

Firstly, Hydrogen can be combusted in an IC engine vehicle with the oxygen from air, similarly to a conventional petrol vehicle. H₂ICE is often questioned for inefficiency and large fuel tanks [111], the H₂ICE can achieve around 40% efficiency whereas for a natural aspired spark ignited internal combustion petrol engine it is 35.74% according to the Second Law Of Thermodynamics [112]. With chamber direct injection (DI) of hydrogen, 45.5% thermal efficiency has been recorded by ANL in 2011 achieved the DoE 2015 goal in efficiency [113], however the cost and durability has not been published. Furthermore, the advanced

hydrogen storage technologies (700 bar compressed gas or liquid) would render storage of sufficient amount of hydrogen on-board feasible.

Secondly, hydrogen can be used in a fuel cell, generating electricity and water with a maximum efficiency of 60%, which is twice as much as that of the normal combustion process. The electricity then powers the motor to drive the vehicle [114].

In order to understand the problems of hydrogen as fuel on vehicles, a comparative test of two vehicles was undertaken - one vehicle was an IC engine Transit van available from CENEX [115] and the other was a Micro-cab vehicle sponsored by Royal Mail, as shown in Figure 3.2.



Figure 3.2 Royal Mail Collaborated Hydrogen vehicle projects, Micro-Cab HFCV (left), H₂ICE Transit Van (right)

3.2 Hydrogen Internal Combustion Engine Vehicles (H₂ICE)

Generally speaking, using an internal combustion engine running on hydrogen is not difficult.

However, to run the engine smoothly and efficiently is far otherwise. The properties of hydrogen that could contribute to its use as combustible fuel are:

- Wide range of flammability – the flammability limit of hydrogen is from 4 to 75 vol%, allowing hydrogen combusted in an internal combustion engine over a wide range of air/hydrogen mixture, making hydrogen ideally suited for ultra-lean burn operation, as lean as $\lambda=10$, to as rich as $\lambda=0.17$ ($0.1 < \phi < 7.1$)³, The flammability limits are even wider if temperature is raised, at 300 °C, the lower flammability limit decreased to $\lambda=20$ ($\phi=20$) [116].
- Low ignition energy – energy need to ignite hydrogen is only 0.02mJ, 14 times less than standard Octane petrol [116]. Enables H₂ICE prompt ignition even with lean mixtures.
- High auto ignition temperature – allows higher compression ratios to be used in a hydrogen engine than in a petrol engine, therefore greater engine efficiency can be achieved. Since the auto ignition temperature is significantly higher than diesel, it is not easily reached with normal compression ratio alone; hence hydrogen is better suited for spark ignition IC engine. H₂ICE has seen used at compression ratios from 7.5:1 to 14.5:1 [117].
- High flame speed at stoichiometric condition – The laminar flame speed of air and hydrogen mixture at stoichiometric condition is about 10 times that of petrol.

³ λ stand for air to fuel ratio and ϕ stand for fuel to air ratio

Therefore hydrogen engines can more closely approach the thermodynamically ideal engine cycle [118].

- High diffusivity – this make possible the formation of a uniform mixture of hydrogen with air, and hydrogen disperses quickly if there is a leakage.
- Extremely low density – Firstly, this posed the challenge to store enough hydrogen on-board of vehicle for an acceptable driving range, as discussed previously. Secondly, the energy density of a hydrogen-air mixture, and hence the power output, is reduced for port fuel injection IC engine. See diagram demonstrations in Figure 3.3.

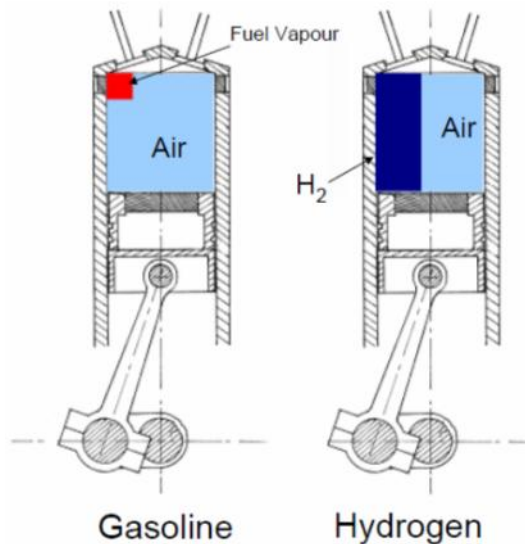


Figure 3.3 Diagrams of Petrol and Hydrogen with Mount of Air Mixture in IC engine.

3.2.1 Results of Comparative Tests

In partnership with CENEX [115], the author studied and tested one of the hydrogen internal combustion engine vehicles on behalf of CENEX. The objectives of the test were to evaluate safety, reliability, and practicality of use, as well as to quantify vehicle emissions, running cost and performance. Key findings were;

- Range – up to 97 miles on hydrogen.

- Carbon free tail-pipe emission, but Well to Wheel CO₂ emission from 0 to 533 g/km depends on the hydrogen production pathway.
- Average Hydrogen cost per mile: £1.35 as in April 2009⁴.
- Engine heat up quicker by 8.5% on hydrogen than petrol.

3.2.2 Vehicle Modification – The Royal Mail Hydrogen IC engine Van

A Ford Transit 2.3L petrol engine van was employed as the testing vehicle. The internal combustion engine had been modified to operate using compressed hydrogen gas but can also operate on petrol fuel. There was a fuel selection switch located on the dashboard panel to the right hand side of steering wheel. An additional fuel rail and injectors to inject hydrogen fuel direct to manifold branch were installed purposely (Figure 3.4).

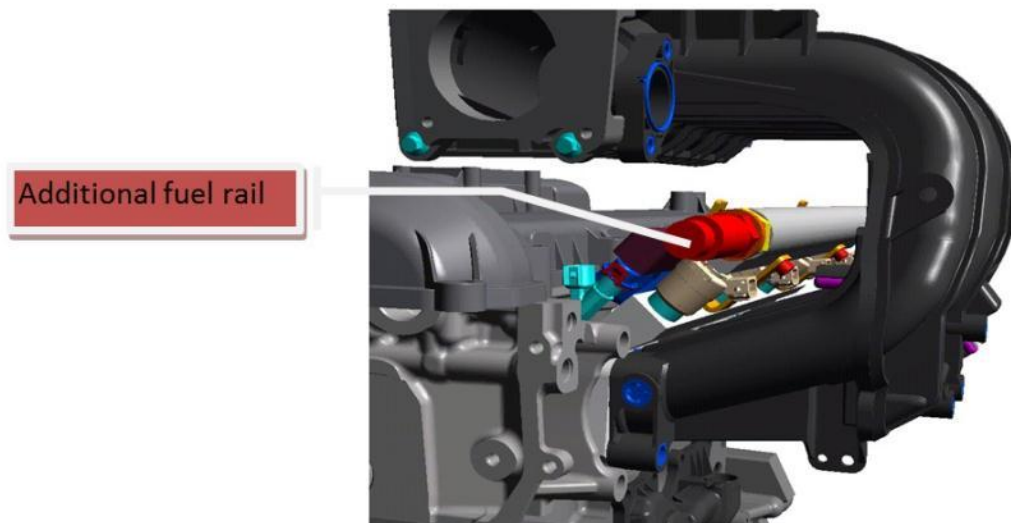


Figure 3.4 Modified IC engines for Hydrogen Fuel

A belt driven supercharger has been installed to provide extra air when fuel mode is selected to hydrogen only; an intercooler is also installed to cool the air. Hydrogen was stored

⁴ The calculation based on hydrogen cost of £20 per kilo (green hydrogen hence the cost), due to there was a hydrogen leakage; the actual average cost is lower than £1.35.

compressed in three tanks under the vehicle (Figure 3.5), with storage capacity of 4.5 kg of hydrogen at 350 bar.

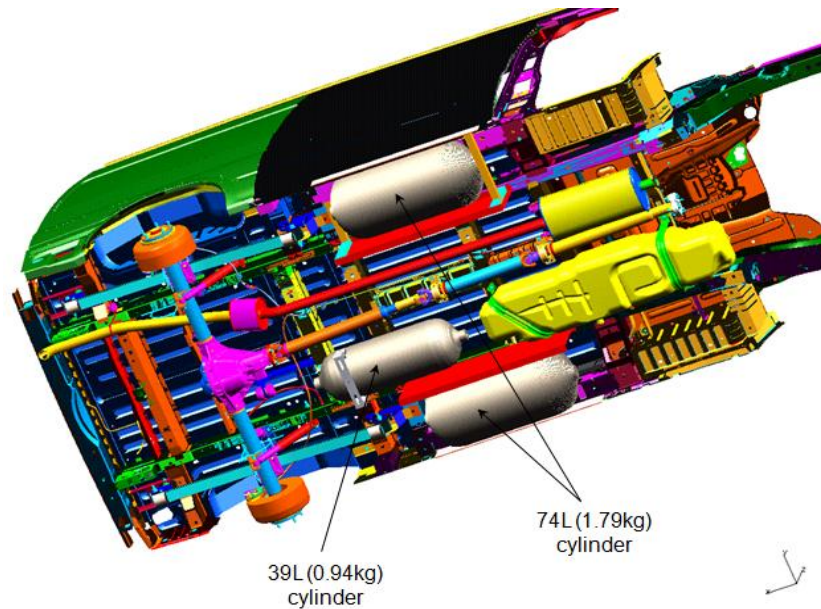


Figure 3.5 Hydrogen Storage Tank Layouts and Position

3.2.4 Hydrogen Consumption and Cost

The H₂ICE was refuelled 8 times through an Air Product 100 hydrogen refueller. Total 14.4 kg H₂ has been consumed and 212 miles have been driven. To evaluate the fuel economy, the estimation method 'Miles per Bar drop' has been used. Although the 'Miles per Bar drop' calculation is not purely linear, it could give an indication of how much hydrogen was consumed for typical driving. From Figure 3.6, it can be seen the most desired result is from the motorway test, about 0.28 miles per bar drop, even higher than the theoretical computer calculated figure given from REVOLVE - 0.25 miles per bar drop [119]. However, driving in urban and campus which involved frequent stops caused dramatic decrease on the figure to 0.06-0.09 miles per bar drop⁵.

⁵ The figures also was affected by hydrogen leaking in pipeline.

Date	10-Mar-09	16-Mar-09	24-Mar-09	27-Mar-09	30-Mar-09	09-Apr-09	20-Apr-09	28-Apr-09
	#23	#28	#32	#34	#35	#37	#38	#39
Start Pressure	19 Bar	177 Bar	38 Bar	97 Bar	178 Bar	181 Bar	295 Bar	241 Bar
Finish Pressure	234 Bar	304 Bar	252 Bar	268 Bar	330 Bar	311 Bar	349 Bar	336 Bar
Hydrogen filled	3.2 Kg	1.2 Kg	3.0 Kg	2.3 Kg	1.1 Kg	1.7 Kg	0.7 Kg	1.2 Kg
Refuel Start Time	15:04:34	15:37:32	16:08:54	15:23:25	11:49:10	11:25:56	15:47:56	14:14:51
Refuel Finish Time	15:06:49	15:39:38	16:11:54	15:25:11	11:51:21	11:27:45	15:48:40	14:16:24
Time Used	135 Sec	126 Sec	180 Sec	166 Sec	131 Sec	109 Sec	104 Sec	87 Sec
Range	3.5Miles	58Miles	27.6Miles	0	27.8Miles	0	9.9Miles	85.8Miles
Condition	Campus	Combined	Combined	Parked	Urban	Parked	Urban	Combined

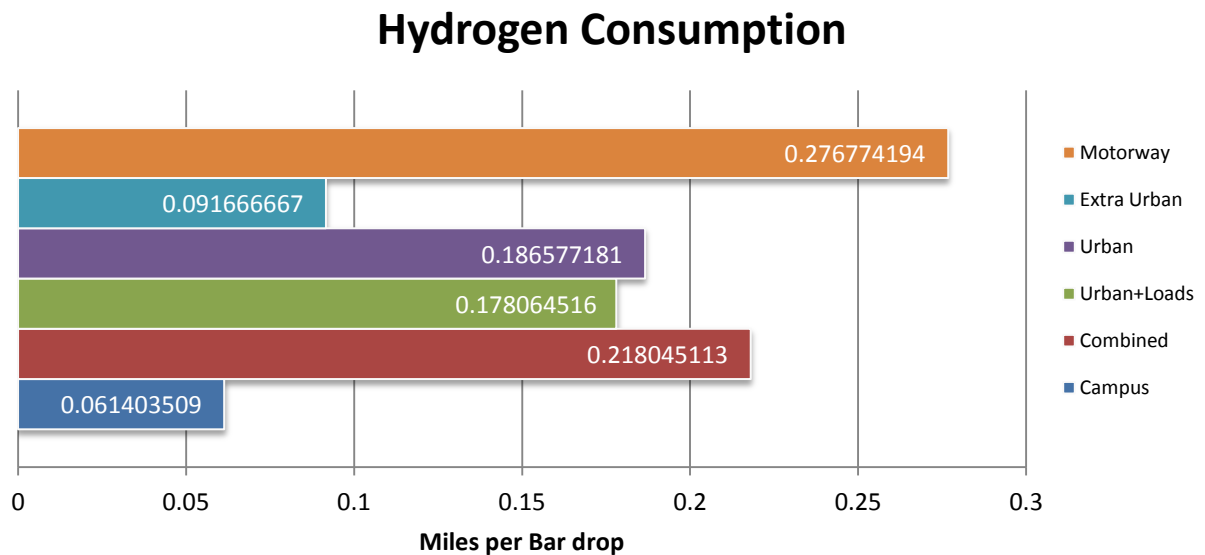


Figure 3.6 Hydrogen Consumption (miles per bar drop)

The H₂ICE van had good feedback overall from the driver during the trial. The performance and drive range were satisfactory for fleet operation. This result shows that the H₂ICE system may provide a cost-effective alternative to fuel cell technology and traditional combustion engines, therefore bridging the gap between today's petrol/diesel powered vehicles and the fuel cell vehicles of the future.

Technologically this is less challenging than the development of fuel cell vehicles and H₂ICE is seen by both leading automotive manufacturers and smaller SME developers as a bridging technology, until fuel cell vehicles become widely available. For instance, BMW has introduced six generations of hydrogen powered internal combustion engine vehicles since 1979; Ford and Mazda have demonstrated the H₂ICEs since 1990s [116].

3.2.4 H₂ICE-electric Hybrid

Like the standard IC engines vehicles, the H₂ICE vehicles could also hybrid with secondary power source (i.e. batteries), therefore improve their efficiencies and reduced emissions. In a hybrid electric vehicle (HEV), the IC engine operates with an electric motor in different configurations. For instance, in series hybrid configuration, it allows H₂ICE to operate at single speed at maximum power with minimum emissions. Van Blarigan and Keller [120] report the single speed H₂ICE peak has been achieved thermal efficiency of 44% at 1800RPM with compression ratio of 14:1, at the same time, the H₂ICE HEV can operate lean enough to output near zero NO_x emissions, these make the H₂ICE electric hybrid a very attractive option toward future low carbon vehicle.

3.2.5 A Bridging Technology for Fuel Cell?

H₂ICE technology can be developed faster and more reliably than fuel cells at the moment, as the IC engines technology has been developed and perfected for more than 150 years.

The U.S. Department of Energy (DoE) has set challenging goals for H₂ICE, as following:

- A brake thermal efficiency of 45%.
- Tier 2 Bin 5 emissions (less than 0.07 g/mi NO_x emissions).
- Equal or better power output than a comparable petrol engine.
- A cost target of \$30/kW in 2015 (same as PEMFC goal).

In addition, H₂ICE vehicles could solve the 'chicken-and-egg' situation of which comes first i.e. the fuel cell vehicle or the hydrogen infrastructure [121]. Furthermore, H₂ICEs normally allow dual fuel operations - the engine can run on both petrol and hydrogen. This makes the start-up of a hydrogen infrastructure much easier and the experience gained from it can be directly translated to fuel cell vehicles in a more practical and efficient way in the future. The H₂ICE engines are capable of running on a lower purity hydrogen supply than fuel cell systems (standard industrial grade purity hydrogen is adequate for IC engines). But the key problem is the hydrogen storage volume plus the weight of pressurised containers.

3.3 Hydrogen Fuel Cell Vehicle HFCVs

Hydrogen also can be used in fuel cell vehicles (FCVs); FCVs are attractive potential replacements for conventional IC engines vehicles because they can offer similar (even better in some aspects) performance, greater efficiency, more environmental friendly, therefore receiving increasing attention in recent years. Many of the leading auto manufacturers have demonstrated their fuel cell vehicles, and are even beginning to put fuel cell vehicles rental to selected customers onto their agenda [122, 123].

FCVs have the potential to perform functions for which conventional vehicles are poorly suited, such as providing remote electrical power (acting as electricity generators) when needed, such as Honda home hydrogen station [124]; and eliminating mechanical and hydraulic subsystems in conventional vehicles hence providing greater design flexibility, FCVs also offer the potential for using fewer vehicle platforms and therefore more efficient

manufacturing approaches, a good example is the GM ‘Autonomy’ skateboard FCV, allowing different body shells to share one vehicle chassis.

Experiments (Chapter 7) showed that the fuel cell hybrid was twice as efficient as the combustion van. Also performance in start-up and drive-cycle testing was good for the campus testing.

3.4 Key Problems for Hydrogen Fuel

3.4.1 Storage

Sufficient storage of hydrogen is the key to commercialising this new technology for vehicle power systems. Table 3.1 demonstrates the varied densities of hydrogen in conventional fuels under different conditions.

Fuel	Density			Energy Density (LHV)		
	(kg/L)	(kg/M ³)	MJ/kg	MJ/L	kWh/kg	kWh/M ³
H₂ at 20°C, 1 atm	0.0000899	0.0899	120	0.01006	33.3	2.79
H₂ at 20°C, 350 bar	0.025	25	120	2.8	33.3	775.86
H₂ at 20°C, 700 bar	0.039	39	120	4.4	33.3	1210.34
H₂ Liquid at boiling point, 1 atm	0.0708	70.8	120	7.92	33.3	2197.24
Petrol	0.702	702	42.7	31.2	11.86	8666.67
Diesel	0.855	855	41.9	36.5	11.64	10138.88

Table 3.1 Densities of hydrogen in conventional fuels under different conditions

By weight the energy density of hydrogen is three times larger than that of petrol and diesel, with 120 MJ/kg versus 42.7 MJ/kg for petrol and 41.9 MJ/kg for diesel. However, the extraordinary low density of hydrogen determines its immense volume that is much larger than petrol and diesel thus requiring vast space for storage under room temperature and pressure. Even when hydrogen has been liquefied, it is still one quarter of the volumetric energy content of petrol, figuring at 7.92 MJ/L for liquid hydrogen compared to 31.2 MJ/L

for petrol. However, this could be partly offset by the higher efficiency of fuel cells related to IC engines.

For transportation applications, the principal challenge is how to store the necessary amount of hydrogen required for considerable driving ranges (>300 miles), with the constraint of weight, volume, durability (>1,500 cycles), efficiency and costs. A hydrogen fuelled vehicle may need to carry 5-13 kg of hydrogen on board in order to match the current conventional vehicles' performance [125].

At the present, the main methods for hydrogen storage in vehicles are:

3.4.1.1 Compressed Hydrogen

Compressing hydrogen is the most accessible and economical way for direct use in automobiles [126]. Currently, both 350 bar and 700 bar carbon fibre reinforced hydrogen tanks are commercially available at low production volumes and high cost.⁶ In addition, compressing hydrogen to 350 bar and 700 bar would require an additional 7%-15% energy which can be lowered providing the hydrogen was initially produced at high pressures [127].

3.4.1.2 Liquid Hydrogen

Hydrogen can be liquefied for on-board vehicle storage, in order to store hydrogen in a liquid state, it is necessary to maintain it at -253°C at ambient pressure [128]. Therefore a highly insulated liquid hydrogen tank is required for such applications.

⁶ From Dynetek Industries Ltd (<http://www.dynetek.com/hydrogen>).

3.4.1.3 Metal Hydride

Many metals and alloys are capable of repeatedly absorbing and releasing large amount of hydrogen, meanwhile storing it at solid state under low pressure. The process absorbing hydrogen into the lattices through cooling and releasing hydrogen through heating [129, 130]. It is known to be one of the safest methods, however the low energy density of hydrogen when stored using metal hydride obstructs the process of successfully achieves the challenging 9% U.S. DoE storage target by 2015 [131]. However, there are other shortcomings such as the longer refuelling time, heavy weight, and slow release rate at normal temperature which is not fitting for automobile applications.

3.4.2 Production

Hydrogen can be produced from a diversity of natural resources, for instance, water, plants, as well as fossil fuel and therefore could potentially reduce countries' dependency on foreign oil when either burnt or used in a fuel cell as previously discussed in Chapter 2. However the main disadvantage of hydrogen is that, it is always chemically 'bonded' with other elements such as oxygen (e.g. H_2O) or carbon (e.g. CH_4). It has to be released from such compounds before it can be used as an energy carrier.

Traditionally, hydrogen is produced by using oil, natural gas, and coal. These currently account for ~ 95% of the global hydrogen production [125] and only 4% and 1% is generated from water using electricity and biomass respectively [127].

Hydrogen can be produced from vehicle on-board, small to medium size distributed on-site facilities and large centralised plants [125].

- **On-board production** – Hydrogen can be produced on-board of vehicle from hydrogen-rich resources such as methanol, ethanol, natural gas, and petrol/diesel fuels [132]. In practice, hydrogen distribution infrastructure and on-board storage are still posing number of difficulties for automotive sector. Generating hydrogen from on-board via reformer is considered to be a more feasible and approachable solution for automotive applications [133]. The main disadvantage of on-board reforming systems is high cost, the extra space required for installation of equipment and storage of hydrogen, the increasing weight of vehicle, the delay on response, and the limited efficiency and durability.
- **Small to medium size distributed on-site production** – probably the most viable solution for introducing hydrogen as a fuel. It needs less initial investment for the smaller capacity production, without excessive requirement of hydrogen transport and delivery infrastructure. The distributed station could reform natural gas or liquid fuel, and electrolysis of water to produce hydrogen, and in need of hydrogen storage to meet the variable demand for hydrogen during a 24-hour period.
- **Large centralised production** – Centralised production of hydrogen benefits from the lower cost approach, allowing more sensible management of greenhouse gas emission through methods such as Carbon Capture and Storage (CCS). Central production of hydrogen could potentially include a more diversified feedstock base, such as fossil fuels, nuclear and other renewable sources. However, it needs the infrastructure in place.

3.4.3 Infrastructure

Like oil and natural gas, hydrogen can be transported via pipeline or shipped in containers, currently 90% of commercial hydrogen is transported via liquid tankers [134]. Due to the characteristic of low density, hydrogen distribution at any stage is inevitably challenging and costly. The U.S. DoE target for hydrogen distribution is < USD1/gge by 2019 against the current figure of USD 4-9 /gge depending upon the amount and quantity [135].

There are primarily three ways to distribute hydrogen from centralised plant:

- a. Distribution in gaseous form through pipeline and high pressure tube trailer
- b. Liquefying and transporting hydrogen in cryogenic tank trucker.
- c. Higher volumetric energy density carriers.



Figure 3.7 University of Birmingham hydrogen dispenser

However, all the methods of hydrogen delivery still present infrastructure challenges. It is predicted that hydrogen fuelled vehicles will first penetrate to commercial and public transport sectors, such as buses, taxis, logistics industry, university fleet vehicles which operate from central depots to multi-destinations, as it is easier to store and dispense hydrogen, before the network of hydrogen infrastructure is established and popularised

[109]. For example, University of Birmingham has 5 hydrogen vehicles and a dispenser as shown in Figure 3.7.

3.4.4 Cost

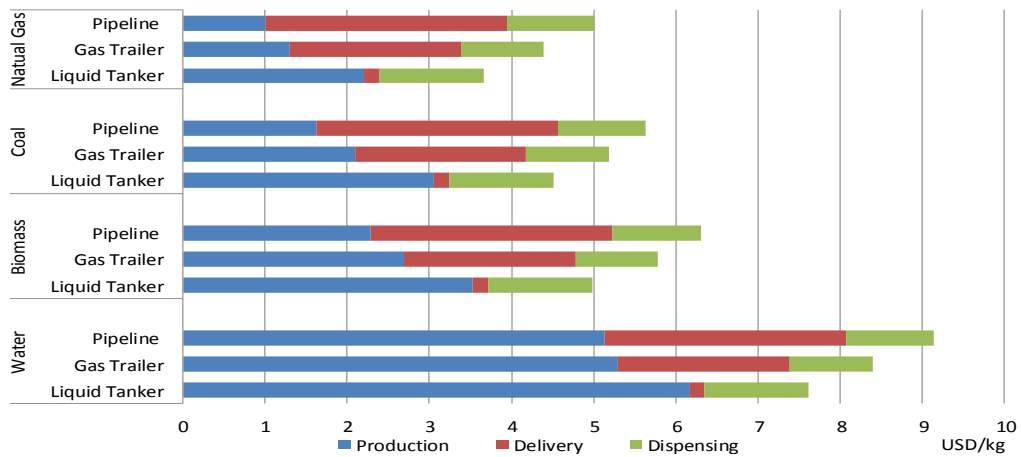


Figure 3.8 Cost of hydrogen from a 150,000kg/d central plant (estimated)

	Delivery Pathway	Liquid Tanker Lorry, \$/kg	Gas Tube Trailer, \$/kg	Pipeline, \$/kg
Natural Gas	Production	2.21	1.30	1.00
	Delivery	0.18	2.09	2.94
	Dispensing	1.27	1.00	1.07
	Total	3.66	4.39	5.00
Coal	Production	3.06	2.09	1.62
	Delivery	0.18	2.09	2.94
	Dispensing	1.27	1.00	1.07
	Total	4.51	5.18	5.62
Biomass	Production	3.53	2.69	2.29
	Delivery	0.18	2.09	2.94
	Dispensing	1.27	1.00	1.07
	Total	4.98	5.77	6.29
Water	Production	6.17	5.30	5.13
	Delivery	0.18	2.09	2.94
	Dispensing	1.27	1.00	1.07
	Total	7.62	8.39	9.13

Table 3.2 Cost of hydrogen produced from various feedstock [136]

The cost of hydrogen production, storage and dispensing is still too high. Figure 3.8 summarises the hydrogen cost estimates from various feedstock and delivery/dispensing methods for large centralised hydrogen plants [136]. The Table 3.2 shows that hydrogen can

be produced presently at costs of USD 1/kg and USD 1.62 /kg from natural gas and coal respectively with pipeline delivery and dispensing adding an estimated cost of USD 4/kg H₂, which is up to 4 times more than the cost of its production. Even when liquid hydrogen tanker could effectively offer more cost effective solutions, liquefying hydrogen is energy intensive and inefficient, as mentioned previously in this Chapter.

3.4.1 Safety

For historical reason, hydrogen has been mis-reputed to be a highly risky element supported by the couple of notorious accidents in the past, such as the fire that destroyed the Hindenburg airship in 1937 [137]. For many years, it has been widely believed that the reason of the fire was the ignition of the hydrogen gas used for lifting the airship, which is not truly justified. An investigation by former NASA researcher Addison Bain in the 1990s reported evidences that the airship fabric skin was coated with highly reactive chemicals, similar to the one used in solid rocket fuels, that easily ignited the airship envelop by an electrical discharge [138].

As a matter of fact, hydrogen is not more dangerous than any other flammable fuels; it is simply a different type of fuel that motorists are yet to be familiar with. Like other fuels in use today, hydrogen can be handled safely if its physical properties are understood and precautions are made [139]. In fact, some of hydrogen's features actually provide extra benefits on safety compared to petrol or other fuels. An official study [16] by Ford Motor Company concluded that, with proper engineering, a future hydrogen fuel cell vehicle would potentially be more reliable and controllable than petrol fuelled IC engines vehicle in

operation. The following list describes the most notable potential safety consideration for using hydrogen in automobiles:

Hydrogen refuelling - Proper 'electrical' grounding of the vehicle and experienced or/and well-trained operator will be essential for safe refuelling in public use.

Vehicle parking - Hydrogen gas is extremely light and diffuses rapidly and as a result when it is released due to leaking, there is a risk that it may gather under roofs in closed environments, and hence indoor parking facilities requisite good ventilation systems and detection, or it may be necessary for vehicles to be kept outside. Similarly, operating hydrogen vehicles in tunnels and confined areas may lead to some issues.

Vehicle collision - In a collision, the hydrogen tank may rupture, like a petrol/diesel tank may do. Limited accident experiences suggests that, when a vehicle carrying hydrogen, the peril is effectively less than that of petrol powered vehicle as hydrogen dissipates very rapidly. However, the immediate release of hydrogen into confined spaces like a garage may lead to explosions.

Hydrogen leaking and detection - Hydrogen is odourless, colourless and tasteless, so the hydrogen leakages become very difficult. Upon the fact that hydrogen rises at a speed of 45 mph (20 m/s) [140], in case of a leakage, it would quickly rise up from ground to the roof. In industry, hydrogen sensors are widely used to detect hydrogen leakage and have so far

maintained a high safety record for many years. Alternatively, researchers are investigating to add odorants which can be detected by human without contaminating the fuel cell [141].

Flammability - Hydrogen has a very wide range of flammable concentrations in air, typically from 4% to 75% by volume. As a result, the release of hydrogen presents a larger probability of ignition than other gaseous fuel.

Ignitability - The hydrogen-air mixture can be ignited either by a spark or by heating the mixture to its auto ignition temperature. The minimum spark energy required for the ignition of hydrogen in air is as low as 0.02 MJ (10 times less than petrol vapour), so even an electricity spark produced by the human would be sufficient to ignite hydrogen. When it burns, the flame is pale blue which is nearly invisible in the daylight.

High pressure tank - The high pressure generally causes public concern about hydrogen safety. One may consider the hydrogen tank as an 'hydrogen bomb' prejudicially although the advanced Carbon fibre reinforced 10,000-psi tanks have demonstrated a 2.35 safety factor (23,500-psi burst pressure) as required by the European Integrated Hydrogen Project specifications. To further ensure the safety, these tanks undergo a series of testing including cycling, dropping, shooting with a rifle, burning, and exposing to acids, salts, and other road hazards to validate that they are safe even under severe and even unusual conditions [142].

Hydrogen Embrittlement - Hydrogen could embrittle metal and non-metallic materials, such as steel and plastics, this is a potential hazardous phenomenon. It consists of the penetration

of hydrogen into the molecular structure the material. Consequently, it causes a severe loss of strength of the material and the possibility of catastrophic ruptures of hydrogen containment systems. This makes it more challenging to design equipment, materials, seals, valves and fittings for high pressure hydrogen use, such as 350 bar.

Healthy and Environment risks - When risks to public health are considered, all sources agree that hydrogen is a non-toxic and a non-carcinogenic compound, thus it does not present any concern for medium- or long-term health implications [143]. When hydrogen is substituted for hydrocarbon fuels in the energy and transportation sectors, it will improve air quality and, consequently, benefit public health. Currently, hydrogen is present in the atmosphere at about 500 ppb (parts per billion) as a mole fraction, which is very likely to be increased with development of Hydrogen Economy. To add to this, hydrogen is not a greenhouse gas itself, but several recent investigations have addressed it may cause indirect greenhouse effects if released in large amounts into the atmosphere, by affecting the chemistry that rules the overall cycle and budgets of greenhouse gases [144-147].

To summarise, hydrogen has been safely used for many years around the world and although there have been some very tragic accidents caused by improper hydrogen use, the dangers and phenomena are now very well-understood and gradually will be well recognised by the public. With appropriate safety measures, hydrogen can be handled safely. The continued safe usage of hydrogen will change public attitude and perception to the Hydrogen Economy as a whole thereby convincing the mass market to accept hydrogen as a possible fuel for vehicular applications in the nearest future.

3.5 Conclusions

Hydrogen provides the potential to develop a more sustainable transport system. The use of hydrogen as long-term replacement for hydrocarbon fuel for transportation is technically feasible, including both H₂ICEs and HFCVs. H₂ICEs are more efficient than conventional petrol-fuelled engines while generating much less toxic and GHG emissions. However the improvement is not sufficient to offset the limitation of hydrogen storage systems, it is yet a bridging technology at current stage. As the H₂ICEs normally allow bi-fuel operations - the engine can run on both petrol and hydrogen. This makes the start-up of a hydrogen infrastructure much easier and the experience gained from it can be directly translated to fuel cell vehicles in the future. Fuel cells operate with much higher efficiency than IC engines, especially at partial loads, however they are limited by high cost and poor durability.

Finally, it should be emphasised that although hydrogen used in fuel cells seems to provide a promising option for a sustainable transport system, it still has to overcome many barriers. This is similar to other alternative technologies, such as Battery Electric Vehicles.

4. Chapter Four

Hydrogen and Fuel Cell Hybrid Scooter with Plug-In Feature - An Early Project⁷

⁷Chapter 4 is based on the published paper “Hydrogen fuel cell hybrid scooter (HFCHS) with plug-in features on Birmingham campus” in International Journal of Hydrogen Energy.

4.1 Introduction

Petrol and diesel powered scooters are popular means of transport in many countries such as in Southern Europe, Asia and South America. This is mainly due to limited space and high population density in large cities [148]. Combined with this is affordability, in an area of the world where the average GDP per person per country is 10% or less of European countries, scooters are a more affordable options than automobiles [149]. For example, there are also issues with the infrastructure in urban Asian cities; the typical city layout does not support an extensive transport support network, as well as a lack of parking space. Scooters are therefore more popular as they can manoeuvre around traffic more easily than larger vehicles, especially if there is congestion. However, scooters are different from cars as they are normally not equipped with advanced engine management and catalytic converter systems to reduce harmful emissions. It has been shown by Sripakagorn and Limwuthigraijirat [150] that conventional petrol motorcycles emit 95% more pollution than larger sport utility vehicles due to the lack of emission control technologies not available on motorcycles.

A commercially available 'pure' lead-acid battery electric scooter (GOPED) [151] was converted to a hydrogen fuel cell hybrid scooter (HFCHS) in order to investigate the effect of hybridisation on driving duty cycles, range, performance, recharging times, well-to-wheel CO₂ footprint and overall running costs.

4.2 Experimental Methods

The electric scooter used for these experiments was a modified 2008 Go-Ped ESR750H [151]. The original scooter had four batteries powering a 24V brushed DC electric motor with “Electro Head” finned heat sink capable of producing over 1HP in continuous operation and reaching a top speed of 20 mph. The manufacturer claims that the maximum riding range is 8 miles in ideal conditions (flat ground, no stops). The modification of the scooter - HFCHS was designed for riding in the University of Birmingham campus with a speed limit to 20 mph and a variety of up hills and down hills. In order to choose the appropriate fuel cell stack, the average cruising power needs to be calculated (assuming a cruising speed of 15 mph).

4.2.1 Theory

There are two forces opposing the motion of a vehicle, namely: the rolling friction force and the air resistance force. A typical μ_r (rolling resistance coefficient) value for a properly inflated scooter on hard pavement is 0.015. The scooter with auxiliary has a mass of 57 kg plus rider 80 kg and a weight of $(57 \text{ kg} + 80 \text{ kg}) (9.81 \text{ m/s}^2) = 1343.97 \text{ N}$, and so the resisting force of rolling friction on a level road (where the normal force $n = mg$) is:

$$F_{roll} = \mu_r n = (0.015)(1343.97\text{N}) = 20.16\text{N} \quad (1)$$

where this force is nearly independent of the car speed.

The air resistance force, F_{air} , is approximately proportional to the square of the speed as shown in Equation (2):

$$F_{air} = \frac{1}{2} C A \rho v^2 \quad (2)$$

where C is the drag coefficient which depends on the shape of the moving body, A is the silhouette area of the vehicle (seen from the front), ρ is the air density (ca. 1.2 kg/m^3 at sea level and STP) and v is the scooter speed. Values of C for a typical scooter range from 0.60 to 1.3 [152]; in our conditions, the Go-Ped is not aerodynamic due to its design hence assume $C = 1.3$ and $A = 0.6 \text{ m}^2$. The maximum speed of this scooter is 20 mph (8.94 m/s) with an air-resistance force of 37.41 N as shown in Equation (3):

$$F_{\text{air}} = \frac{1}{2} C A \rho v^2 = \frac{1}{2} (1.3) (0.6 \text{ m}^2) \left(\frac{1.2 \text{ kg}}{\text{m}^3} \right) \left(\frac{8.94 \text{ m}}{\text{s}} \right)^2 = 37.41 \text{ N} \quad (3)$$

Here, the inertia of the vehicle is negligible, therefore in an ideal condition, the total force required to power the scooter is shown in Equation (4):

$$P = (F_{\text{roll}} + F_{\text{air}})v = (20.16 \text{ N} + 37.41 \text{ N}) \left(\frac{8.94 \text{ m}}{\text{s}} \right) = 514.68 \text{ W} \quad (4)$$

The total power train efficiency is 80% (including motor and drive chain), the maximum power required is therefore 650W, slightly less than the motor rated power. Hence based on our calculations, a 500W PEMFC stack is sensible for our HFCHS in normal ride condition, where full power 650W not always required.

4.2.2 Components

PEMFC Stack - A 500W air cooled PEMFC (Horizon Fuel Cells) [153] of a maximum efficiency of 40% at 21 VDC with a maximum current output of 24A was used (Figure 4.1). This stack consists of 36 cells with a rated hydrogen consumption of 6.5 L/min. It has an external 12V battery power source to supply the hydrogen inlet valve, hydrogen purging valve and cooling fans.

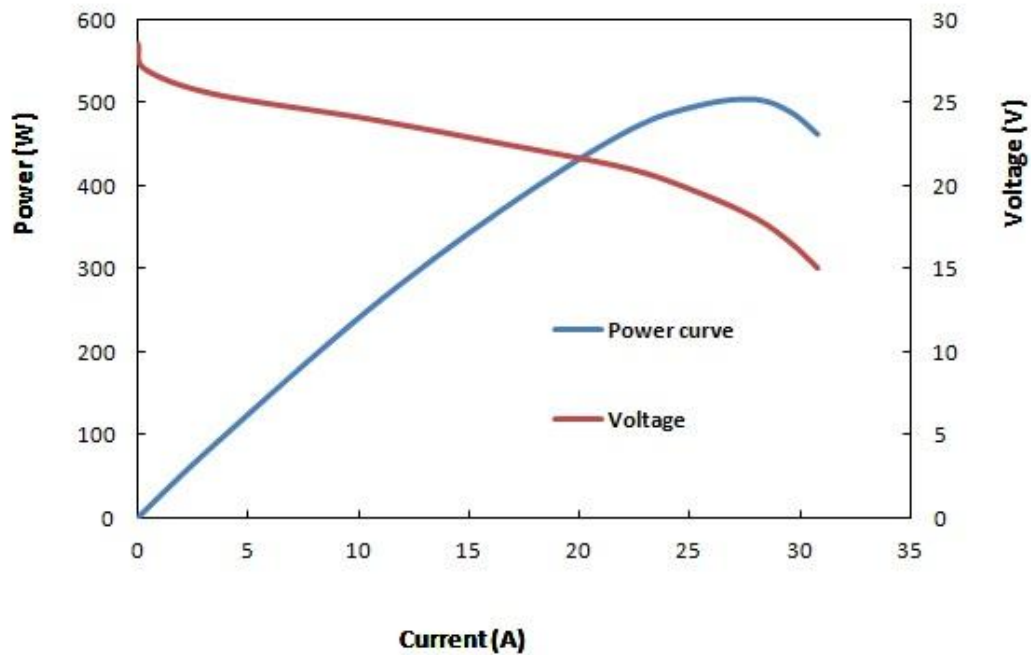


Figure 4.1 Horizon Fuel Cell 500W PEMFC stack characteristics showing cell voltage and power vs. current.

Hydrogen Storage - Two Highland metal hydride cylinders [154] were used to store 600NL pure hydrogen with a discharge pressure of 0.3 bar and a flow rate of 2-3 NL/min at 20°C. The metal hydride storages could take up to 54 grams of hydrogen which contained 1.8kWh energy. The metal hydride storages were connected to the PEMFC stack via a pressure regulating valve to control the pressure output. The cylinders were attached on the top of the motor in order to use the motor heat to boost the hydrogen release, as well as to cool down the motor temperature.

Battery - Four 12VDC lead-acid rechargeable batteries were fitted under the board. Two batteries were connected in series and then paralleled with two others. These batteries had a total power of 576Wh, capable of discharging a maximum current of 360A in 5s. The battery discharge characteristics at room temperature are shown in the Figure 4.2. The

batteries also continuously supplied 15W power to the PEMFC stack controller through a 24V-12V DC-DC converter.

HR SERIES BATTERY DISCHARGE CHARACTERISTICS (25°C/77°F)

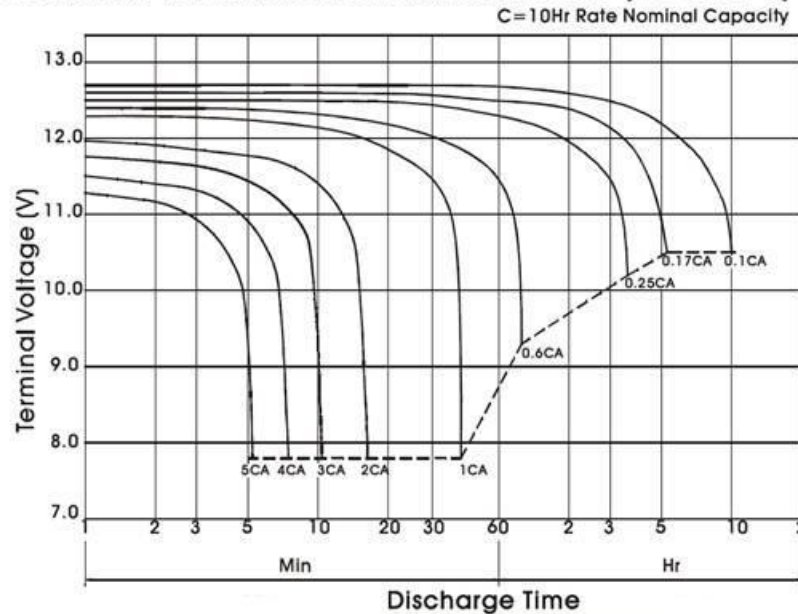


Figure 4.2 12V lead-acid discharge characteristics showing voltage vs., discharge at various amperages and at 25°C [155]

Motor - The 24V DC brush type motor with aluminium heat sink of 80% efficiency was capable of producing 1,000W of power in continuous operation and up to 3,000W in short period of times.

4.2.3 Data collection

In order to determine the range and performance of the HFCHS under different driving conditions, data logging was performed. The speed, power and range of the HFCHS were logged for each experiment. The current was monitored using a current clamp adaptor (TECPEL CA1000D) connected to a data logger (Grant Squirrel 2010) under driving. The power output from the PEMFC stack was also logged.

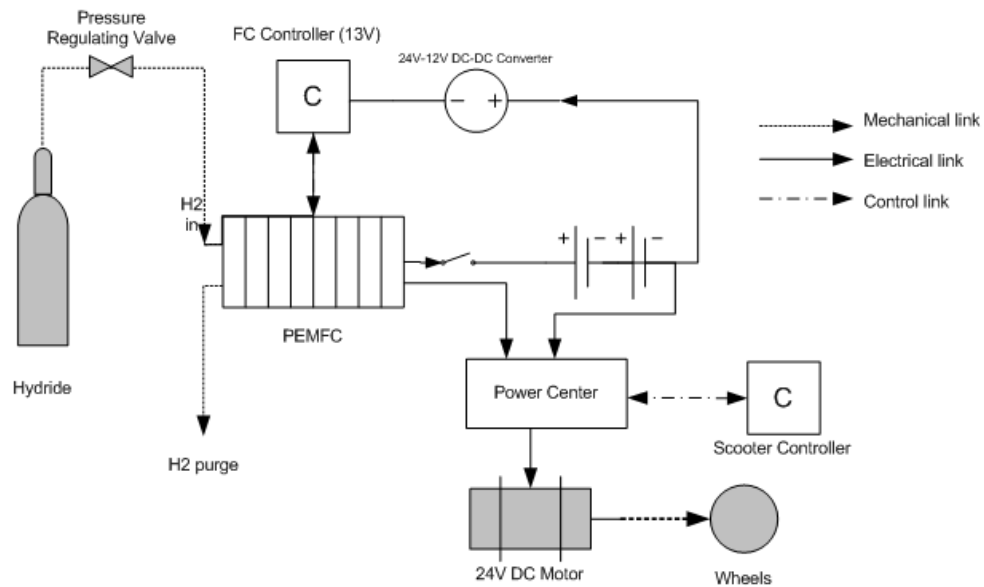


Figure 4.3 Component diagram of the HFCHS showing all components.

A GPS logging system (Racedrive 2090) was also installed on board the HFCHS to monitor speed and distance ran. The GPS results combined with the power data allowed clear indication on how the power train performed. Figure 4.3 and 4.4 shows the system integration and components.



Figure 4.4 Photo of the HFCHS.

4.2.4 Modelling

In order to validate functionality of the concept, a mathematic model has been built to preview the performance of this hybridization using the following parameters, as shown in

Table 4.1.

PARAMETERS		
$m =$	57	vehicle mass (kg)
$m_G =$	137	mass incl. driver (kg)
$P_{Tot} =$	0.8	total power available (kW)
$\eta =$	88%	vehicle transmission efficiency
$P_{Wheels} =$	0.704	power delivered to the wheels (kW)
$C_D =$	1.3	coefficient of drag
$A_f =$	0.9	frontal area (m ²)
$C_dA =$	1.17	(m ²)
$h =$	0.2	height of the centre of gravity (m)
$L =$	1.2	wheelbase length (m)
$WD_f =$	20%	weight distribution (front)
$f_o =$	0.015	rolling resistance coefficient
$f_1 =$	6.25E-05	rolling resistance coefficient
$\rho =$	1.2	air density (kg/m ³)
$g =$	9.80665	gravity (m/s ²)

Table 4.1 Parameters used to build modelling

The mathematical results show on Figure 4.5 clearly shows the performance is excellent, presenting an acceleration rate which of 2.26 second to 10mph and 27.13 second to top speed 20mph.

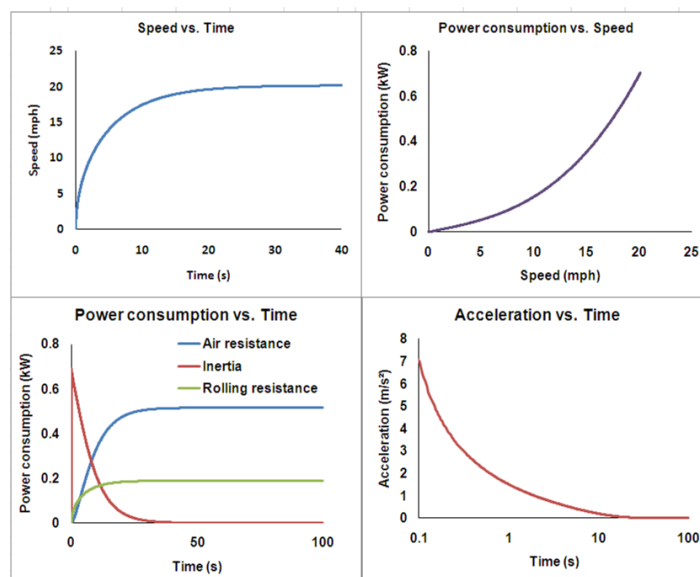


Figure 4.5 Mathematical Performance of modelling.

4.3 Results and Discussion

4.3.1 Hybrid with Low State of Charge (SoC)

Figure 4.6 shows the performance of the HFCHS when driving at low battery level (SoC = 20%). The green plot shows the speed of the HFCHS with time where an average speed of 8-10 mph is achieved. The motor current was between 20A-30A (blue plot) giving a motor power demand of 480W-720W. The pink plot represents the current output from the PEMFC stack, starting from 12A and gradually increasing up to 18A, giving a power output of 250W-380W. The figure also shows that the power demand from the motor is higher than the power output from the PEMFC stack, and the extra power required comes from the batteries. For this experiment, the run lasted for 42 mins before the PEMFC stack cut off due to the lack of hydrogen in the cylinders.

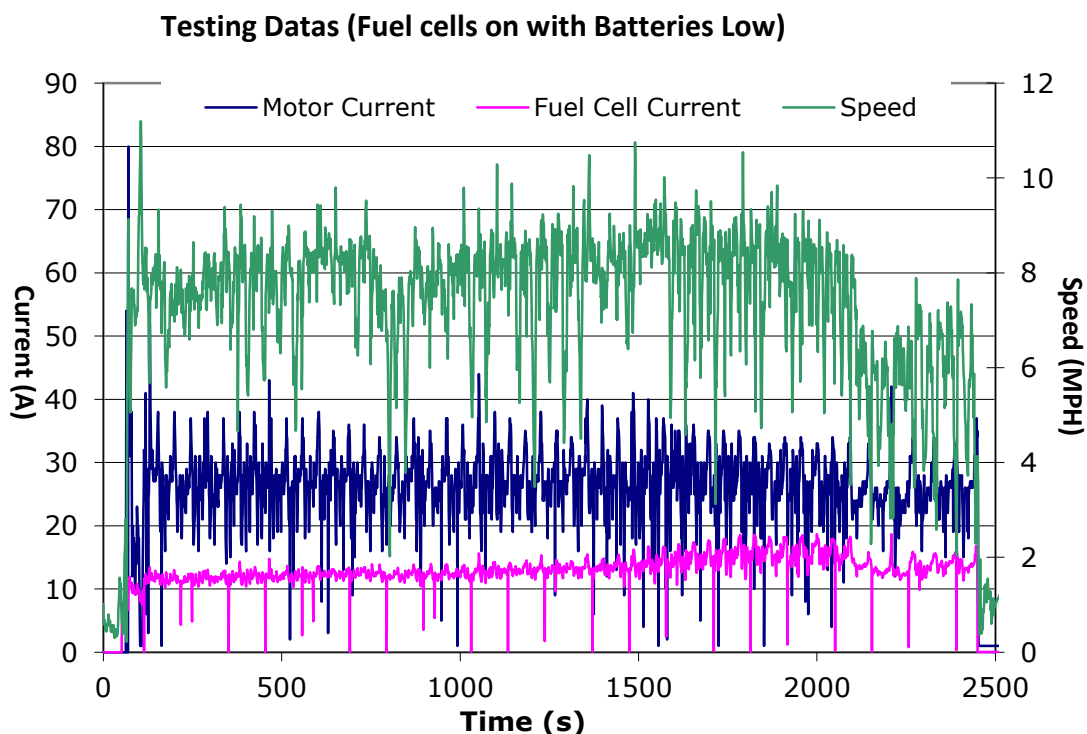


Figure 4.6 Performance of HFCHS when the batteries are low [SoC = 20%].

4.3.2 Hybrid with High SoC

Figure 4.7 shows the performance of the HFCHS when driving at full battery level (SoC = 100 %). Here, the batteries were fully charged in 5 hours. In our conditions, the average speed was approximately 8 mph with again, a motor power demand of 480W-720W. Unlike the previous tests at low battery level (20% SoC), the PEMFC stack power output varied between 200W-320W, in other words less power was required from the stack at full battery SoC. This test lasted longer i.e. 1 hour 7 minutes. Obviously, during these experiments, the PEMFC stack functioned below its rated maximum power, possibly due to the following reasons: a) the metal-hydride canisters cannot supply enough hydrogen to the stack, b) the power demand is low or c) lack of power management system. This is further explained below.

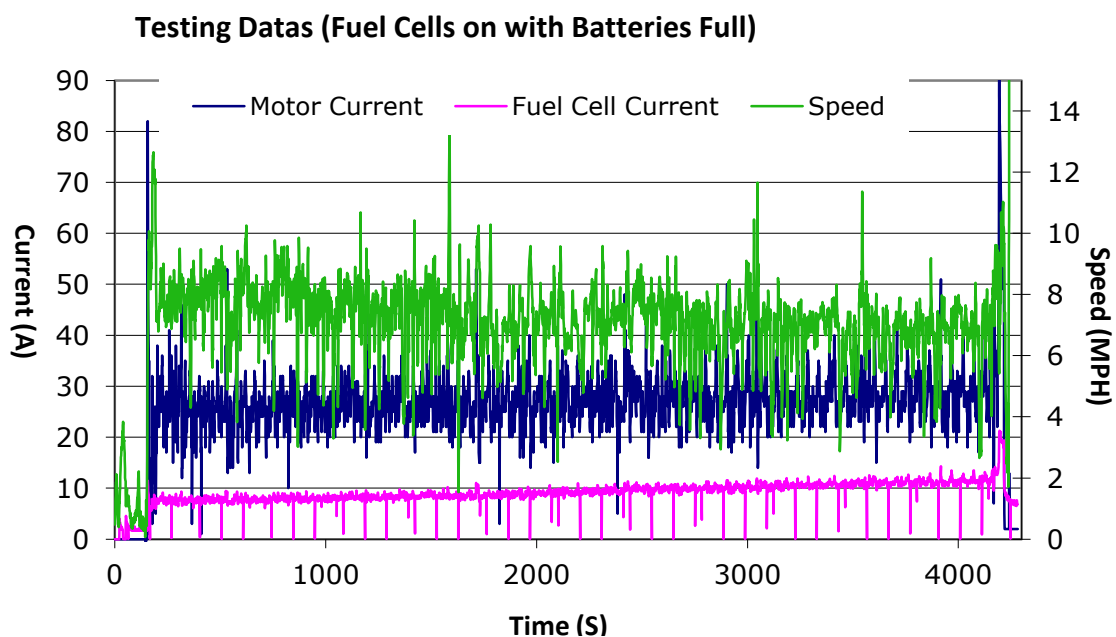


Figure 4.7 Performance of HFCHS when the batteries are fully charged [SoC = 100%]

4.3.3 Hydrogen Supply

The metal-hydride canisters were 'charged up' directly from high purity hydrogen (99.999%) at a pressure of 10 bar. It took 20 mins for full charge at room temperature but only 12 mins at 0°C (ice-water bath) at 25 bar. The PEMFC stack consumes 6.5 litre hydrogen per minute to reach a maximum power of 500W, however, in this testing conditions; the metal hydride canisters only supplied 2-3L/min of hydrogen at room temperature. Although the metal-hydride canisters were placed onto the 'hot' motor to gain some heat, this design didn't seem to work to achieve a minimum flow rate of 6.5L/min to the stack; for example, the metal-hydride canisters surface temperature dropped from 30°C to 0°C in 20 minutes, and at this point, the flow rate dropped even further.

4.3.4 Power Management

As seen from Figure 4.6 and Figure 4.7, the PEMFC stack always functioned below its optimum power due to the lack of advanced power management systems. For example, the motor withdraw power from the highest voltage power source first, in this case the lead-acid batteries are at 22 V (Figure 4.2), compared with 18 V for the PEMFC stack. In our conditions, by using a DC-DC converter, the load is higher than the fuel cell rated power and the batteries work in order to provide the power needed to satisfy the load.

	Go-Ped FC Plug-in	Go-Ped Plug-in	Go-Ped (29 cc)
Vehicle Cost	£3,000	£1200	£800
mpg Equivalent	500mpg (H ₂)	383mpg	100mpg
Energy Efficiency	37%-75%	75%	20%
Tail-Pipe Emission	None/H ₂ O	None	Harmful Air Pollutions
Well-to-Wheel CO₂	9.37-40.95 g CO ₂ /km	42.4 g CO ₂ /km	90-120 g CO ₂ /km
Running Cost on Fuel	£0.01-£0.11/Mile	£0.01/Mile	£0.06/Mile
Refuelling Time	15 Minutes - 5 Hours	5 Hours	1 Minute
Range	15 miles	8 miles	32 miles
Top Speed	25.8 mph	20 mph	24 mph
Noise Level	55 db	55 db	75 db

Table 4.2 Summary of fuel cell hybrid, battery and petrol powered scooters characteristics.

Even with the lack of power management systems, the range of the HFCHS was 15 miles after 70 mins riding at a top speed of 25.8km/h. For comparison purposes, experiments on ‘pure’ battery and petrol scooters were performed as shown in Table 4.2. The table shows that HFCHS offers many advantages over electric and petrol scooters, for example, higher energy efficiency (up to 75%), lower running costs, higher speed and better MPG equivalent. For example, using two 600NL (0.054 kg) hydrogen metal hydride canisters give an energy of 1.8kWh and a 40% efficient PEMFC stack gives a total energy of 0.72kWh which is higher than battery only powered and lower than petrol powered scooters of 0.42kWh and 1.71kWh respectively. However, the estimated cost of the HFCHS is much higher than that of the pure electric and petrol scooters. For example, the donor vehicle Go-Ped cost around £1,200 (inc. seat and basket kit), the 500W PEMFC stack costs ca. £1,200, the Highland metal hydrides cost approximately £500, and other components like DC-DC converters, and switches cost approximately £50. The total cost of this HFCHS is ca. £3,000 compared with only £800 for the pure electric Go-Ped. Furthermore, well-to-wheel CO₂ footprint values showed that the HFCHS gives a total of 9.37 g CO₂/km to 40.95 g CO₂/km depending on where the hydrogen comes from (Table 4.3).

H ₂ Source	[g CO ₂ /kg H ₂]	Total CO ₂ produced [g]	Total Carbon Emission [g CO ₂ /km]
Steam Methane Reforming (SMR)	11374.90	614.24	40.95
Solar	3804.00	205.42	13.69
Wind	2604.00	140.62	9.37
Hydro	3324.00	179.50	11.97
Biomass	4284.00	231.34	15.42

Table 4.3 Well-to-wheel carbon Footprint from different energy sources.

4.4 Conclusions

To conclude, the range of the scooter has been extended and the top speed has been increased by adding the fuel cell and hydrogen store. There are several advantages over the traditional scooter in terms of mpg equivalent, energy efficiency, tail-pipe emission also the well to wheel CO₂ footprint, and lower running cost compare to petrol Go-Ped.

These findings give a more clear idea about the fuel cell and battery hybridisation and can give an insight into FCHV. The technology and experience gained from this project also transferred to local SMEs (Valeswood Fuel Cell Ltd and Spencer Ashley Ltd), who built a similar HFCHS for a Royal Institute Lecture, as seen in Figure 4.8.



Figure 4.8 Scooter built for Royal Institute Lecture

5. Chapter Five

Novel Hydrogen PEM Fuel Cell and Battery Hybrids without DC-DC Converters⁸

⁸ Chapter 5 is on the basis of the published paper “Hybrid Hydrogen PEM Fuel Cell and Batteries without DC-DC Converter” in International Journal of Low-Carbon Technologies.

5.1 Introduction

The Hydrogen Fuel Cell Electric Vehicle (HFCEV) is generally recognised as one of the optimum technologies for long term future low carbon automobiles [10, 22, 156, 157]. This combines the Proton Exchange Membrane (PEM) Fuel Cell (FC) stack with a battery and electric drive train to optimise the starting time, operating temperature and efficiency of the vehicle [158]. Using PEM fuel cells to generate electricity from high purity hydrogen; the electricity could drive the electric motor of the vehicle or be stored in the energy storage device, either battery or ultra-capacitor. Since fuel cells generate electricity via chemical reactions, no pollutants will be produced and much less heat is generated compared to an internal combustion engine. The by-product of a hydrogen fuel cell is only water vapour for PEMFC [159]. Fuel cells have few moving parts and are fabricated by stacking repeatable components together; hence they have the potential for high reliability and low manufacturing cost.

PEM fuel cells are best operated at a constant load in order to achieve peak efficiency and maximum lifespan [160], whereas the power required for the automobile varies substantially, because of the variety of accelerations and decelerations under real-life driving conditions. However, a battery can accommodate these dynamic power changes better, while also capturing the braking energy using electromagnetic deceleration [161]. Hence the HFCEV not only solves the problem, but also offers additional benefits:

- Smaller fuel cells stack therefore lower cost.
- Fuel cells stack can operate at optimum efficiency most of the time.
- Fuel cells stack lifetime is extended.

- The fuel cells stack designer is able to optimise the cells for power efficiency instead of cycle life.
- Deep discharging from the battery is eliminated, therefore improving the batteries' lifetime.
- Fast start-up of the fuel cell stack.
- Improves power train efficiency through capture of regeneration energy.

In general, there is a difference between the FC stack voltage and battery voltage, and a DC-DC converter is required in this hybrid system. According to a study of the Micro-Cab HFCEV, nearly 20% of energy generated by the FC was lost through this DC-DC converter [162], mainly because the DC-DC converter obtained its peak efficiency at full load, which is rarely achieved in real driving cycles, especially under urban drive cycles which involved many stops. To minimise this power loss in the DC-DC converter, the present project aimed to match the fuel cell, the battery pack and the electric motors, in a 48V system.

5.2 Experimental Methods

The experiments comprised a bench tests to examine the PEMFC hybrid with both Lead-Acid (PbA) batteries and Li-Ion phosphate (LPB) batteries with a Battery Managing System (BMS) under different State-of-Charge (SoC) and load conditions. In order to investigate the fuel cell performance, rate of battery charging, State-of-Charge of batteries (SoC) and power distribution character from both batteries and fuel cells, the bench test was developed with three electric loads to simulate the electric motor.

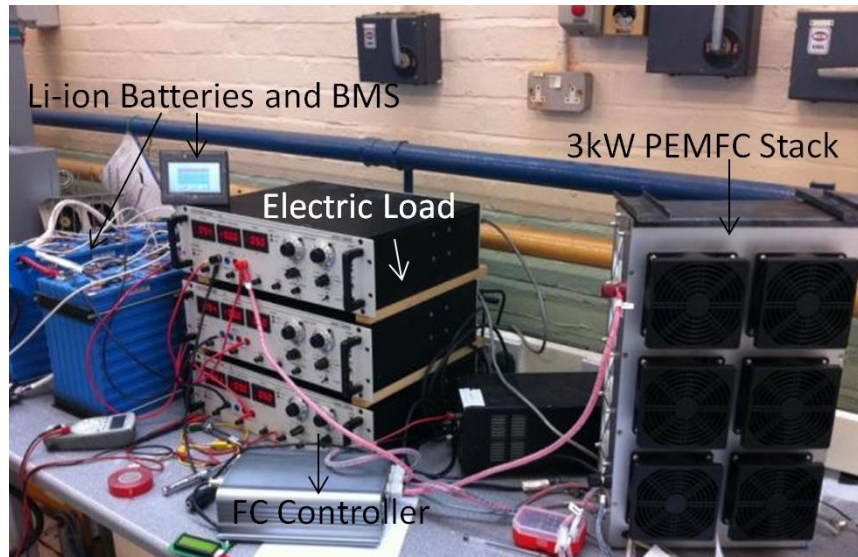


Figure 5.1 Configuration of the FC and batteries hybrid system

Equipment	Specifications
FC Stack	3 kW PEM, Self-humidified
Load	3 x 1 kW Electric Loads
Peak Power Source (PPS)	4 x 12V 22 Ah Sealed Lead Acid batteries
	16 x 3.4V 180 Ah Li-ion Phosphate batteries with BMS
	15 x 3.4V 180 Ah Li-ion Phosphate batteries with BMS
H₂ Supply	99.999% purity H ₂ at 0.55 bar

Table 5.1 Bench test components and specifications

Figure 5.1 shows the bench test configuration of the hybrid system. Table 5.1 shows the equipment used and its specifications. The fuel cell stack and batteries were connected in parallel. The FC stack may not only supply power to electric loads but also charge batteries at the same time when needed. Also, the batteries may assist the FC stack to supply extra power to the electric loads when required. The power flow relies solely on the voltage difference. The current flow between them will be examined.

The testing procedures were as follows:

1. Charge/discharge the batteries to the required SoC.
2. Turn on the FC, start to withdraw current from it after it is fully started.
3. Increase the electric load by 50W with every 15 second interval.
4. Record the voltage, current and temperature of electric loads, FC and batteries where applicable.

5.3 Results and Discussion

5.3.1 Hybrid with 4 x 12V Lead-Acid Batteries

Firstly, the 3 kW Horizon PEM fuel cell [153] was connected with 4 x 12V Valve Regulated Lead-Acid (VRLA) batteries, connected in series to provide the nominal voltage of 48V and total energy capacity of 1kWh. The lead acid battery has high specific power and is capable of producing high power for short periods of time (e.g., during maximum acceleration in an automobile). In addition, its low cost, reliability and highly recyclable character make it a good option as Peak Power Source (PPS), despite its heavy weight [163].

Figure 5.2 shows the fuel cell stack output against the electric loads when hybridised with these batteries at different SoC from 20% to 100%. It can be seen that different SoC of batteries share a similar trend; the FC stack output gradually increases along with the electric load increase, at the same time, the FC stack charged the lower SoC batteries more rapidly than higher SoC batteries. For instance, with the battery's SoC at 20%, the FC stack charged the batteries up to 25.88A at the beginning of the experiment, then steadily decreased as the electric load increased, to approximately 1A at the end of the test (see Table 5.2). In this experiment, no current flowed from the batteries to the electric loads

during whole process; the FC stack not only supplied the required power to the electric loads, but also charged the batteries continuously. This was because the battery's voltage was too low to provide any electrons to the electric loads, compared to the FC stack at the same point. As a result, the battery pack had been charged 164.8Wh by the fuel cell stack during the 15 minute experiments and the SoC increased by 16%.

Batteries SoC	20%	50%	80%	100%
Maximum Charged/Discharge rate	+25.88 A	+16.64A	+3.43A	+0.5A
Minimum Charged /Discharge rate	+1.02A	-8.16A	-6.06A	-9.8A
Charge/Discharge Turning Point	N/A	Load to 2100 W	Load to 1800 W	Load to 1350 W
Change of Capacity	+164.8 Wh	+64 Wh	+13.6 Wh	-9.8 Wh
Change of SoC	+16%	+6%	+1%	-1%
Change of Voltage*	54V-48V	55V-49V	61V-50V	64V-50V
Fuel Cell Temperature	24 °C -42 °C	22 °C -39 °C	22 °C -38 °C	21 °C -36 °C

Table 5.2 Results from FC stack hybrid with 4 x 12V PbA batteries at 20% SoC, 50% SoC, 80% SoC and 100% SoC

*- True voltage under load condition, not open-circuit voltage, data from electric load display.

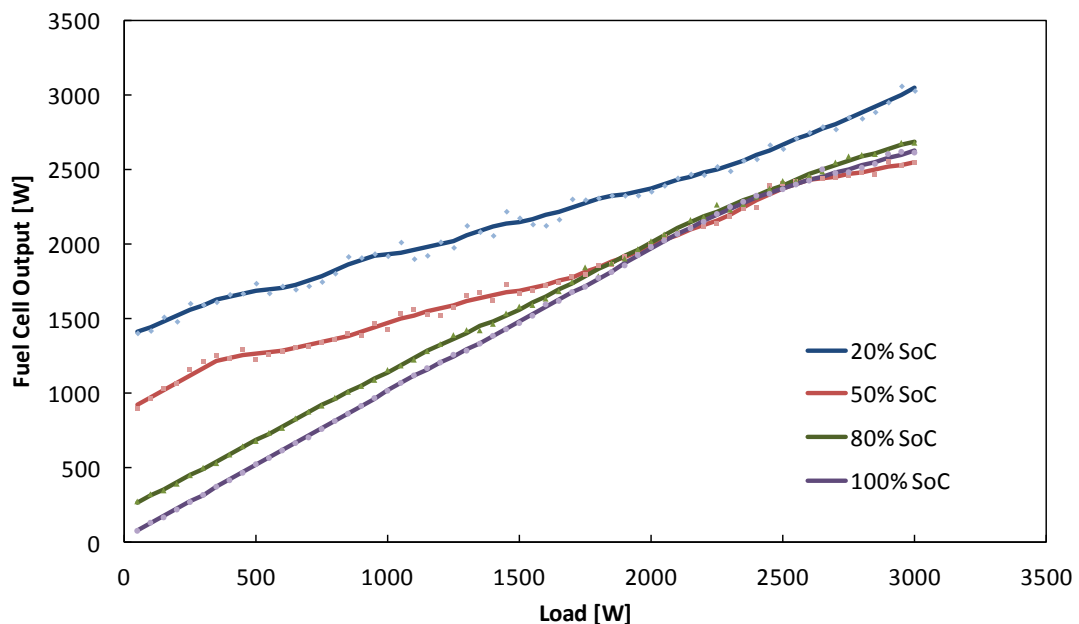


Figure 5.2 Fuel cell stack output against electric load when hybrid with 4 x 12V lead acid batteries

When battery's SoC is 100%, the FC stack provides power to the electric loads by itself until the load is greater than 1300W, then the battery pack starts to provide a small amount of

power to assist the FC stack, see Figure 5.3. This is not because the FC stack cannot supply the extra power, but because the battery's voltage is now higher and able to share some of the load; the batteries shared 370W out of 3000W when approaching the end of this experiment. Consequently, the battery pack lost 9.8Wh of energy and its SoC decreased by 1%. The FC stack output was lower in this test and therefore the temperature change was relatively small too.

Not surprisingly, most results from 50% SoC and 80% SoC are between low 20% SoC and high 100% SoC discussed above; they had both been charged by FC stack at the beginning while the electric load was small, and both assisted the FC stack when the electric load was high.

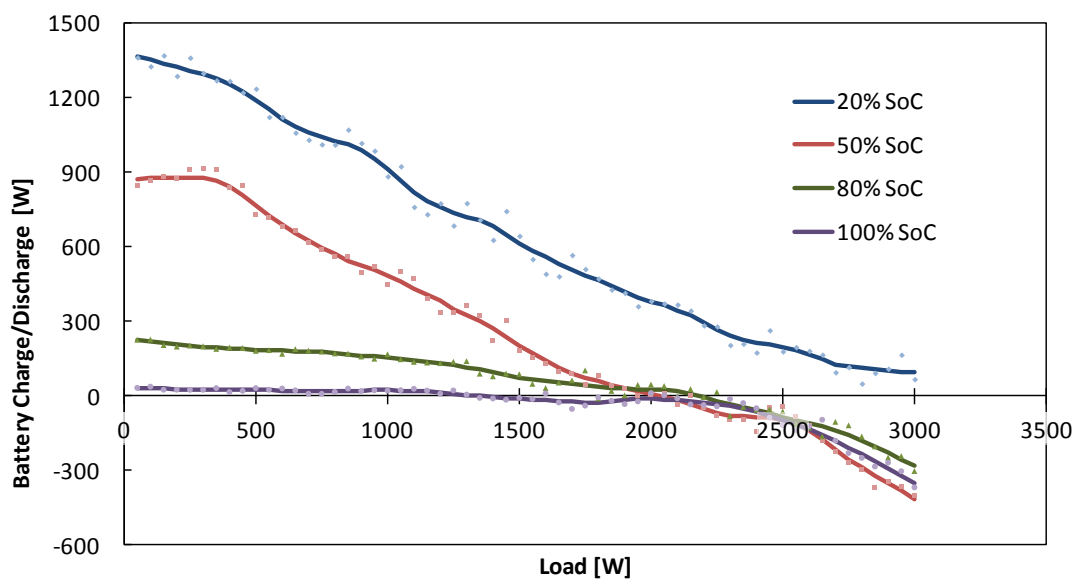


Figure 5.3 Change of battery power distribution against electric load with 4 x 12V lead acid batteries

5.3.2 Hybrid with 16 x 3.4V Li-ion Phosphate Batteries (LPB)

Lithium-ion batteries are the fastest growing and most promising batteries for automobiles [164]. Lithium is the lightest of all metals, has the greatest electrochemical potential and

provides the largest energy density by weight. There are many types of lithium based batteries with different cathode materials, such as lithium cobalt oxide, lithium manganese oxide, lithium nickel oxide and lithium iron phosphate. It is believed that the lithium ion phosphate battery is the best option for automobile application owing to its high safety factor [165]. In addition, it does not include noble elements such as cobalt, hence the price of raw materials is lower and both phosphorus and iron are abundant on earth which lowers raw material availability issues. Nevertheless this battery's cathode is heavier and its capacity is about 25% less than other lithium batteries per unit weight [166, 167]. However, for automobiles, the top priority is safety rather than capacity. The LPB cells used in this experiment have a nominal voltage of 3.4V per cell and 180 Ah capacities, and with 16 cells the LPB pack could supply more than 9 kWh of energy at 54.4V. This capacity is 6 times higher than that of the PbA batteries, which were capable of producing high power for longer periods of time.

With the Battery Managing System (BMS), this LPB pack can be tested at any precise SoC: for comparison purpose, 5% SoC, 20% SoC, 50% SoC, 80% SoC and 100% SoC have been tested. At the beginning of the testing for low SoC, it was observed that the voltage potential between the FC stack and LPB pack is large enough to make the FC output its maximum 3 kW power, and charge the batteries at the rate of 62.5A. Although the LPB could take such a high current, heat would build up quickly due to the high current flow and the battery's life may be affected [168], and with such high demand from the FC stack, its temperature increased dramatically to 42°C at the beginning of the test; hence this circumstance should be avoided

if possible. While approaching the end of this low SoC test, unlike the PbA batteries, the LPB could assist FC stack to provide a small amount of power to electric loads.

When testing the higher SoC, from 20%-80%, it can be seen from Figure 5.4 that the LPB have a similar charge/discharge character, with the FC stack constantly running at the range of 1500W to 2500W, which is within its high efficiency range. In all cases, the batteries provide a reasonable amount of power to electric loads when the requirement is above 2.1 kW. After the tests, the batteries SoC increased moderately by up to 1.7%.

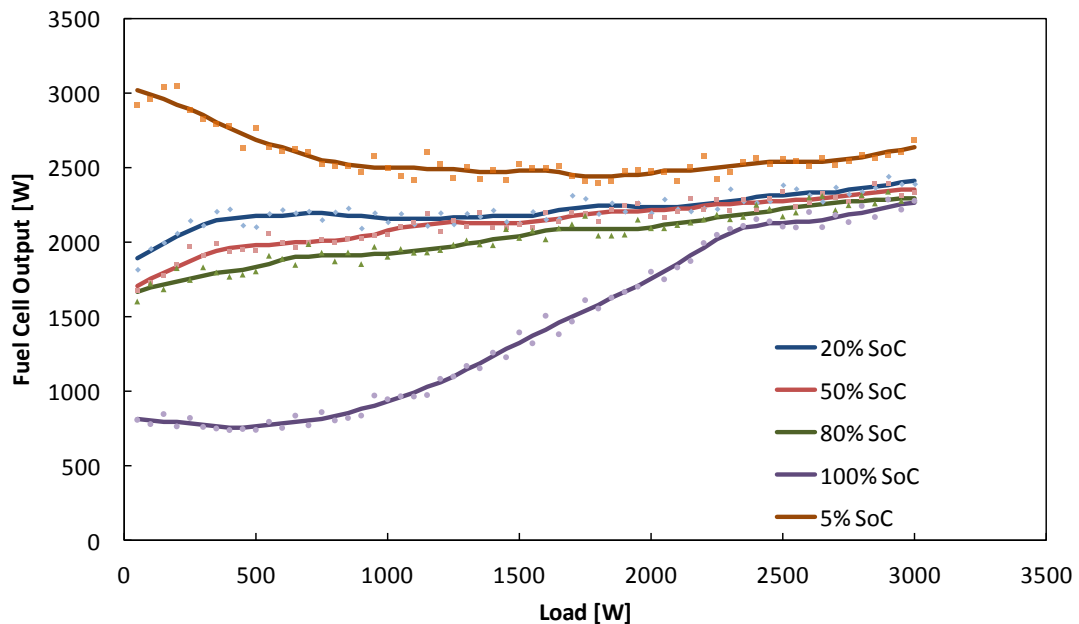


Figure 5.4 Fuel cells stack output against electric load when hybrid with 16 x 3.4V Li-Ion batteries

A fully charged battery was also tested; from Table 5.3 it can be observed that the FC stack still charges the LPB in the beginning, but at a much lower rate of 13.65A. This is because the FC stack has a high voltage of 64V when the electric load was small. Once the electric load was greater than 0.85 kW, the batteries assist the FC stack to provide power to electric loads. As a result, the SoC decreased 0.2% after the test. By estimation, in a real-life vehicle, the

power required is normally greater than 0.85 kW most of the time; hence the SoC should further decrease.

Batteries SoC	5%	20%	50%	80%	100%
Maximum Charged /Discharge rate	+62.6A	+36.68 A	+31.97A	+30.25A	+13.65A
Minimum Charged /Discharge rate	-5.85A	-11.28A	-11.81A	-13.15A	-13.18A
Charge/Discharge Turning Point	Load to 2600 W	Load to 2250 W	Load to 2300 W	Load to 2150 W	Load to 850 W
Change of Capacity	270 Wh	+117.2 Wh	+155.7 Wh	+131 Wh	-22.2 Wh
Change of SoC	+3%	+1.3%	+1.7%	+1.5%	-0.2%
Change of Voltage*	46V-48V	51V-50V	53V-52V	53V-52V	64V-50V
Fuel Cell Temperature	34 °C -39 °C	26 °C -39 °C	24 °C -37 °C	24 °C -37 °C	19 °C -36 °C

Table 5.3 Results from FC stack hybrid with 16 x 3.4V LPB at 5% SoC, 20% SoC, 50% SoC, 80% SoC and 100% SoC

*- True voltage under load condition, not open-circuit voltage, data from electric load display.

5.3.3 Hybrid with 15 x 3.4V Li-ion Phosphate Batteries

After testing the 16 x 3.4V LPB pack, one battery cell was removed and the nominal voltage lowered to 51V. From the previous test, it was proved that lower SoC, such as 5%, should be avoided due to the high current at the beginning. By removing one cell, the voltage difference further increased, causing higher current flow at the beginning. The 5% SoC test was therefore not conducted in this experiment, as well as 100% SoC to avoid LBP over charging. Again from the previous test, it was shown that even when the battery pack was full, the FC stack still charged the LBP at the beginning, as shown in Figure 5.5.

For these reasons, only 20%, 50% and 80% SoC have been tested, yet the results were not satisfactory. This was because for all three cases, the FC stack not only charged the batteries at high current at the beginning, but also over its rated output for most of the time, see Figure 5.5. Furthermore, the batteries were charged from start to end, and were not able to assist the FC stack throughout the whole process. The worst case was at 20% SoC; the FC stack operated over its rated power at all times, and the stack's internal temperature

reached its highest point across all tests of 49 °C. This would reduce the efficiency as well as shorten the stack life span. In addition, Table 5.4 shows 443.7 Wh of energy was transferred to the batteries in 15 minutes. In fact, 70% of that energy was transferred during the first 5 minutes while the electric load was small; this rapid energy transfer would also reduce the battery life if it occurred frequently [168].

Batteries SoC	20%	50%	80%
Maximum Charged/Discharge rate	+60.93 A	+55.82A	+53.36A
Minimum Charged /Discharge rate	+9A	+4.63A	+1.55A
Charge/Discharge Turning Point	N/A	N/A	N/A
Change of Capacity	+443.7 Wh	+398.2 Wh	+367.5 Wh
Change of SoC	+5.3%	+4.8%	+4.4%
Change of Voltage*	50V-49V	51V-49V	51V-50V
Fuel Cell Temperature	29 °C -49 °C	20 °C -46 °C	20 °C -45 °C

Table 5.4 Results from FC stack hybrid with 15 x 3.4V LPB at 20% SoC, 50% SoC and 80% SoC

*- True voltage under load condition, not open-circuit voltage, data from electric load display.

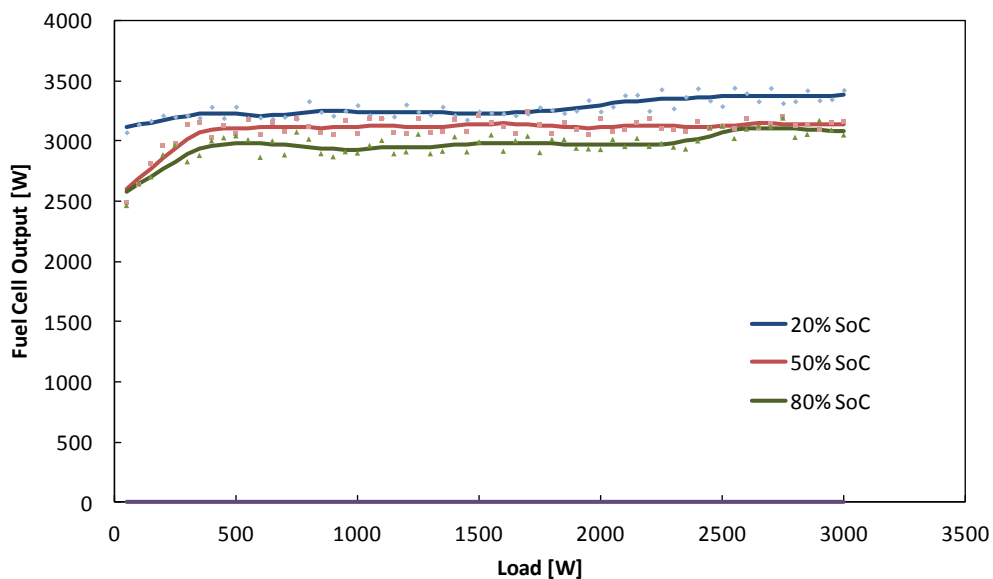


Figure 5.5 Fuel cell stack output against electric load when hybrid with 15x 3.4V Li-Ion batteries

From the test results of hybrid FC with PbA batteries and different LPBs, it is clear that the absence of a DC-DC converter in this hybridisation is not a problem. However, the type, voltage and capacity of the batteries have to be carefully selected for a defined FC stack. As

most commercial PbA batteries are either 12V or 24V, the flexibility is narrower than for LPBs with 3.4V. For example, developing a PbA battery with nominal voltage of 54.4V (with around 26 individual cells), the curve shown in Figure 5.2 would be more constant like that of the LPBs. In other words, the voltage of the batteries and their ability to keep on this voltage would directly determine the FC stack output.

Comparing the FC stack output when hybridised with 15 LPBs and 16 LPBs at 20% SoC, 50% SoC and 80% SoC (Figures 5.4 and 5.5), it can be seen that the curves give a similar trend but in a different range. These LPBs have a stable performance from 20% SoC to 80% SoC when hybridised with this 3 kW PEMFC stack. In terms of the FC efficiency and lifespan, the 16-cell pack is superior to the 15-cell pack, because with 16 cells, the FC output power is maximised at 2.5 kW, irrespective of the SoC.

It is proven that 16 x LPB pack is the best possible solution; this is shown by Figure 5.4 and Table 5.3. Except in the low SoC condition below 20%, the FC stack and batteries work perfectly at all other times. It can be speculated that the battery's SoC may hardly ever be lower than 20% in real life conditions. Because in the low battery SoC situation, the FC stack would provide most of the power before the batteries when the power need is greater than 2.6 kW, while when the power need is low, the FC would replenish the battery at a slower rate than the bench test. Of course, it would be recommended that the batteries are always kept at a higher SoC, controlled by BMS.

To summarise, this 3 kW fuel cell stack is likely to achieve the best efficiency and a longer life span if hybridised with 16 x Li-ion phosphate batteries.

5.4 Limitations

- The PbA battery SoCs were estimated by measuring the cell voltage after the batteries had cooled down, therefore error range is ± 5 V or 10%.
- Battery SoCs were changing continuously during the experiment, because the batteries either had been charged by the fuel cell, or discharged to the electric load.
- The experiment only demonstrated that the fuel cell and batteries could hybridise without a DC-DC converter to reduce energy losses. The power needed in a real vehicle is more complex than this simulation; hence the behaviour of the fuel cell and batteries maybe different.
- The effects on the life cycle in both the batteries and the fuel cell were not investigated.
- This study is limited to a DC power train only, a DC-AC converter will be needed for an AC drive.
- The number of batteries can affect the performance and thus the durability of the components. Further investigation is needed into the component-level design. This system will be trialled on a hydrogen fuel cell hybrid vehicle.

5.5 Conclusions

Improving the energy flow efficiency of HFCEV is crucial, especially whilst all the elements such as hydrogen, the fuel cell stacks and batteries are still very expensive, compared to

conventional vehicles. The efficiency of electrical flows within the system is paramount in electric power train design; eliminating components such as the DC-DC converter not only reduces the cost, but also improve the overall efficiency by simplifying the power train. In addition, fewer components mean less can go wrong in term of reliability. However, absence of this voltage controlling device not only requires matching the voltages of the fuel cell stack, batteries and electric motors, but also requires the components to work effectively with each other. For example, the batteries need to have a matching nominal voltage, as well as an appropriate charge/discharge curve for the fuel cell discharge curve; then this matching system will work as a whole to supply the power to the motor effectively.

In this study, all the components were commercially available and carefully selected to suit this experiment. There is still room for improvement in terms of suitability, because the components could have been designed specifically for automobile use. Optimising the compatibility of fuel cell, battery and motor components could further improve the power train efficiency. To conclude, this simplified approach to a HFCEV without DC-DC converter is workable, and could lead to further improvements in the future.

6. Chapter Six

Study of Micro-Cab H4 Fuel Cell Hybrid Vehicles

6.1 Introduction

The purpose of this Chapter is to describe theory and experiments methodology on the early prototype Micro-cab H4 designed and manufactured by Micro-Cab at Coventry University. This was an innovative design due to its light weight and economic components, but the overall range was poor because of low efficient conversion in the system and lack of regenerative braking.

6.1.1 History of Micro-cab

Starting from a student design project, the founder of Micro-cab Prof. John Jostins has been working on the hybrid urban vehicle designing since 1998. From the early pedal/electric hybrid 3-wheeler model, to the most recent H₂EV hydrogen fuel cell hybrid model, all models have no tail-pipe carbon emission and are potentially to be fossil oil independent; Figure 6.1 shows the timeline of Micro-cab development, ending with the 2012 version which is part of the EU SWARM project (HFC UJ 302485).



Figure 6.1 Development timeline of Micro-cab (courtesy Micro-cab)

6.1.2 UK Automotive - Chance to Re-bounce

The UK has a long history of automotive manufacturing; in the 1950s, UK was the second largest automotive manufacturing worldwide and was the largest vehicle exporting nation. The sales dropped to 12th place by 2008 because of the competition from nations such as Germany, France and Japan. Given the future emerging 'automotive revolution' as introduced in Chapter 1, the UK needs to take positive steps to take advantage of the IC engines to fuel cell changeover, as the conventional IC engines automotive manufacturers are likely to be constrained while the new automotive industry is trending to low carbon vehicle technology orientation, such as the higher involvement of hydrogen fuel cell vehicles (HFCVs) [169].

For the 15 years, Japanese and American auto manufacturers have been leading the development of HFCVs, while the UK was lacking of either major OEMs committed to or extensive hydrogen HFCV R&D projects. But now a consortium of Micro-cab Industries, Delta Motorsport⁹ and RDM Automotive¹⁰ has designed and built five fuel cell vehicles in the West Midlands, named Micocab-H4. This model is the first fuel cell vehicle in the UK, and is positively a significant step towards developing next-generation OEM and supply chain capabilities within the UK.

⁹ Based in Silverstone – specialist engineers developing 'green' chassis and drive train for eco industry, as well as traditional motorsport activity

¹⁰ Tier 1 automotive supply chain company supplying to Jaguar Land Rover, Aston Martin etc. with specialism in electronic and telematic vehicle systems

Five Micro-cab H4 cars were produced as experimental and demonstration vehicles that were to be used on the campus of University of Birmingham, as shown in Figure 6.2. They were delivered to the university in April 2008, at the same time as the UK's first hydrogen fuelling station had been installed on campus by Air Products to provide compressed hydrogen at 350 bar. These projects were part of the Hydrogen Energy Project which has received funding of GBP 6.3 million from regional development agency Advantage West Midlands (AWM) regarding the usage of hydrogen energy as a green fuel, and were also part of the overall Birmingham Science City initiative.



Figure 6.2 Five H4 series Micro-Cab HFCVs in Campus University of Birmingham

6.2 Micro-cab H4

6.2.1 Construction

Improved from previous lightweight concepts models shown in Figure 6.1, the platform of the Micro-cab H4 series was specially designed for hydrogen fuel cell and battery hybrid

drive train; and was the first 4-wheel model in its production line. From the 'engineering design' point of view, there is better flexibility for electric drive train design than IC engines drive train in the vehicle configuration. This is because the electric energy flow is more flexible than mechanical energy flow, the arrangement of components can be kept in minimum volume, and hence more useful space can be achieved compared to similar size conventional vehicles, even though the measurement of H4 series is only 3000 L x 1500 W x 1850 H mm (length, width, height). With the compact electric drive train under the rear seats, the Micro-cab could comfortably carry 4 adult passengers.

The H4 series were initially planned to weigh up to 500kg with lightweight space frame chassis (engineered by Delta Motorsports) and Glass Reinforced Plastic (GRP) body panels. The space frame chassis offers great rigidity and safety, with light weight benefit. Light GRP body panels are ideal for prototype vehicles in small quantities. However, the finished vehicle weighed 667kg as a consequence of the limited budget which restrained the use of lighter components (such as the standard Ford seat with bracket weighs up to 50kg each was chosen, and steel wheels were used as substitution of lighter alloy wheels). In addition, the prohibitive costs of carbon fibre, engineering and tooling have induced major compromise on weights. Furthermore, the effort required for electrical integration of the fuel cell and other vehicle systems was underestimated and a wide range of electrical system revisions has taken place, such as adding additional batteries, power converters, and chassis materials to protect the hydrogen tank and fuel cell. Although the vehicle weight was one-third over the designed target, it was still only half of the weight of today's conventional vehicles with similar carrying capacity [170].

Figure 6.3 illustrates the frame of the vehicle with major components; the lower chassis contains a sandwich structure on the floor to hold the batteries and other electronic device, a steel frame underneath the rear seats is to accommodate the fuel cell stack, hydrogen tank and electric motor. The front space of the vehicle was left empty to enhance crash protection; however it also offers potential for future upgrade, such as to install additional batteries, a secondary fuel cell or hydrogen tank.

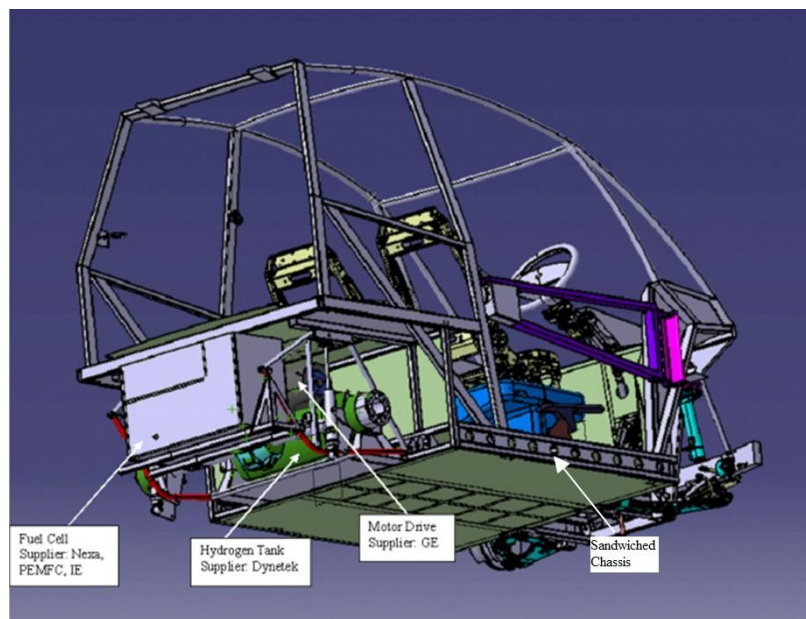


Figure 6.3 Design of frame showing the layout of the fuel cell, hydrogen tank and motor (courtesy Micro-cab)

6.2.2 Design Configuration and Operating Strategies

The H4 series employed hydrogen fuel cell and batteries in series-parallel hybrid configuration, as shown in Figure 6.4. The fuel cell connected in parallel with both traction batteries and motor controller, so it could provide power to both components at the same time, and also could provide solely to each individual component, purely determined by the voltage of motor and batteries. For example, when the vehicle was at a standstill, the fuel cell replenished the batteries up to full SoC; but when the vehicle was accelerating, both fuel

cell and batteries supplied power to the motor. This power train has a strong degree of hybridisation because the fuel cell was only able to meet the average campus driving demand, which includes many stops and starts. At each stop the fuel cell had enough time to replenish the batteries. With a 1.2kW nominal output of the fuel cell, continuous driving over 15km/h was impossible; however, with the power from the batteries, the Micro-cab could achieve 45km/h top speed in practice for a short period, with an accelerating time of 6 seconds from stand status to 30km/h.

In order to maintain the SoC of the traction battery, a straightforward timer based controlling strategy was applied – the fuel cell started with the vehicle ignition to provide instant power; but the fuel cell was kept running for 7 minutes after the ignition was turned off to allow the fuel cell to replenish the battery pack up to 140Wh energy (timer based on the fuel cell output and battery capacity), in order to keep the same SoC of batteries packs after the typical drive cycles experienced on campus [171].

In this vehicle, high pressure hydrogen stored in a Dynecell tank at 350 bar was firstly pressure-reduced to feed the Ballard NEXA fuel cell through a 10 bar hydrogen gas regulator. The fuel cell then converted the hydrogen to electricity via the electrochemical process, producing 26 Volts at rated full power. In order to charge the 48V batteries packs and provide power to the 48V motor controller, the voltage was stepped up to between 48V and 58V via a DC-DC converter. The fuel cell itself needs a 24V power supply for its starting system, whereas other auxiliaries used a standard lead-acid 12V battery. Therefore a 12-24V step-up DC-DC converter was used. However, in order to keep enough SoC of this auxiliary

12V battery, an additional step-down DC-DC converter was used to take unregulated power direct from the fuel cell (26-43V). Figure 6.4 shows the three DC converters, all of which were dissipating heat, at an estimated 80% efficiency.

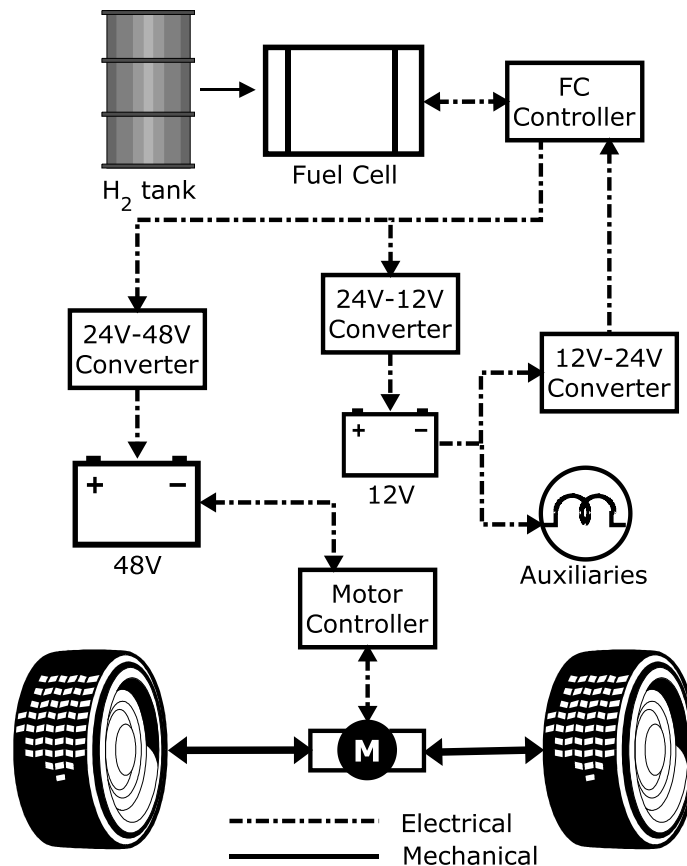


Figure 6.4 Schematic of H4 Configuration

6.3 Main Components

6.3.1 Fuel cell

The fuel cell stack in a HFCV is similar to the role of an IC engine in a conventional vehicle. In this Micro-cab H4 series, the 1.2kW Ballard Nexa™ PEM fuel cell was used, the world's first volume produced proton exchange membrane (PEM) fuel cell, introduced in 2001. It was designed for integration into a wide variety of stationary and portable power generation applications. It was not recommended by manufacturers for automobile application, due to

the rated operating and life cycle being far away from standard automotive requirement (5000 hours). However, it is well suited for small size prototype demonstration vehicles, as it was compact and relatively low cost, and provided the durability required by the demanding operating environment. Also during the vehicle construction, it was the only affordable PEMFC that could be purchased off the shelf.

These PEM fuel cell stacks produce unregulated DC power from hydrogen and air. Water and heat are the only by-products of the reaction. In order to operate the fuel cell, it must be provided a 24V power supply to support start-up and shut down process. Table 6.1 lists the specification of the fuel cell.

Rated Power at standard condition	1200W at 26V
Operating voltage range	22-50V
Rated current	46A
Dimensions	56 x 25 x 33 cm (L x W x H)
Number of cells	47
Area of cells	121CM ²
Total system mass	13kg
Operating and Cycle Life	1500 hours or 500 Cycles
Hydrogen purity	99.99%
Fuel pressure	0.7 to 17 bar (10 to 250 PSIG)
Pprice	£3000

Table 6.1 Specifications of Ballard Nexa™ 1.2kW PEMFC stack

The fuel cell achieves its maximum efficiency at partial load. Figure 6.5 illustrates the NEXA fuel cell efficiency against its output, and it can be seen that it operated up to 50% net efficiency at 300W output, but decreased to 39% while operating at full power 1200W. An appropriate controlling strategy will be needed to be applied in order to achieve higher system efficiency.

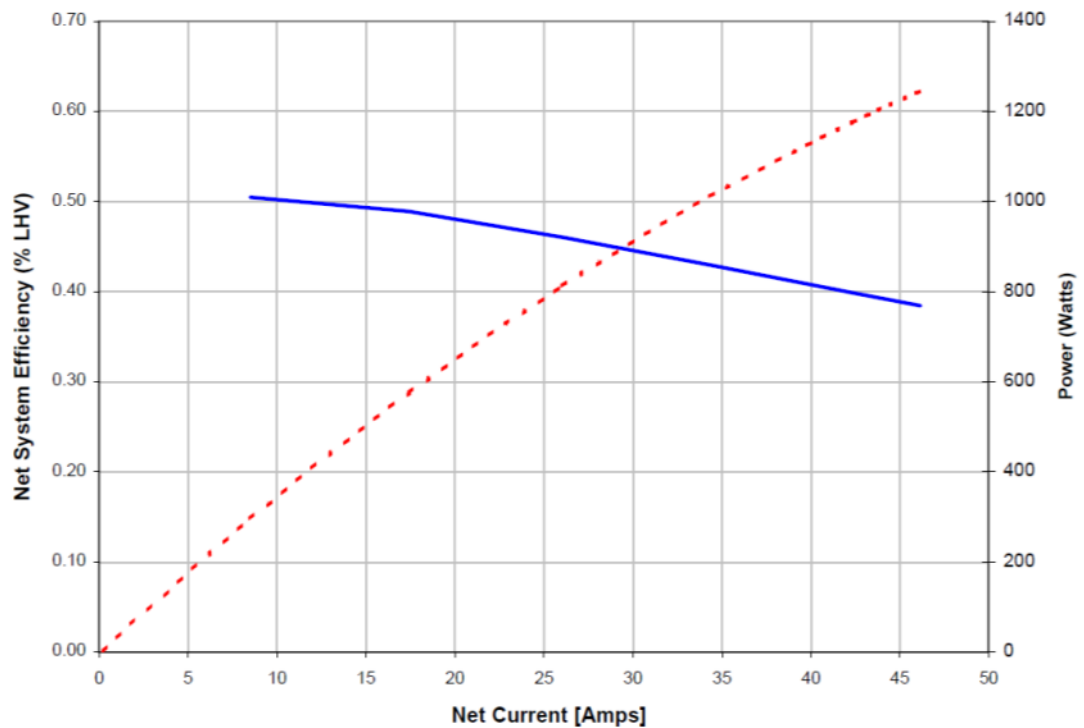


Figure 6.5 Ballard Nexa™ fuel cell efficiency curve[172]

6.3.2 Hydrogen Supply Storage and Refuelling

- **Hydrogen source** - In order to achieve sustainability and CO₂ reduction of those hydrogen fuel cell vehicles, hydrogen from renewable sources has been used; the hydrogen used in University of Birmingham was purchased from Green Gases Ltd. The hydrogen is produced by 'green' means – it is manufactured from renewable energy, resulting in a considerable reduction in greenhouse gas emissions when compared with conventional production of hydrogen via SMR. The hydrogen used has a very high purity of 99.999%, more pure than required by this low temperature PEM fuel cell stack which is 99.99%.

- **Hydrogen storage** - Hydrogen is stored on board in a Class III DyneCell tank (Model L026) from Dynetek Industries, it was an aluminium cored, fibre reinforced high-pressure hydrogen storage tank, specification listed as following:
 - Stored 0.61 kg of hydrogen at 15°C and 35MPa (350 bar), giving a total of 73.2MJ (20.33kWh) of chemical energy storage (LHV). When combined with a conservative estimate for the NEXA fuel cell efficiency (39%), this storage was equivalent to at least 265kg of lead acid batteries which were used in this vehicle.
 - The tank has an internal storage space of 25 litres; however, it stored 6676L of hydrogen in standard atmosphere.
 - The tank has a 15kg system weight [173].
 - Maximum fast fill pressure: 6344 psi / 438 bar.
 - 4.1wt % hydrogen storage (not including pipework).

- **Hydrogen refuelling** -The Air Products Series 100 fuelling station has been installed at the University's School of Chemical Engineering on 17th April 2008 [174], this was England's first hydrogen gas fuelling station, the station satisfied the fuelling needs of the Micro-cab H4 series hydrogen fuel cell vehicles. This fuelling station comprise of an integrated compression, hydrogen storage and dispensing system. It is capable of fuelling six vehicles per day up to 350 bar¹¹. It was equipped with standard WEH TK16 nozzle, see Figure 6.6, which could fuel other FCVs from OEMs and H₂ICE as well, for example, Nissan X-trail FCV and Honda FCX Clarity both refuelled from this hydrogen station.

¹¹ Calculation based on 0.6kg on board hydrogen storage. It can also re-fuel 700 bar fuel tank up to 350 bar.



Figure 6.6 Hydrogen fuelling station in University of Birmingham with nozzle zoomed in

6.3.3 Batteries

Eight Odyssey PC680 heavy duty Valve Regulated Lead Acid (VRLA) batteries (12V) have been used for traction, Table 6.2 shows the specifications of this type of battery; they have been positioned inside of the sandwich part of the chassis as shown in Figure 6.3, four batteries were connected in series to supply the required voltage, and two strings of them were connected in parallel to provide higher power capacity, as illustrated in Figure 6.7. This arrangement also gave a low centre of gravity for the vehicle and good weight balance. The battery pack provided a 48V battery power supply, which was capable to provide up to 12kW for peak power when the vehicle is undergoing extensive load, such as climbing steep hill with passengers. An additional 12V battery with same specification was installed to provide power for the in-car electronics such as:

- Data logging system, dashboards, lights, electric windows, screen wipers, etc.
- Start-up power for the fuel cell.



Figure 6.7 Traction and auxiliary batteries located under the vehicle floor

Odyssey PC680 Specifications	
Power Figures	Pulse Hot Cranking Ampere (PHCA): 680 amps for 5 seconds Hot Cranking Ampere (HCA) at 0 °C: 370 amps Cold Cranking Ampere (CCA) at 26.6 °C: 220 amps Capacity (20 hour): 17 Ah at 12V
Life Cycle	Design life 8-12 Years Cycles 80% D.O.D. 500 Cycles Cycles 100% D.O.D. 400 Cycles
Dimensions	185 L x 79 W x 187 H mm
Weight	6.525 kg including fixtures (measured)
Cost	Around £100 each [175]

Table 6.2 Traction and auxiliary batteries specifications

The weight of all 9 batteries was in total about 60kg, which stored around 1.5kWh energy at standard constant discharge rate. The useful energy will be less in the real-life use due to the Peukert's Effect¹² of batteries.

6.3.4 Motor

The Micro-cab H4 Series are driven by a General Electric (GE) Separately Excited DC electric motor on the rear wheels, as specified in Table 6.3, it rated at 3hp (2.24kW) nominally but can deliver transient power up to 12kW. The motor operated at 48V and up to 360A, and

¹² The capacity of a lead-acid battery will decrease if discharge rate increase.

was connected to the wheels with COMEX D585 differential reduction (8.47:1 ratio) gear, which provided a top speed of 45km/h at 3650RPM. This motor was controlled via its integrated motor controller. Total costs around £1900.

Model	5BC49JB1108A
Motor Speed (RPM)	3650
Voltage (V)	48
Current (A)	64
Horsepower (HP)	3
FR	49
Max ambient temperature °C	40
Price	£1900
Weight	25kg

Table 6.3 Specification of motor used in H4

6.4 Data Monitoring and Collection

The vehicle has employed a digital interface to monitor the key parameters for its users, including vehicle speed, travelled distance, voltage of auxiliaries' battery, voltage of traction batteries, hydrogen tank pressure, operating status of fuel cell and other common indications as conventional vehicles. See Figure 6.8:



Figure 6.8 Driver interface on Micro-Cab H4

As a prototype vehicle for research and demonstration purpose, extensive data logging equipment has been integrated into the vehicles, from vehicle movements to the power flows of each component in the powertrain. RDM Automotive¹³ designed and installed the 'Green Track' GPS fleet management system for the vehicles, which enables live tracking of each vehicle from a web interface, and they also built a set of tools in to analyse vehicle utilisation, journey distances and typical patterns of movement. Tempus Computers¹⁴ custom designed and installed a data logging system which measures and records 113 parameters in total, including:

- Voltage and current throughout the electrical flow at 100Hz.
- Individual cell voltages and temperatures of fuel cell.
- Apart from Ballard default monitored data, extra sensors were used to measure the air and hydrogen flows into and out of the stack (including humidity and temperature).
- Vehicle pitch, roll and fuel cell vibration.
- Ambient temperature, humidity and hydrogen concentration within the vehicle.

The data logging systems cost around £20,000 per vehicle installed and extensive data has been collected for analysis. The data has collected and processed by a central field-programmable gate array (FPGA), and then sent to an SQL database via satellite modem.

¹³ Tier 1 automotive supply chain company supplying to Jaguar Land Rover, Aston Martin etc. with specialism in electronic and telematic vehicle systems.

¹⁴ Providing technology based solutions to propose and deliver 'off the shelf' solutions to fully 'bespoke solutions'.

6.5 Conclusions

The five Micro-cab vehicles and the hydrogen dispenser provided an ideal test environment for the theory of hybrid HFC vehicles presented in this thesis. The next chapter goes on to report the test results and compare them to the computer model. Later these results will be used to improve the drive-train components to give improved performance and energy economy.

7. Chapter Seven

Testing of Micro-cab H4 Vehicles

7.1 Introduction

Having defined the components and design performance of the Micro-cab prototypes supplied by Professor John Jostins, it was necessary to install data loggers and to run tests on the vehicle efficiency, analysing the results in terms of the hybrid model theory.

7.1.1 Test of Vehicles

According to the government regulation of prototype hydrogen vehicles, such vehicles can only be used on private roads. Therefore most drives and tests were undertaken inside the 1 km square University of Birmingham campus, where the ring road covered about 2 km with a speed limit of 20 mph, combining many uphill/downhill slopes and speed ramps. This raised an issue that the data collected was not directly comparable to other HFVC tests under standard drive cycle conditions. However the data are well comparable with equivalent runs on the Ford Connect vans used by the University fleet, which also had duties such as:

- Postal service within campus (partnership with Royal Mail), Figure 7.1 shows the typical mail delivery run.
- Service in the waste recycling department.
- Providing rides for university VIPs and visitors.
- Academic test drives.
- Short-distance leisure drives.

Therefore, the following results were compared with controlled runs in the diesel Ford Connect van. Table 7.1 summarised the use of four vehicles from 08/10/2008 to 29/06/2010, with thousands of trips which covered 4173.9 km in 18 months, mainly with the postal van (H4 005) which contributed most because it was used on a daily basis and made several trips a day.

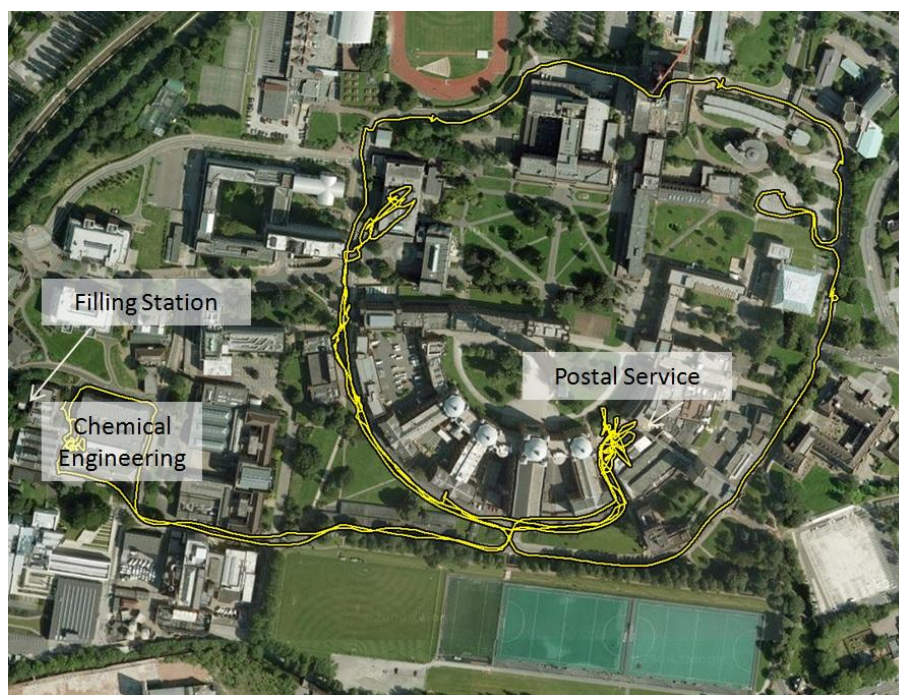


Figure 7.1 Postal service route[176]

Vehicle	H4 002	H4 003	H4 004	H4 005	Total
Time	From 08/10/2008 to 29/06/2010				
No. of trips*	163	479	653	983	2278
Maximum day trip distance (km)	7.2	8.9	10	42.9	
Top speed recorded (km/h)	48	46	50	49	
Total distance done (km)	519	810.8	1266.4	1577.7	4173.9

Table 7.1 Summary usage of each vehicle

*Trips from RDM GPS data logger only, since May 2009.

7.2 Results

The results discussed in this section were collected in collaboration with Dr. Iain Staffell.

7.2.1 Hydrogen Refuel and Consumption

More than 150 hydrogen refilling were done with 100% safety record during the trial period.

Table 7.2 shows the recorded data of amount of hydrogen refuelled and distance travelled for each vehicle. In total 61.7kg hydrogen were consumed to cover 3347km travel, giving an average fuel consumption of 18g/km, or 2.21MJ/km.

Vehicle	No. of Refuel	Amount of H ₂ in kg	Distance Covered	Avr. Fuel Economy	Avr. Range
H4 005	56	25.1 kg	1333 km	2.26 MJ/km	34.9 km
H4 004	41	15.7 kg	961 km	1.96 MJ/km	38.6 km
H4 003	36	13.2 kg	692 km	2.29 MJ/km	33.3 km
H4 002	16	7.7 kg	361 km	2.55 MJ/km	29.5 km

Table 7.2 hydrogen refuelling record and fuel economy of each vehicle

7.2.1.1 Temperature Change and Expansion

The temperature change of the hydrogen tank (outer wall) during the refill process has been measured via laser thermometer; the temperature behaviour of a typical refill is illustrated in Figure 7.2. The temperature observed increased dramatically from 23°C to 55°C in 5 minutes while refilling, and took 90 minutes to cool down to the initial temperature. In this process, the hydrogen tank was filled from 7 bar to 354 bar and it was estimated that 0.6 kg hydrogen were transferred. The starting pressure (7 bar) was measured from the on-board tank itself during the pressure equilibrium process between fuelling station and hydrogen tank, whereas the final pressure (354 bar) was measured from canister (final stage) of fuelling station, which presents a more accurate result as the pressure of the fuelling station changes relatively small compare to the vehicle tank. The hydrogen tank pressure decreased to about 300 bar (estimated¹⁵) after cooling down; therefore the hydrogen content weighed slightly less than the initially calculated results (44 gram less for this particular refill). To minimize this error, the fuelling station was re-programmed to reduce its filling rate from 100 'bar per minute'¹⁶ to 50 'bar per minute' since 2012, for a typical refilling, the temperature rose from 19 °C to 38 °C, which was significantly lower than the initial range and the tank pressure dropped from 351 bar to 315 bar (estimated) while cooling down.

¹⁵ Pressure reading from the vehicle on-board dial, as the hydrogen fuelling station won't operate if the tank pressure is relatively high, hence no pressure reading from it.

¹⁶ This is non-linear estimate pressure exchange rate between fuelling station and hydrogen tank.

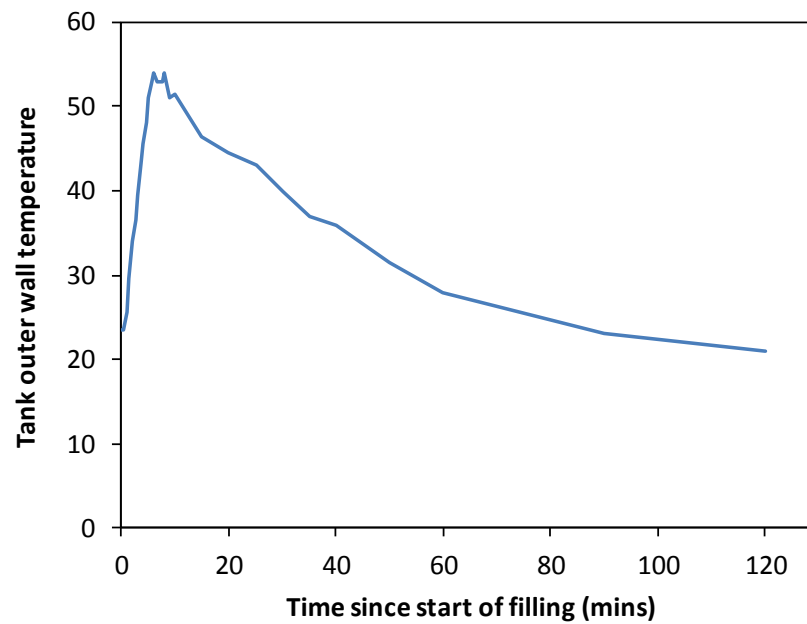


Figure 7.2 Temperature change before and after the hydrogen refuelling process

7.2.1.2 Refill Time

As displayed in Figure 7.3, most of the refill processes have been done within 4 minutes during the test, depending on the initial pressure of the tank; even if when the tank was empty, it took no more than 5 minutes to fill the tank. On average, the filling rate was around 0.16kg hydrogen per minute. This energy (LHV) transfer rate equals that of charging a battery at a rate of 1350A from a 240V power supply. Hence, refilling a hydrogen fuel cell electric vehicle is hence more than 100 times quicker than charging a battery electric vehicle from a UK household plug.

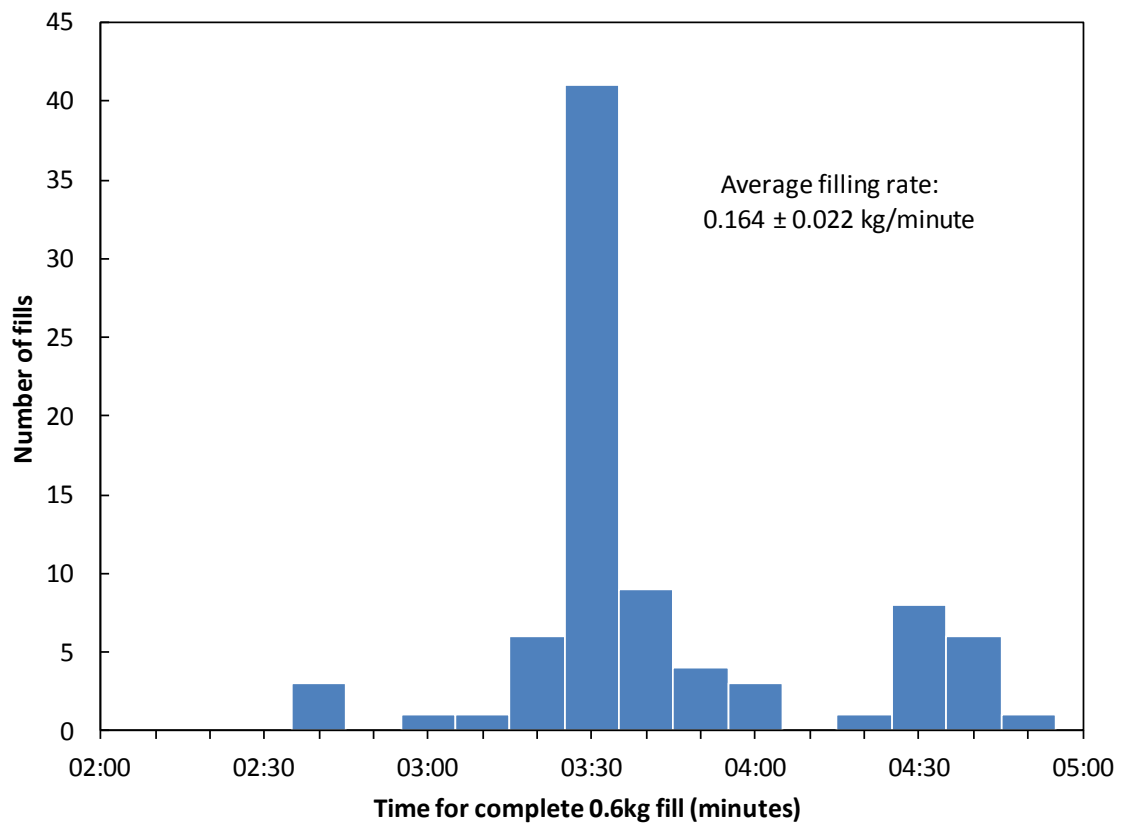


Figure 7.3 Time of refilling process

7.2.1.3 Hydrogen Consumption

To compare hydrogen fuel cell vehicles' energy consumption with other type of vehicles, the measurements of fuel consumed, either in volume per one hundred kilometres (i.e., L/100 km) or in distance per volume fuel consumed (i.e., MPG-miles per gallon) are not comparable because of the different physical properties. Therefore, the energy consumption per distance travelled in MJ/km has been used, or vice versa (km/MJ), however this can be converted to equivalent value of L/100 km or MPG. Figure 7.4 shows the fuel consumption of each vehicle during the trial, according to the data of hydrogen refilled and distance travelled. The energy consumption of all the vehicles was calculated to be around 2.1 MJ/km, equivalent to 6.07 L/100 km or 46.54 MPG on petrol, a result affected strongly by the drive

cycle and traffic condition on the campus. Therefore the energy consumption ranged from 0.9MJ/km to 3.6MJ/km. When the condition was ideal, a 100MPG could be achieved.

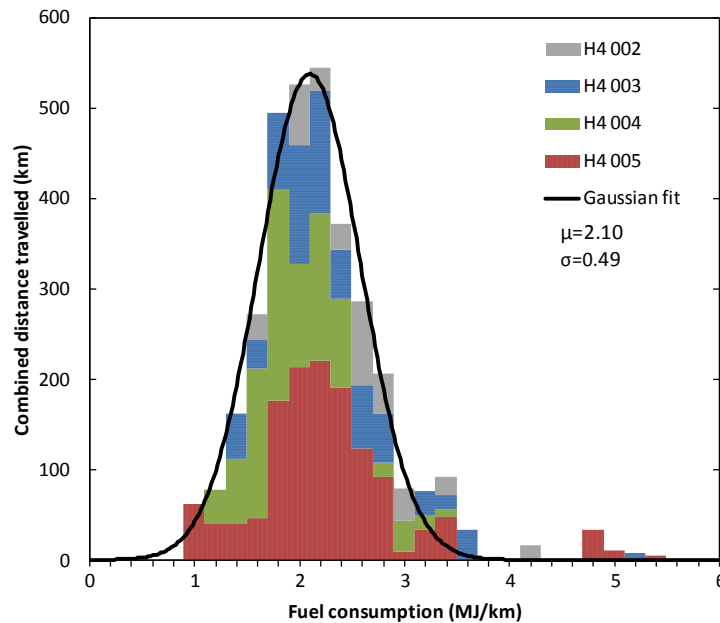


Figure 7.4 Combined fuel consumption of each vehicle under campus drive cycle

7.2.2 Fuel Cell Performance and Efficiency

The Ballard Nexa™ fuel cells have performed very robustly during the trial in all four vehicles, underwent the sub-zero winters down to -5°C without problems and showed no observable degradation after more than 800 hours¹⁷ of operation, see Figure 7.5.

The control strategy of the fuel cell was straight forward because it followed the requirement of a ‘current limited’ DC-DC converter which replenished the traction battery. Due to the strong hybridisation configuration, the fuel cells normally operated at full power, sometimes even over the rated output, allowing the fuel cell to take advantage of operating

¹⁷ Fuel cell operating time on H4 005, total operating time across all 4 vehicles more than 2000 hours.

under a reasonable static condition, but compensated by the low energy efficiency at high current output due to the concentration effects and internal resistance.

7.2.2.1 I-V Curve

The Nexa™ has integrated monitor systems which can measure the stack's voltage and current output during operation; this was recorded by the Tempus data logger via RS232 connection. Total 137,000 data points have been collected from real-life operation from all four vehicles rather than from controlled laboratory tests. The I-V curves of fuel cell stacks from all four vehicles are illustrated in Figure 7.5, compared with the manufacturer specifications given by Ballard. It can be seen that all four stacks have performed well and sometimes were even over their rated manufacturer specifications.

When the stacks operated less than the maximum rated output of 46A (1500W gross, 1250W net) there were no statistically significant differences between the individual I-V curves. However, three of the stacks were operated over their rated power, occasionally reaching the maximum shut-down limit of 75A (equals to 1850W gross or 1600W net). In the range of 50A to 75A, the I-V curve fluctuated irregularly. This generally took place at the start-up process in normal operation and accounted for less than 5% of their operating time.

The H4 002 (as illustrated on the bottom right) was an exception to this, as its DC-DC converter was purposely limited to take an input current of 40A, thereby keeping cell voltages above 0.65V.

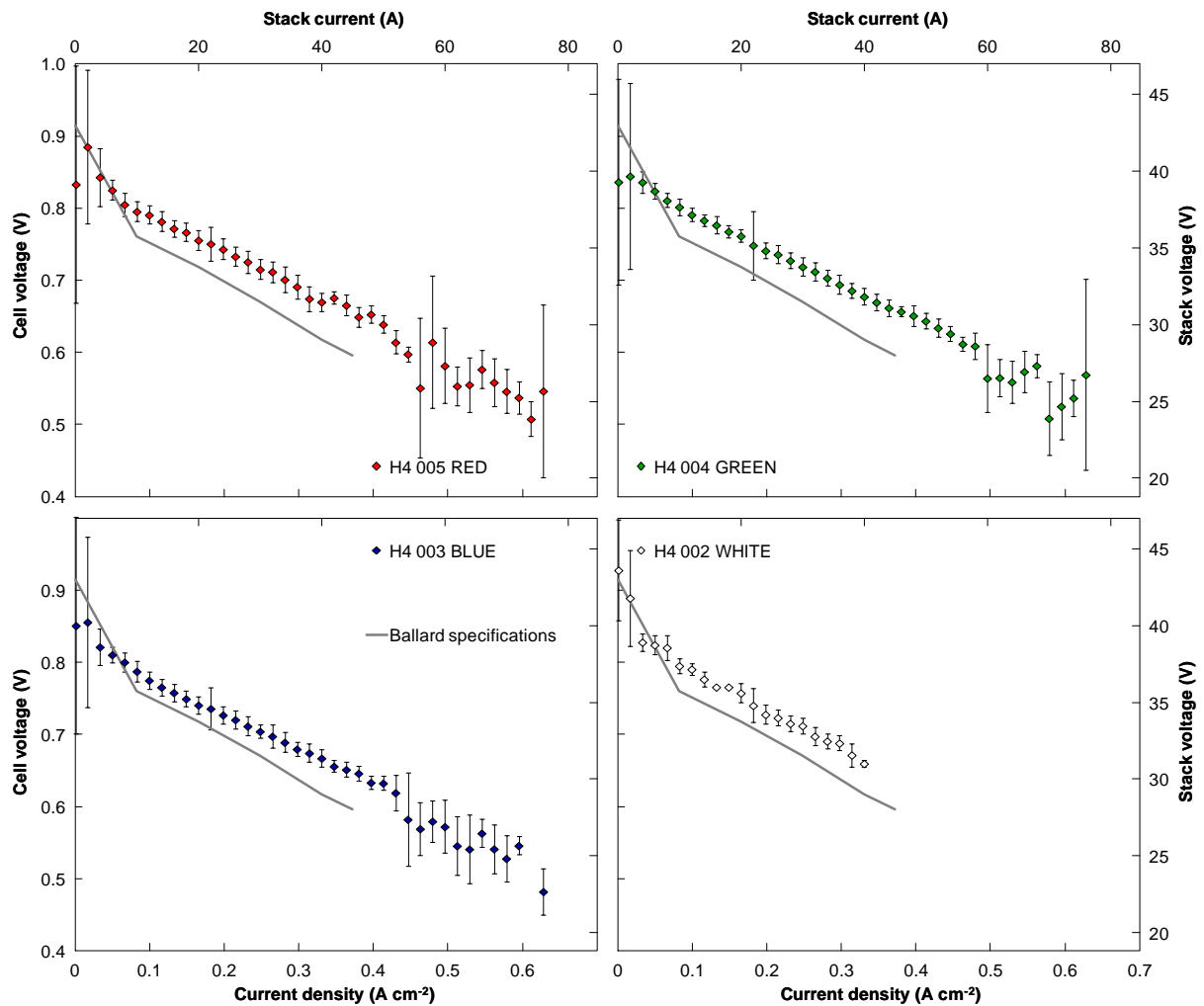


Figure 7.5 I-V curve for the fuel cell stacks measured in each vehicle in comparison to manufacturer rated specification[162]

7.2.2.2 Hydrogen Consumption and Purge

The high pressure of hydrogen from the tank was firstly reduced through a pressure regulator to approximately 11 bar to feed the fuel cell stack. With a 1/4" tube used in the system, the hydrogen discharge rate was satisfactory at every stage of fuel cell performance (less than 18 Standard Litre Per Minutes-SLPM as manufacturer suggested). Figure 7.6 plotted the hydrogen consumption rate SLPM against fuel cell current for a typical 'postal operation', is shown when the fuel cell requires less than 13 SLPM hydrogen most of the time, with higher rates that were up to 19 SLPM occasionally. The average of this particular drive cycle had an average hydrogen flow rate of 11.08 SLPM with a total

hydrogen consumption of 412.5L, so that, given the hydrogen stored on-board was approximately 6676L, the amount of hydrogen stored could power the vehicle up to 10 hours of duty or 15 postal duty cycles (around 2Km long).

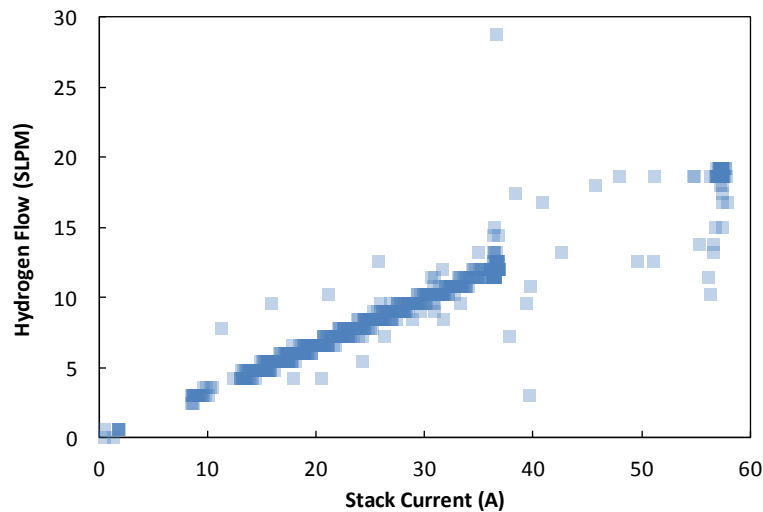


Figure 7.6 Hydrogen consumption rate (SLPM) against fuel cell stack current in typical 'Postal duty cycle'

Only a small amount of hydrogen was purged from the system, occupying less than 1% of the overall fuel consumption rate. Purged hydrogen was discharged into the cooling air stream before it left the Nexa™ system.

7.2.2.3 Cell Temperature

In the same postal duty cycle (see Figure 7.1), the temperature measured from the air exhaust stream was up to 10°C lower than the actual cell temperature: the cell was designed to operate at 65°C, and the air exhaust stream temperature was 55°C [172]. Figure 7.7 illustrates the temperature behaviour of the fuel cell; it can be seen that temperature rose from the ambient 20°C to the operational temperature of 55°C in 7 minutes, and kept in the range 52 – 59 °C across the whole cycle. It was observed that the temperature dropped slightly with current decrease (when the traction battery SoC was close to 100% during the stops), and stayed constant when the fuel cell stack operated continuously at rated full

power. The air-cooled Nexa™ maintained the temperature at 65°C by varying the speed of the cooling fan, extracting the heat to the top of the fuel cell and dissipating it via the vent near the rear bumper. The fuel cell shut down if the cell temperature rose over 73°C, but this was never realised.

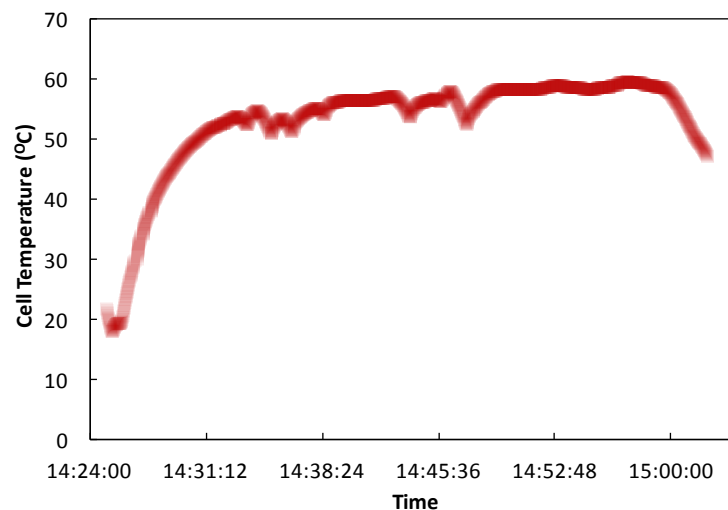


Figure 7.7 Cell temperature behaviour in a typical postal duty cycle

7.2.2.4 Fuel Cell Efficiency

The data used to calculate fuel cells efficiency was the same as in-situ data used to plot the I-V curve. This data was gross power output data, and it therefore needed to be corrected to get the net data, i.e. subtract the parasitic loads such as air blower and control electronics.

To identify the characteristic stack efficiency and the impact of parasitic loads, one hour of controlled driving testing was accomplished. From these results, both gross efficiency and net efficiency were plotted in Figure 7.8 against the net power output. The gross efficiency plot used the raw data from the Nexa™ integrated monitoring system, which came out with an average efficiency of 50%, with a peak of 60%. This included internal parasitic loads which needed to be subtracted, as the stack efficiency was expected to be 38% LHV at full load,

rising to a peak of 50% based on the specification. Therefore, net efficiency was plotted using the corrected data¹⁸ from the net efficiency curve and it can be seen that:

1. Starting the fuel cell from cold: the maximum power output and efficiency increased slightly while the stack was warmed up to its optimum temperature of 50°C.
2. Operating at full power: when at steady-state, the net power output and efficiency remained consistent at $1140 \pm 4\text{W}$ and $41.6 \pm 0.6\%$.
3. Reduced power output: when the batteries SoC was high, the stack power fell, and the increase in cell voltages led to improved efficiency, reaching $47.3 \pm 0.4\%$ at the minimum of 330W ¹⁹.

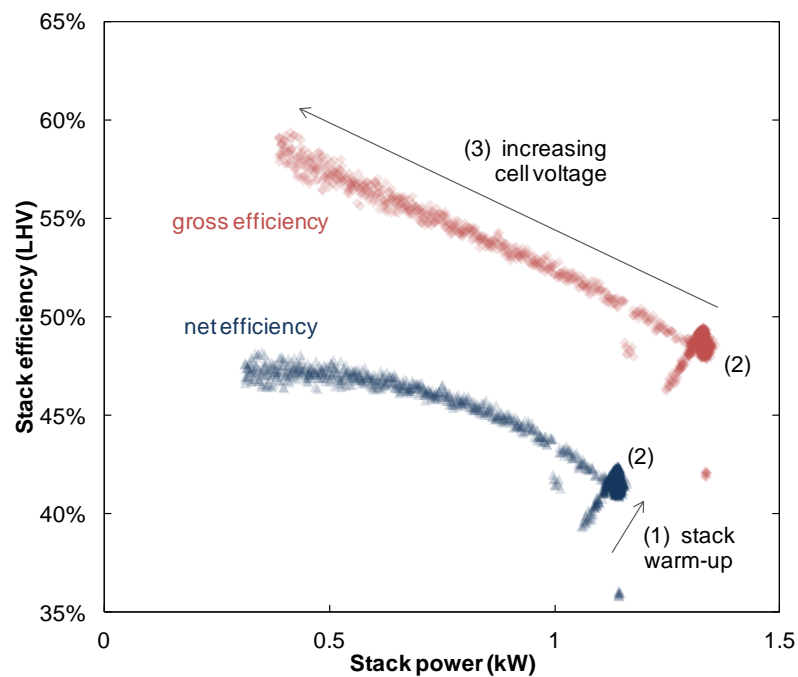


Figure 7.8 Gross and net efficiency of the red vehicle's fuel cell stack for a representative drive cycle

¹⁸ Correction equation from Excel fitting $y = 0.0267x^2 + 3.4759x + 37.817$

¹⁹ This was the reasoning behind limiting the output of the fuel cell in the white vehicle; net efficiency could be kept above 45% by operating the stack above 0.65 V per cell.

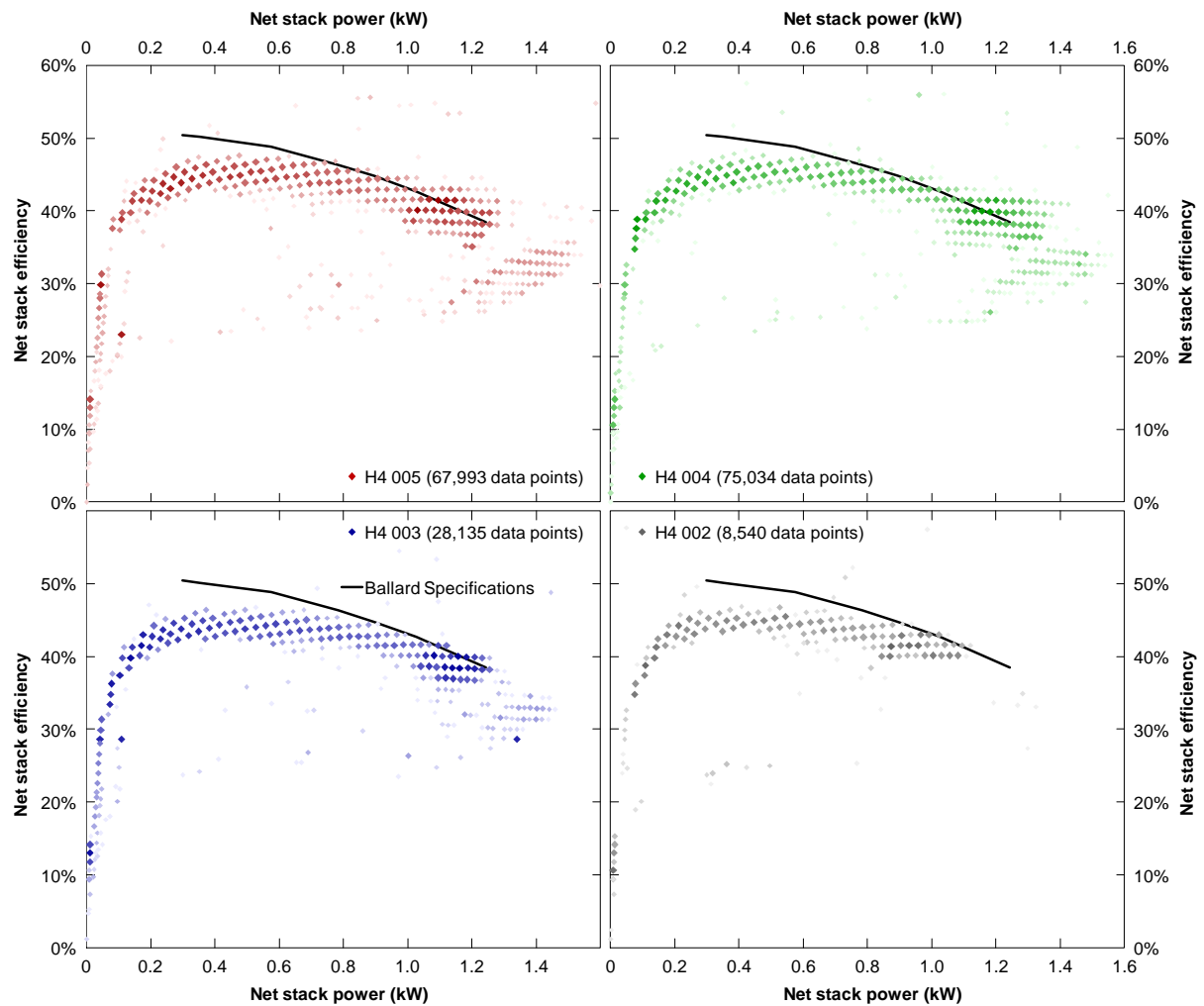


Figure 7.9 Net efficiency for the fuel cell stacks measured in each vehicle against instantaneous power output. The colour intensity of each data point indicates how frequently the stack operated at that point.

The overall efficiency of all four vehicles' stacks over 250 hours operation has been plotted against power output in Figure 7.9. It is seen that each of the curves follows the trend expected, the efficiency increasing as power output decreased, up to the point where auxiliary loads began to dominate the requirement for hydrogen consumption, and the system efficiency started to decline rapidly. The results showed that the efficiency $36.7 \pm 1.3\%$ (averaging across the four vehicles) at full load was close to the rated value 38%, but when the fuel cell output was below 600W, the average efficiency was just $41.1 \pm 1.7\%$ across the four vehicles, lower than the manufacturer rating. This was very likely caused by the greater

parasitic loads than rated, since the fuel cell stack being enclosed in a metal box that reduced the air flow, therefore needing greater pumping power in comparison with operating in an unconfined condition. In addition, the efficiency of supplying power for these parasitic loads was lowered due to the repeated voltage conversions. The fuel cell needs external 24V power supply but the H4 auxiliary voltage is 12V as in most light duty passenger vehicles. Consequently, auxiliary power came from the fuel cell initially from a step-down DC-DC converter, and step-up back to 24V via another DC-DC converter, the overall conversion efficiency being only around 71%, 1.4 times worse than expected.

7.2.3 DC-DC Converters

The H4 has two main voltage networks, 48V traction network and 12V auxiliaries network²⁰, both drawing power from the fuel cell 24V output, hence two different DC-DC converters have been used.

7.2.3.1 Main Converter 24V-48V

In order to charge the traction batteries effectively, the fuel cell's output was stepped up to 48 volts using a voltage regulated 1.7kW Zahn Boost DC-DC Converter (DC6350F-SU). This converter has an input of 24–42 V and adjustable output up to 60V, Figure 7.10 shows that this converter has a peak efficiency of just $81.2 \pm 4.0\%$ in a narrow window between 1100 and 1250 W, where the fuel cell output is at full power. The efficiency then decreased more than 10% on either side of this power range, with more dramatic decrease occurring when input power was below 750W. However, the histogram of input powers in Figure 7.11 also shows that the fuel cells operated for considerable time between 300 to 600 W, providing 150 to 400 W to the main DC converter. In this region, the converters' efficiency ranged

²⁰ The power for Ballard 24 V controlling system is included in 12 V auxiliaries' network.

from 58% down to just 21%, which pulled the average efficiency during the trial down to 73.6%.

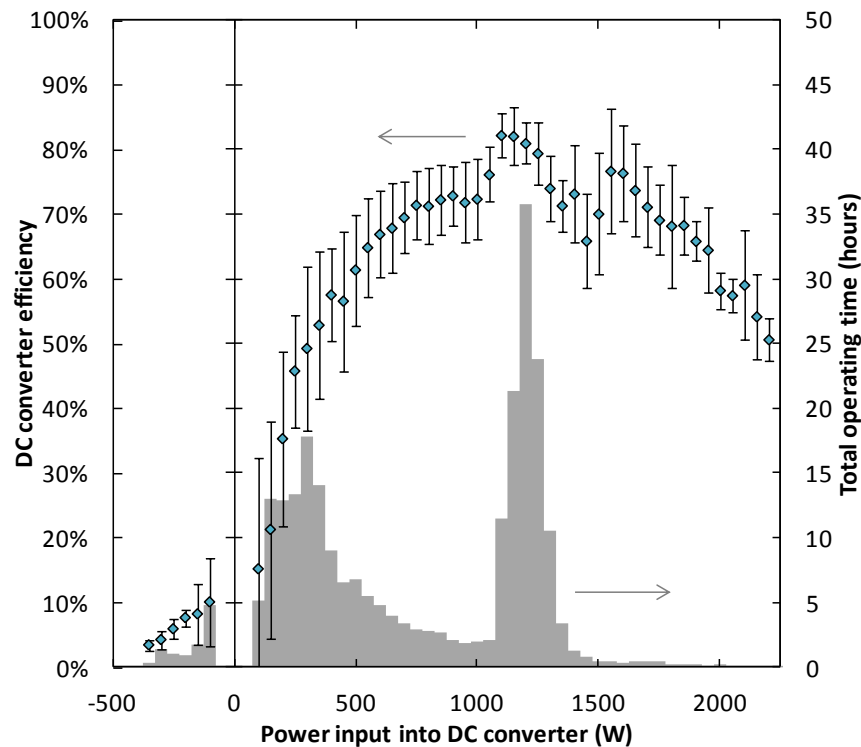


Figure 7.10 The efficiency and usage profile of the main DC converters averaged across all four vehicles

Figure 7.10 also shows some negative power went into the DC converter up to 350W. As the regenerative braking was disabled (described in following sections), this negative power was possibly caused when all the traction batteries were completely charged and the fuel cell was turned off. This was a very inefficient mode of operation, as the unidirectional DC converter could provide only 2–16% efficiency; however, it was only experienced for 4% of vehicle's operating time. This could be limited by a diode between the 48V battery pack and main DC converter.

7.2.3.2 Auxiliaries' Converter 24-12 V

The combined power needed for the vehicle electronics and data logging equipment ranged from 50W up to 300W at 12V. Hence a Waeco PerfectPower DCDC20 step-down converter

was used together with a 12V lead-acid battery. The maximum power conversion of this DC converter was 240W, drawn from the 12V battery where needed.

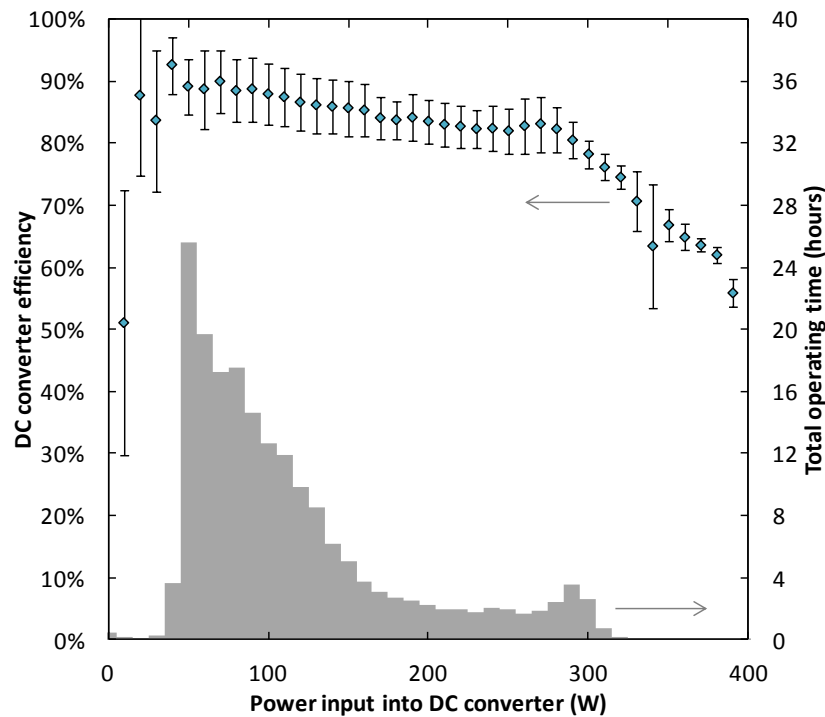


Figure 7.11 Efficiency of the auxiliary DC converters in all four vehicles over their operating range

Figure 7.11 shows a histogram of the power input into the converter during the trial, from which it is seen that the majority of power input was less than 100W. This is because most the tests were undertaken during daytime, when heating and lights were generally switched off. The average power draw from the auxiliary network was 113W, unlike the main DC converter, the efficiency of this auxiliary DC converter was relatively consistent over its operating range (see Figure 7.10), providing an average efficiency of 83.4%. It only declined below 80% when producing more than 24A which rarely occurred.

7.2.4 Batteries

7.2.4.1 Useful Energy Capacity

During the typical campus drive cycle, the fuel cell could not provide enough traction power. Therefore the battery supplied 1-12kW power from time to time, and since the capacity of the batteries was 1.5kWh, the battery could be completely discharged in 7 minutes. In addition, the useful battery capacity was reduced when higher currents were drawn due to the Peukert effect. In extreme cases, less than half of the total battery capacity was available at the high discharge rates, as shown in Figure 7.12. When discharging at 12kW, only 27% of the total capacity was left, indicating that the battery completely discharged in 2 minutes. Increasing the battery capacity by adding more parallel strings would reduce the discharge rate in each string of battery, thus increase the available capacity per string. However, the increase in vehicle weight may offset the benefit (see results in Chapter 8).

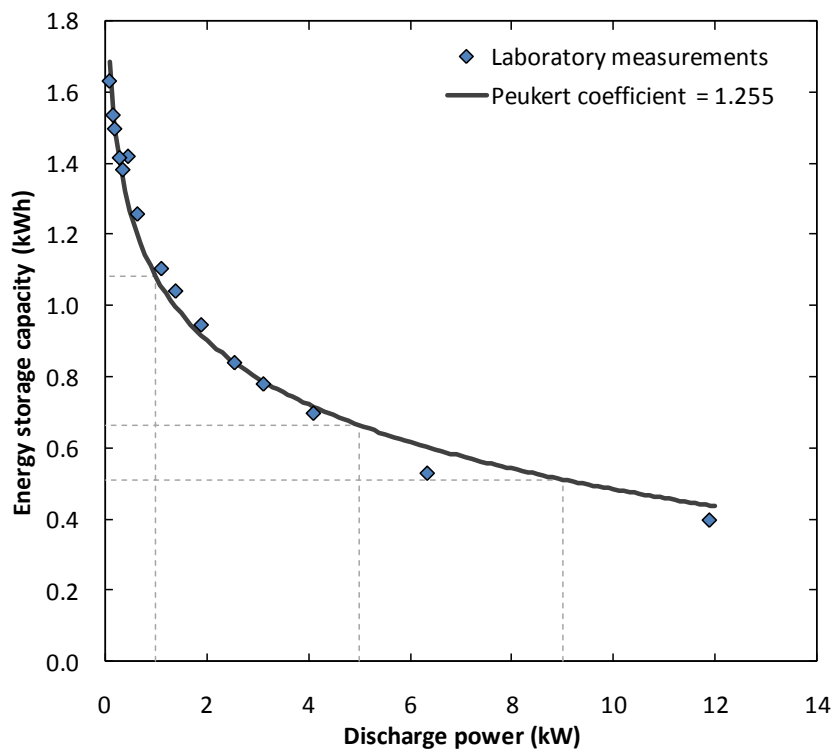


Figure 7.12 Available battery capacities as a function of discharge power, showing the Peukert effect

7.2.4.1 Change of SoC

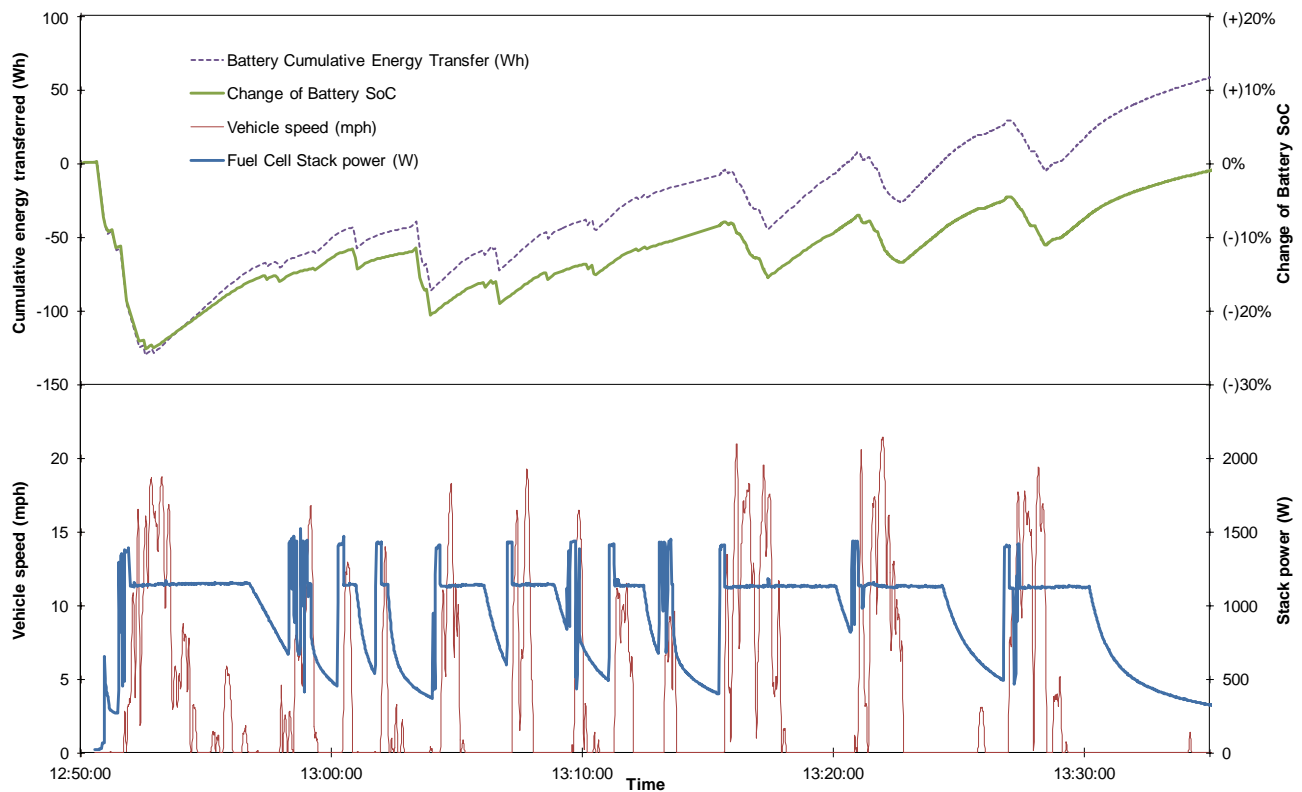


Figure 7.13 State of charge and energy transfer to/from the battery pack during the course of a typical drive

Due to the size of battery, the vehicle needs to operate under charge sustaining (CS) model, i.e. the SoC over a driving profile may increase and decrease, on average, it remain at its initial level. The charge/discharge cycle efficiency of the batteries was measured to be 83% in the laboratory; therefore a 1.5kWh battery pack will need 1.85kWh electric energy to be supplied for a complete recharge. This efficiency was confirmed within the vehicles from analysis of the voltage and charge flowing in and out of the batteries. See Figure 7.13, the top section illustrated the change of SoC and the amount of cumulated energy transfer, the bottom section plotted the vehicle speed and fuel cell power output, it can be seen that when the vehicle ran at higher speed, the fuel cell operated at full power (the flat straight line) with assistance of battery, hence decreasing battery SoC and the capacity has been observed in this stage; when vehicle ran at lower speed and standstill, the fuel cell

continually operated at full power to charge the battery, and started to reduce power output when SoC was within 10% range, a good example was at the end of the drive the fuel cell power gradually decreased to its minimum of 300W before shutting off, when the battery had charged to its initial SoC level.

7.2.4.2 Battery Lifetime

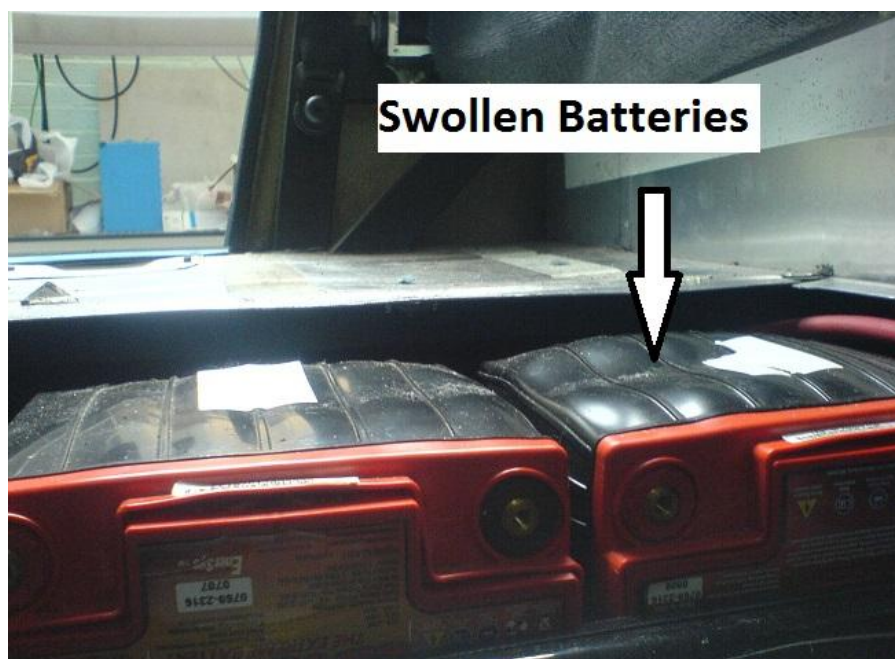


Figure 7.14 Swollen Batteries of Micro-cab H4

The batteries were rated for 500 cycles at 80% Depth of Discharge (DoD). During the campus drive cycle, the DoD of the battery was around 10%-30% as shown in Figure 7.13, which would increase the cycles above 2000 in this case. However, battery life becomes shorter when charge/discharge is at a repetitive high current. With about 4-10 cycles per day on average, the batteries in Micro-H4 would last 2-3 years [177]. In addition, when two strings of battery were connected in parallel, each string may have different resistance, and may give uneven currents flow between strings, therefore reducing the lifetime of the batteries.

Under extreme circumstances this could cause damage to batteries, as Figure 7.14 illustrates with a picture of swollen casings. This was happened after 5 hours of heavy load use in 2 of H4 model vehicles.

7.2.5 Motor and Drive-train

One of the vehicles was tested on a rolling road and its power consumption was measured at different road speeds by TUV NEL, which revealed the motor efficiency peaked at 81% and remained above 77% over the range of 4–12kW. But the efficiency decreased dramatically under 3kW, as shown in Figure 7.15 and the specific efficiency at each power output can be calculated using equation (1). This motor character particularly affected the Micro-cab H4 because of its low speed and mass. The motor required less than 3 kW for the vehicle to cruise at a steady speed of 30km/h (the campus speed limit), meaning that its high efficiency region was only obtained during periods of acceleration or hill climbing. And over the typical drives on campus, which were mostly low speed, the average motor efficiency was reduced to 73.5% when weighted (Excel fitting) by the amount of energy consumed at each power level (input power multiplied by operating time).

$$\eta = 1.0463 - 0.01759P - \frac{0.7618}{P}$$

It can be seen that the efficiency of the motor varied widely over the operating range. The motor controller was able to control the power to the motor field coils and the motor armature in response to driver demand. The motor controller power input and motor net power output has been compared in Figure 7.16. The motor controller withdrew up to 13kW power from battery and fuel cell, where the motor was only capable to deliver max 10kW to the differential gears. The differential with reduction gears was assumed to have a constant

efficiency of 92%, the net power to drive the vehicle should be around 9.2kW with an overall efficiency from the motor controller to wheels about 67.6%.

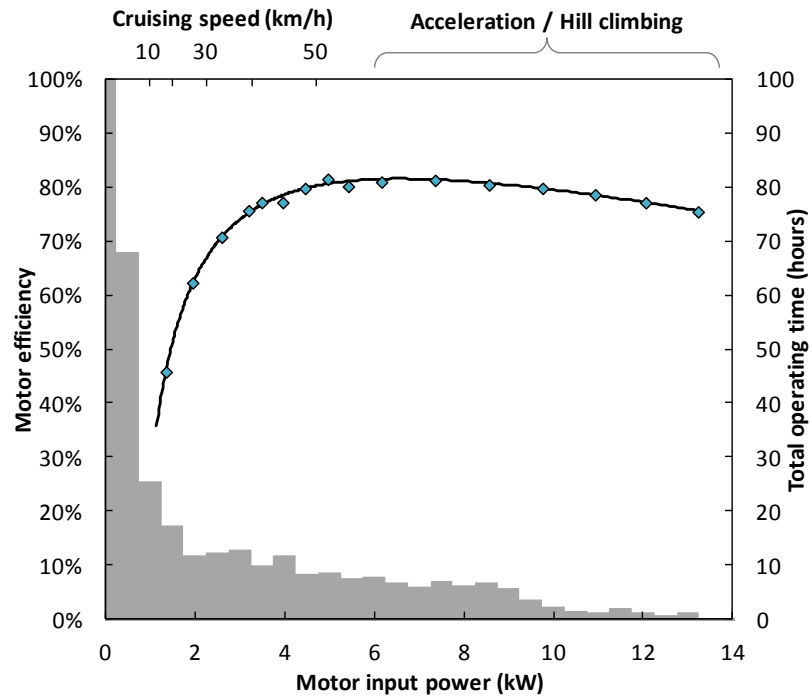


Figure 7.15 Motor efficiency plotted against power input and the corresponding vehicle speed, overlaid with a histogram showing how frequently the motors were operated at each power level

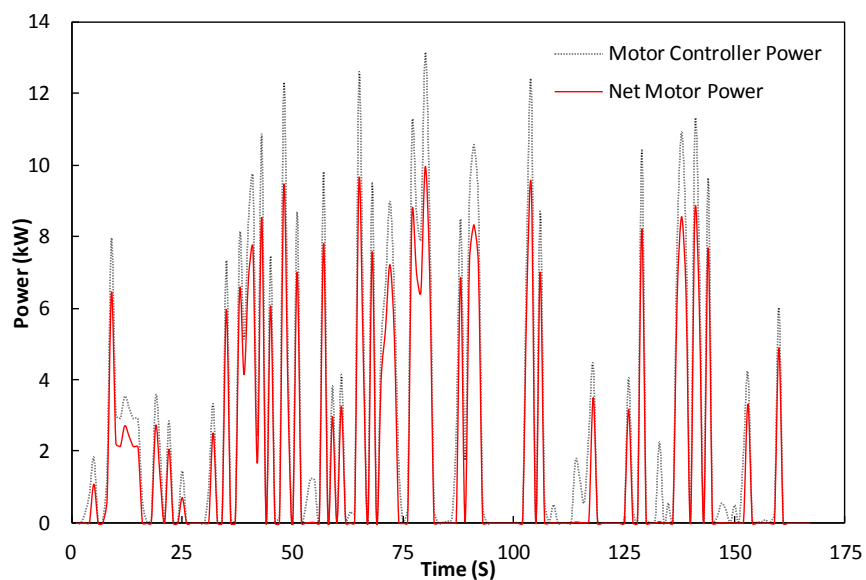


Figure 7.16 Motor controller input power and net motor power comparison

The motor operated over its rated power 2.24kW for half of the time of the campus drive cycle, and amazingly has a greater efficiency to do so. The motor designed to operate above rated power for 60 minutes. Owing to the thickness and size of the motor outer wall, it could dissipate the heat effectively and keep the temperature within the limit. During the test, the motor temperature was about 32°C, and no issues were recorded regarding motor and its controller's temperature. In addition, the motor was continuously draining the battery by an average of 2.25kW. Clearly, if this was typical, there must be frequent stationary periods to allow the battery to recharge, as the fuel cell can only supply half of that power. The motor and its integrated controller were capable of operating as a generator to provide regenerative braking. The efficiency of being a generator is unknown but can be assumed as similar to be a motor. However, this function had to be deactivated because the vehicle's electronics couldn't withstand the surge due to the small capacity of battery, so around 5-10% braking energy could not be recovered.

7.2.6 Overall Performance and Efficiency

The fuel cell vehicle was expected to be twice as efficient as the conventional IC engine vehicle, because the fuel cell stack has higher efficiency than thermal engines by factor of 2 in general. Figure 7.17 shows the combined efficiency of fuel cell and the main DC converters, showing the peak efficiency was $33.4 \pm 1.7\%$. In ideal conditions, the main DC converter has a peak efficiency of 82.2% and the fuel cell has a peak efficiency of 46.2%, offering a combined result of 38%. However the fuel cell achieved its peak efficiency at partial load whereas the DC converter almost behaved in the opposite way. This means that when the fuel cell operated best at low power, the DC converter would pull the combined efficiency down from 46% to just 25%.

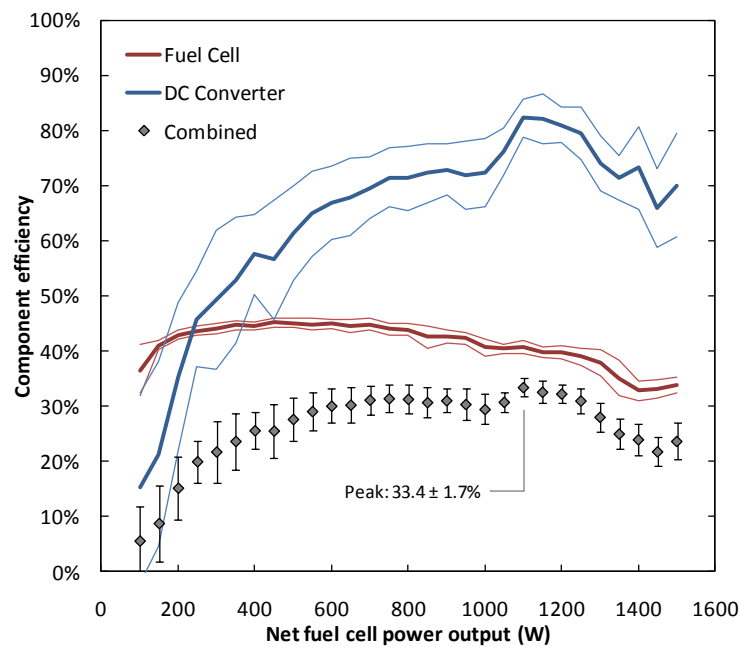


Figure 7.17 The combined efficiency of the fuel cell and main DC converter. For the fuel cell and DC converter, the three lines show the average efficiency plus and minus one standard deviation.

Table 7.3 lists the measured efficiencies of each component to show that the average power-train efficiency was 18.6%, more than one-third lower to its peak efficiency 29.6%, almost double that of the diesel vehicle (Ford Connect diesel Van) under the same drive/duty cycle on the campus.

Component	Peak efficiency	Weighted average efficiency ²¹
Fuel cell	46.2%	40.1%
Gross stack efficiency	56.4%	47.0%
Parasitic consumption	18.1%	14.7%
Vehicle auxiliaries	95.0%	89.4%
Proportion of power required	4.5%	8.8%
DC converter efficiency	89.9%	83.4%
DC converter	82.2%	73.6%
Battery charging	92.1%	92.1%
Proportion of power used for recharging	46.6%	46.6%
Charging efficiency	83.0%	83.0%
Motor	82.0%	73.5%
Overall	29.6%	18.6%

Table 7.3 Average and peak efficiencies of each component in the Micro-cab power-train

²¹ Actual efficiency calculated through real-time data under campus drive cycle.

7.3 Postal Service

The University of Birmingham employs a fleet of 110 vehicles for deliveries and other duties, many of which are small vans with similar format to that of the Micro-cab, such as Ford Connect van for postal service. One Micro-cab H4 was modified in order to serve the postal routine has been shown in Figure 7.1. The records show an average speed of just 2.6 mph due to numerous stop/start involved in this duty cycle. The postal results were also compared with academic drive cycle (as pictured in Figure 7.18) where the vehicles were driven in a loop around the perimeter road, in which stop/start cycles were reduced to a minimum.

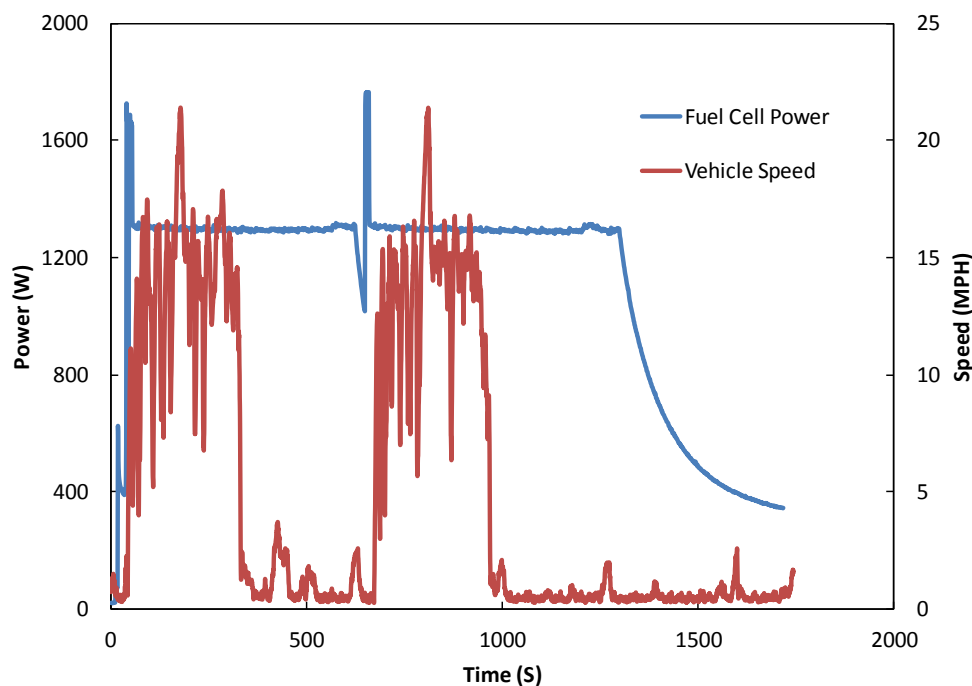


Figure 7.18 Academic drive cycle

7.3.1 Energy Consumption

Figure 7.19 show the results for both Ford Connect diesel van and Micro-cab H4 hydrogen fuel cell vehicle driving under postal and academic cycles in terms of energy consumption. It

can be seen that the postal cycles were worse than those from the academic cycles for both vehicles, and the hydrogen fuel cell H4 has better energy efficiency in both cycles. Under the academic drive cycle, the Micro-cab H4 consumed 1.4MJ/km, which was only about half that of the diesel van. During the 160 individual postal duties, total 281 kilometres has been done and 5kg of hydrogen was refilled. Giving energy consumption was 2.49MJ/km HHV during the postal run, which corresponded to 0.41km/MJ HHV (44 mpg diesel equivalent), this was an improvement on the diesel van which was 28mpg but only half of the efficiency of the academic run.

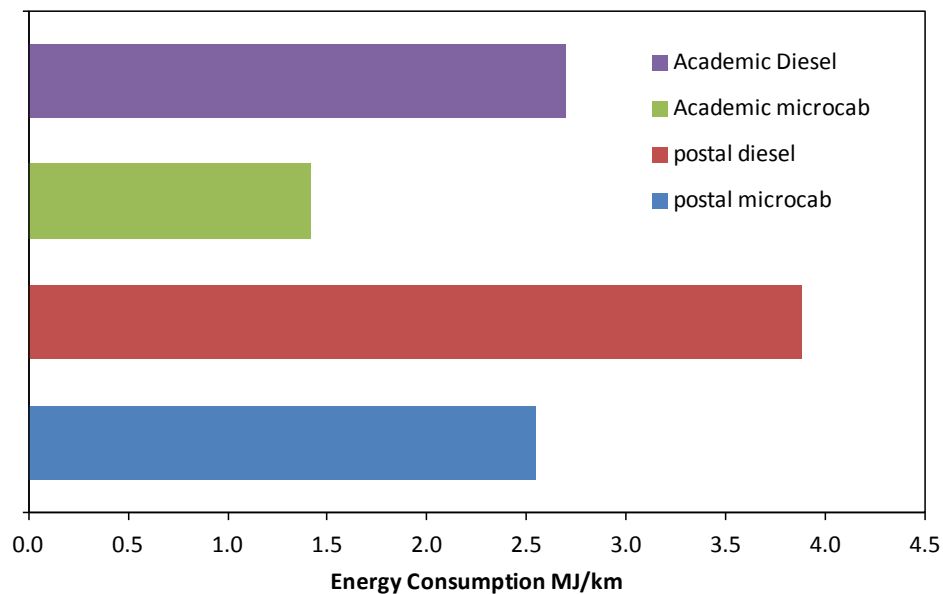


Figure 7.19 Results for both Ford Connect diesel vehicle and Micro-cab H4 hydrogen fuel cell vehicle

7.3.2 Carbon Footprint

The Micro-cab H4 only emits water hence the overall carbon footprint has been compared through energy measurements instead of measuring tailpipe carbon emissions. The postal vehicle drove 27km a week in average, around 1300km a year. The fuel consumption was 28mpg for the diesel van. In total 131.1L or 4712MJ LHV of diesel were required; CO₂

emissions from combusting diesel were 74g per MJ of fuel used. Extraction from the ground and refinery operations added 14% to this. Therefore the well to wheel equals 86g per MJ, so that the carbon footprint annually was 405.2kg.

The Micro-cab H4 need 22.6kg hydrogen a year to provide postal services. The hydrogen used was sustainably-sourced from Green Gases of Cambridge. The hydrogen was generated from renewable electricity that was in turn produced on site from digesting agricultural wastes. The carbon footprint of this hydrogen was estimated to be 18g/MJ. Nearly two thirds of this was for transport from Cambridge to Birmingham in steel containers by truck. So the total carbon footprint annually for Micro-cab H4 was 48.7kg, with a reduction of 88% compare to the diesel van.

7.4 Discussion and Recommendations

From the results shown in the previous sections, giving the reasons for inefficient operation of the fuel cell vehicles, it is clear that the Micro-cab required improvements in the following areas.

7.4.1 Sufficient Fuel Cell Stack with Improved Control

At present the Ballard 1.2kW fuel cell cannot match the average driving power requirements, as operating continuously in the campus duty cycle requires 2.24kW average power. A 4-5kW fuel cell would be ideal to conduct this duty cycle. However, a higher speed drive cycle required for urban applications will further increase the size of fuel cell. In addition, currently the fuel cell is dynamically providing the load demanded by the batteries and motor, and a 7 minutes relay will turn it off after the ignition has been taken out whatever the battery SoC was. But in practice it proved to be problematic as there was no calculation

of how the vehicle had been driven which means if the vehicle had been driven to complete depletion of the battery, 7 minutes is not enough to replenish the battery, leaving the batteries almost empty for the next drive. On the other hand, if the vehicle had been barely driven, the fuel cell will operate at lower output which just covers the parasitic load. Therefore an improved control strategy is to turn off the fuel cell when the batteries have reached an optimal state of charge; this would improve the combined efficiency of fuel cell and DC converter.

A 48V fuel cell stack can be used, as discussed in Chapter 5, to reduce the number of DC conversion stages, therefore improving total system efficiency, as well as reducing cost and weight.

Another approach is to use a current-limited DC converter with two fuel cell stacks connected in parallel, running each stack at 50% power output. In this case the DC converter would operate at full load, then all the components can reach their optimum efficiency, however, the extra parasitic load for additional fuel cell may offset the benefit.

7.4.2 Advanced Battery or Ultra-capacitors

Integrating a larger capacity of battery or super capacitors will provide greater peak cranking power and allow regenerative braking. For example, to replace the lead acid batteries with a state of the art lithium phosphate battery will provide 5 times more energy with the same weight. Larger capacity of electric storage device will also allow the fuel cell to operate at

more steady conditions, and allow the vehicle to have a plug-in feature which will reduce the dependency on hydrogen fuel.

7.4.3 Permanent Magnet Electric Motor

Another improvement could be realised by replacing the Separately Excited GE motor with a permanent magnet electric motor, hence eliminating the power required to generate the magnetic field. AC motors generally have higher voltage efficiency, but the controller costs more and the additional stage of power conversion from DC to AC will not only add the cost and complexity, but may offset the gained efficiency.

7.4.4 Projected Power-train Efficiency

Calculation of the above proposals suggests that the power-train efficiency could be doubled from 18 to 36% whilst keeping the weight similar (see Chapter 9). This would give an estimated fuel economy of 1.0-1.2MJ/km – equals to 85-102 miles per gallon of diesel equivalent (UK), or 64-76 miles per gallon of petrol equivalent (USA).

7.5 Conclusions

The original prototype Micro-cab H4 has been tested for about 2 years on the campus drive cycle, without any major issue regarding hydrogen and fuel cell operation. The performance of the vehicles was competitive with the University of Birmingham fleets; the power train efficiency was only about 18% but was found to be twice as good as the standard diesel vans used in the postal services.

The fuel cells stacks were found to perform better than expected, however, the main DC converters and the motors were found to perform below anticipations. It was also found that optimal operating points of individual components were shown not to coincide with one another, such as combined efficiency of fuel cell and main DC converter, and the motors often operated outside of its peak efficiency range at low power output.

The findings from this chapter were considered as guidance for the future upgrade. It was manifest that optimising the system as a whole is critical. In order to achieve this upgrading, it was necessary to calculate from the computer model how the hybrid system could be improved, as described in the next chapter.

8. Chapter Eight

Drive Cycle Simulation of Various Vehicle Drive-trains

8.1 Introduction

The energy consumption results in Chapter 7 showed that the Micro-cab presented quite different performance in the different duty cycles. In addition, for the same duty cycle, the fuel consumptions showed a discrepancy when different drivers were used, as Figure 7.19 illustrated. At the same time, the results also indicated that the fuel cell Micro-cab was more sensitive to aggressive drive cycle and driver behaviour than the diesel van. In this chapter, the energy efficiency of the vehicles under different drive cycles will be compared.

8.2 Methodology

The objective was to compare the vehicles' energy efficiency and greenhouse gases of different potential propulsion technologies on an equivalent basis assuming that the size and performance of future vehicles were comparable to 2010 models.

8.2.1 Glider Vehicle

The Volkswagen Golf glider has been chosen as a representative as it is not only the best-selling light duty vehicle according to 2010 sales in Europe, but also the most sold vehicle in history. The main characteristics of the glider are defined in in Table 8.1.

Parameters	Value
Glider mass (kg)	990
Frontal area (m ²)	2.19
Coefficient of drag	0.31
Wheel Radius (m)	0.56
Rolling Resistance	0.08

Table 8.1 Parameters of glider, data based on VW MK VI Golf hatchback

8.2.2 Simulation Method

The vehicle system simulation was performed using ADVISOR[®] (Advanced Vehicle Simulator) software, developed by the U.S. Department of Energy's National Renewable Energy Laboratory's (NREL) for Transportation Technologies and Systems based on Matlab [178].

This means that for every instant of a drive cycle, the required torque and rotational speed are first calculated at the wheel, and subsequently traced all the way to the power source, i.e. engine or electric motor. The structure of ADVISOR makes it ideal for interchanging a variety of components, vehicle configurations and control strategies.

In order to optimise the different power train models' accuracy, parameters like fuel consumption, CO₂ emission, and vehicle range testing under New European Drive Cycle (NEDC) were compared, as shown in Table 8.2. The official results from Driver and Vehicle Licensing Agency (DVLA) have been used for already commercialised power trains, including petrol, petrol-hybrid, diesel and diesel hybrid; the BEV fuel consumption was compared using the near-commercialised NISSAN Leaf, and the FCV fuel consumption was compared using demonstration FC vehicle from Honda and Daimler. It can be seen that the differences between simulation results under NEDC are relatively insignificant; it could be assumed that the differences under other drive cycles would have the same trend.

Power train	Equivalent Model	NEDC Dynametre Results	ADVISOR Simulation Results in NEDC
Petrol	VW 1.4 TSI petrol Golf*	6.29 L/100 km or 144 g/CO ₂ , DVLA	6.3L petrol per 100km
Petrol Hybrid	Toyota Auris Hybrid*	3.75L/100km or 87g/CO ₂ , DVLA	3.9L petrol per 100km
Diesel	VW 2.0 TDI diesel Golf*	4.49L/100km or 119g/CO ₂ , DVLA	4.7L diesel per 100km
Diesel Hybrid	Peugeot 3008 Hbrid4*	3.7L/ 100km or 99g/CO ₂ , DVLA	3.8L diesel per 100km
Battery	Nissan Leaf*	175km range or 1.42L/100km equivalent, Nissan	181km range or 1.5L/100km equivalent
Fuel Cell	Honda FCX Clarity*	3.46L/100km petrol equivalent, H ₂ Move	3.2L/100km petrol equivalent
	Daimler Benz B Class F-Cell*	3.62L/100km petrol equivalent, H ₂ Move	

*From manufacturers official website

Table 8.2 Parameters of simulation models under NEDC

8.2.3 Drive Cycles

In order to better understand the differences on energy consumption under different driving conditions, four representative driving cycles have been selected, as listed in Table 8.3.

Drive Cycle	NEDC	ARTEMIS 130	FTP 72 (UDDS)	WLTC Class 3
Distance	10.93km	50.88km	11.99km	23.26km
Duration	1184s	3143s	1369s	1800s
Average Speed	33.21km/h	58.28km/h	31.51km/h	46.5km/h
Maximum Speed	120km/h	131.8km/h	91.25km/h	131.3km/h
Maxi Acceleration	1.06m/s ²	2.86m/s ²	1.48m/s ²	1.75m/s ²
Max Deceleration	-1.39m/s ²	-4.08m/s ²	-1.48m/s ²	-1.5m/s ²
Idle time	298s	331s	259s	235s
NO. of stops	13	28	17	8

Table 8.3 Characteristic of different drive cycles

8.2.3.1 New European Driving Cycle (NEDC)

NEDC was designed to test typical vehicles (light duty and less powerful compared to U.S.) in Europe; it combines four urban routes and 1 extra-urban route, as shown in Figure 8.1. The urban driving cycle is also known as ECE 15 cycle, introduced in 1970 to represent the driving condition of busy European cities, with a maximum speed of 50km/h; the Extra Urban Driving Cycle (EUDC) is more aggressive with a maximum speed of 120km/h (or 90km/h for low-powered vehicle). With this drive cycle it is widely admitted in the research community that it is much less aggressive than real-world driving conditions [179], as the cycle uses a driving speed pattern of low accelerations (1.06m/s² maximum), constant speed cruises, and long idling period (quarter of total testing time). This can also offer possibilities for automakers to optimise vehicle emission relevant operating characteristic to the test cycle, so called 'cycle beating' [180], hence motorists are likely to experience higher fuel consumption than the approved official figure.

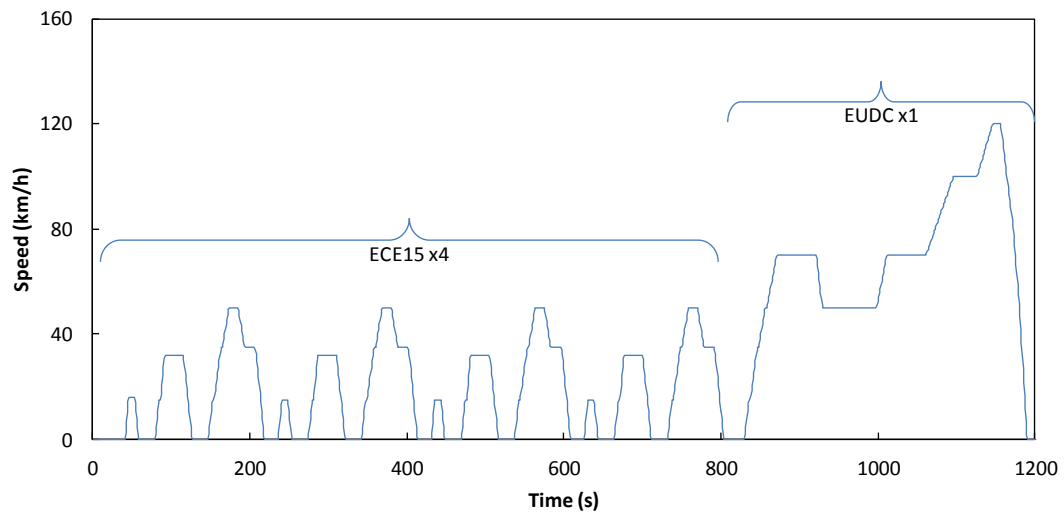


Figure 8.1 New European Driving Cycle

8.2.3.2 Common ARTEMIS Driving Cycles (CADC)

CADCs are chassis dynamometer procedures developed within the European ARTEMIS (Assessment and Reliability of Transport Emission Models and Inventory Systems) project [181]. Unlike the EUDC, the ARTEMIS includes 3 major “real-world” driving cycles (urban, rural and motorway), as shown in Figure 8.2. There are two different motorway sections with top speed of 130km/h and 150km/h respectively. In this analysis, the lower top speed of 130km/h was chosen with the consideration of energy consumption. The cycles are based on statistical analysis of a large database of European real world driving patterns. (totally 12 in specific²²), ranging from congested urban to steady speed motorway [182]. Therefore the drive cycle testing results are representative and are closer to reality.

²² (1) Congested urban (2) Urban dense (3) Urban low speed (4) Urban free-flowing (5) Urban unsteady (6) Secondary roads unsteady (7) Secondary rural roads (8) Rural roads steady speed (9) Main-road unsteady (10) Main-road steady speed (11) Motorway, unsteady (12) Motorway, steady speed.

The ARTEMIS drive cycle covers 50.88km, 5 times more than that of NEDC. It is also much more aggressive with acceleration up to 2.86m/s^2 and deceleration up to 4.08m/s^2 , so that for the same vehicles, ARTEMIS tests are expected to consume a greater amount of energy than NEDC tests.

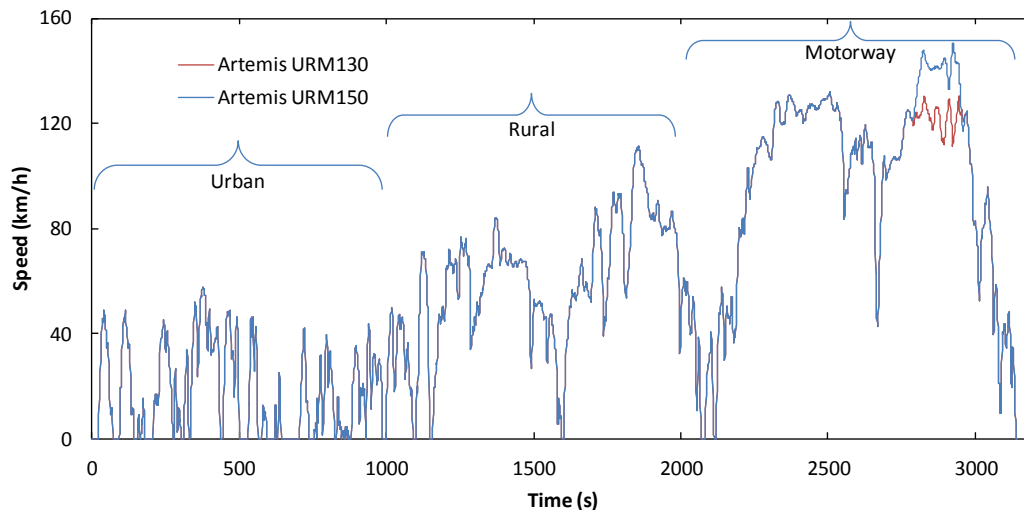


Figure 8.2 ARTEMIS (Assessment and reliability of transport emission models and inventory systems) driving cycle

8.2.3.3 Urban Dynamometer Driving Schedule (UDDS)

The UDDS is also known as FTP 72 (Federal Test Procedure U.S.) which represents the scenario of light duty vehicles under urban drive conditions with frequent stops and starts. This cycle has two phases: the “cold start” phase of the first 5.78km at 41.2km/h average speed, and the “transient phase” after 10 minutes stop follow the first phase, to cover the remaining 6.29km, as shown in Figure 8.3. Since 2000, FTP 75 has been used in emissions certification of light duty vehicles; the first 2 sections are the same as that of FTP 72, but adding another same phase with hot engine and the air-conditioner on. The FTP 72 has been used in this analysis because the focus was on drive cycles rather than on the auxiliary load.

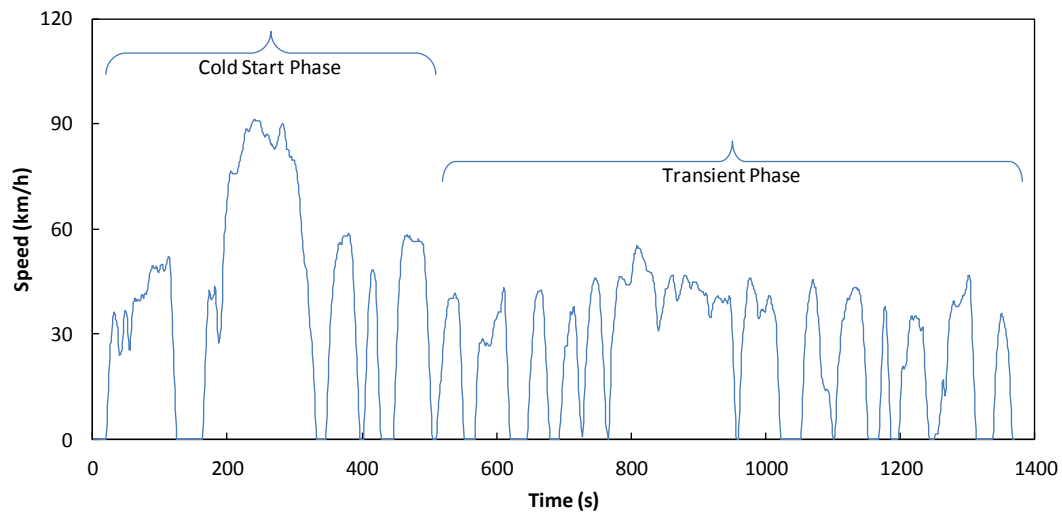


Figure 8.3 Illustration of FTP 72

8.2.3.4 Worldwide Harmonized Light Duty Driving Test Cycle (WLTC)

The WLTC was developed based on combinations of collected in-use data and suitable weighting factors in China, EU, India, Japan, South Korea and U.S., which will include typical driving conditions worldwide [183, 184]. It has 3 different classes defined by the ratio of rated power in W / kerb mass in kg²³,

- Class 1: ratio ≤ 22 , this is for ultralow-powered vehicle, for example, Micro-Cab H4's motor was rated as 2.4kW with kerb mass of 650kg, giving a ratio of just 3.7.
- Class 2: ratio > 22 but ≤ 34 , designed for low-powered vehicles, however there are not many vehicles that could fit in this class, the well-recognised urban vehicles such as Smart, Nissan Leaf and Mitsubishi IMEV all have a higher ratio²⁴, however, fuel cell hybrid vehicle like new Micro-cab H₂EV is in this class [52].
- Class 3: ratio > 34 , most of the vehicles can be allocated in this class; the cycle as shown in Figure 8.4, contains different speed and acceleration requirements from

²³ The total weight of a vehicle with standard equipment.

²⁴ According to the fact sheets on official websites of Smart, Nissan, and Mitsubishi.

low to extra high, and the testing cycle covers 23.26 km with an average speed of 46.5km/h.

Although this drive cycle is still under development with the final version expected in 2013-2014, it is well suited for comparison purposes in this study.

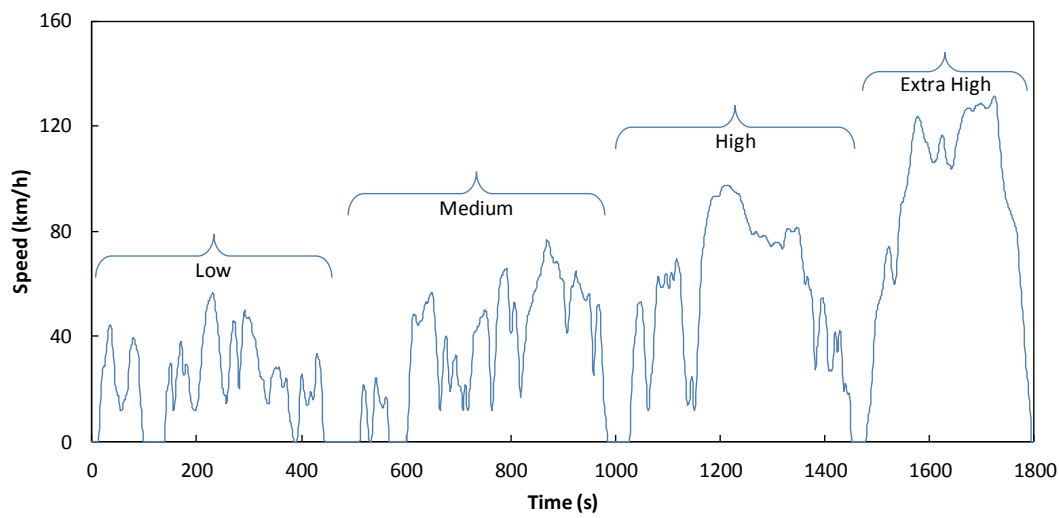


Figure 8.4 WLTC Class 3 drive cycle

8.2.3.5 Cycle Testing Mode

In order to minimise the impact of the 'cold start' phase and to measure the differences between each drive cycle, it is essential to equalise the distance of different drive cycles. Providing the ARTEMIS is the longest cycle of 50.88km, 4 times NEDC and FTP 72, and 2 repeated WLTC were simulated.

In addition to individual drive cycles, a combined drive cycle contains all drive cycles (4 individual cycles were performed consecutively) was also simulated.

8.3 Results

8.3.1 Fuel Consumption

To compare the fuel consumption of different power trains under different drive cycles, the vehicles were firstly simulated without cargo mass, with a hypothesis that a constant electric auxiliary load is available throughout the whole testing and the ambient temperature remains at 20°C. Figure 8.5 shows the fuel consumption (L/100km) of each test. It can be seen that:

- Conventional petrol power train has similar results under NEDC, ARTEMIS 130, WLTC and combined drive cycles, with a stable consumption of around 6L/100km, apart from the result from FTP 72 of 10.6L/100km, which is about 1.7 times higher.
- Petrol electric hybrid power train consumes, as expected, around 1/3 less energy in every drive cycle. Nevertheless this advantage is more obvious in a less aggressive drive cycle, such as NEDC, and vice versa.
- Conventional diesel power train consumes around 20% less energy than petrol vehicle, even though the fuel consumption figures were already converted to petrol equivalent (lower energy density fuel). Basically, the fluctuations between different drive cycles are highly similar to that of conventional petrol vehicle.
- Diesel hybrid power train demonstrates a slightly better performance than conventional diesel vehicle, but the trivial margin of improvement is yet enough to surpass petrol hybrid power train which costs less energy due to the lighter weight in general.
- Battery vehicle displays much lower energy consumption, needs up to 4 times less fuel than others under NEDC drive cycle. Even its worst result occurs in FTP 72 drive

cycle equals to the consumption of the most efficient petrol hybrid power train in the least aggressive NEDC drive cycle.

- Fuel cells vehicle has better results than any IC engine based or IC engine hybrid vehicles, under every drive cycles, but more fuel consumptive than BEV as expected.

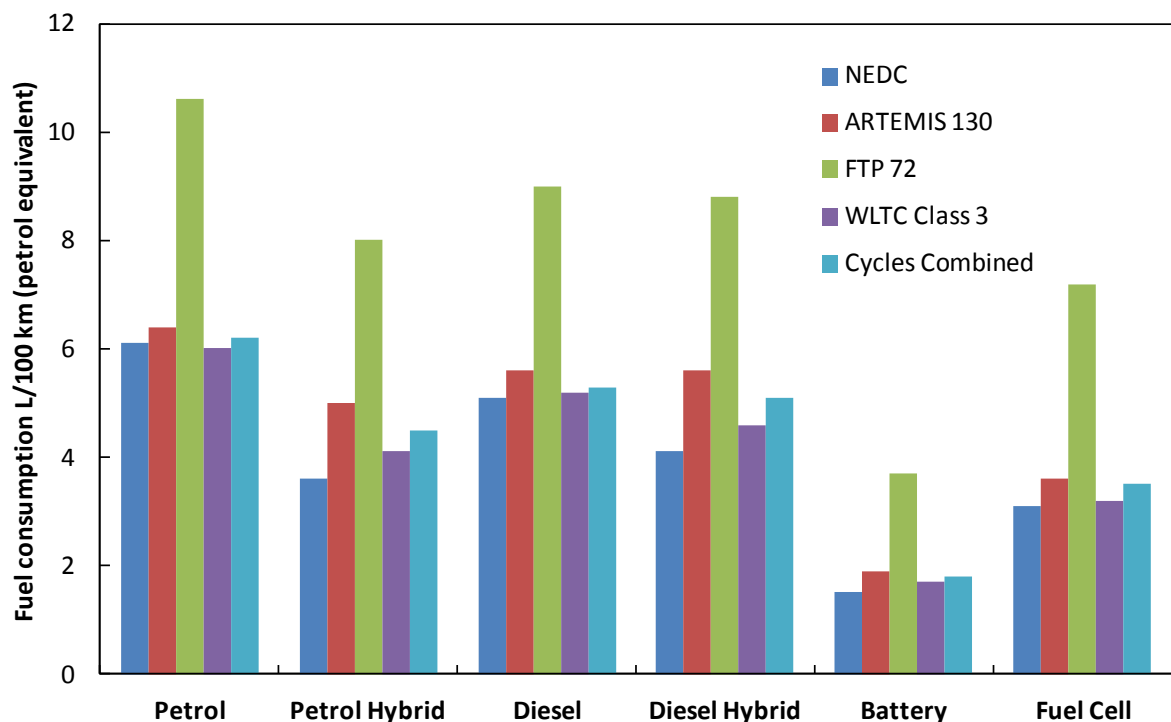


Figure 8.5 Fuel consumption of different power train under different drive cycles

These results prove that different drive cycles would affect the energy consumption greatly. Conventional vehicles such as petrol and diesel power trains are less sensitive compared to their electric hybrid version. As indicated in Figure 8.6, battery and fuel cell electric vehicles are more sensitive on aggressive drive cycles, such as FTP 72, especially for pure battery vehicle, consuming up to 2.5 times more energy from one drive cycle to another (for example, when comparing FTP 72 against NEDC). Figure 8.5 shows both petrol hybrid and

diesel hybrid power train were influenced significantly by different drive cycles, for instance their efficiency under NEDC and ARTEMIS 130 were remarkably altered, while all other power trains were less affected by driving conditions when testing under these two cycles, showing a similar consumption. This simulation also demonstrates that the results from combined drive cycle can be used as the best representative result.

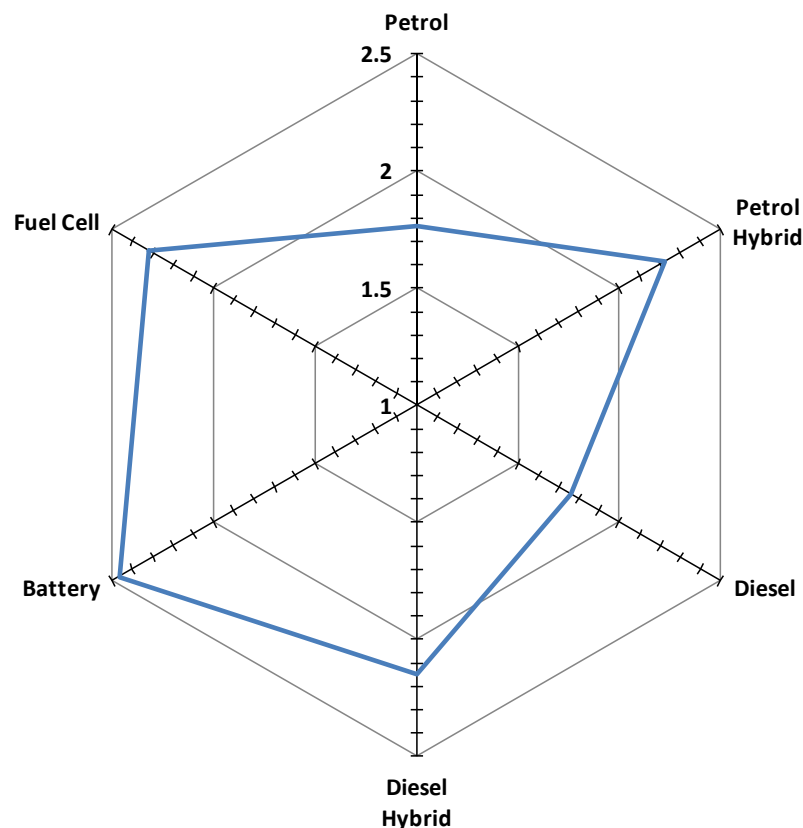


Figure 8.6 Degree of sensitivity of power train to drive cycles (ratio of different drive cycles)

8.3.2 Tank to Wheel (TtW) Efficiency

Figure 8.7 shows the TtW efficiency of all power trains under all 4 drive cycles and the combined trip. It is manifest that the battery vehicle is the obvious winner, achieving up to 70% power train efficiency, and is at least 3 times better than any IC engines power train; followed by the fuel cell vehicle, with about half of the efficiency of battery vehicle, because

the fuel cell itself has a typical efficiency of 50%. However, this result is still superior to any IC engines based and IC engines hybrid power trains.

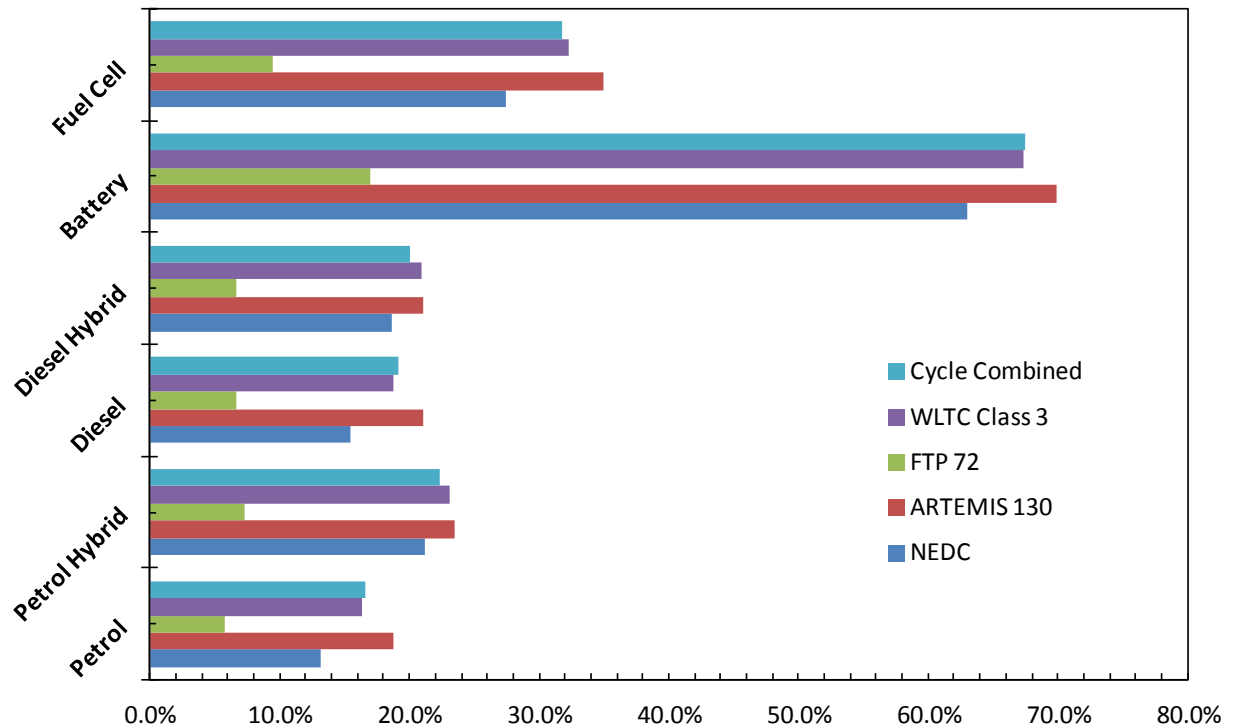


Figure 8.7 Power train Tank to Wheel (TTW) energy efficiency of different power train under different drive cycles

8.3.3 Fuel Consumption with Increased Weight

According Coulomb's friction law, the vehicle weight could heavily affect the energy consumption, hence the fuel consumptions of different power trains with different payload has been analysed. From the manufacturers' specification, the MK6 golf has a maximum payload between 511 and 644 kg. Because the extra weight of the battery in some hybrid models, such as diesel hybrid, the lower limit 511kg was used along with other 2 different loads: 150kg payload (2 passengers) and 350kg payload (4 Passengers with luggage). The simulation runs under the combined drive cycle, totally 97.1km.

The simulation results are shown in Table 8.4, it can be seen that with the increasing payload, the fuel consumptions of all power trains grew accordingly, but rising with different

percentage. For example, from unladen to maximum payload, the petrol power train needs 1 extra litre fuel, and fuel cell power train needs 0.6 litres extra. In theory, one can argue that the fuel cell vehicle is superior to conventional vehicle when carrying extra load. However, the increments shown in Figure 8.8 demonstrate that the fuel cell power train has a very similar sensitivity of petrol vehicle towards payload; it also shows that the conventional diesel power train was least impacted by various weights, whereas the battery power train and petrol hybrid power train were sensitive to weight to a large extent.

	Unladen (L/100kg)	150kg Payload (L/100kg)	350kg Payload (L/100kg)	511kg Payload (L/100kg)
Petrol	6.2	6.5	6.9	7.2
Petrol Hybrid	4.5	4.8	5.1	5.4
Diesel	5.3	5.4	5.8	6.0
Diesel Hybrid	5.1	5.3	5.7	5.9
Battery	1.8	1.9	2.1	2.2
Fuel Cell	3.5	3.6	3.9	4.1

Table 8.4 Fuel consumption with different weight under combined drive cycle

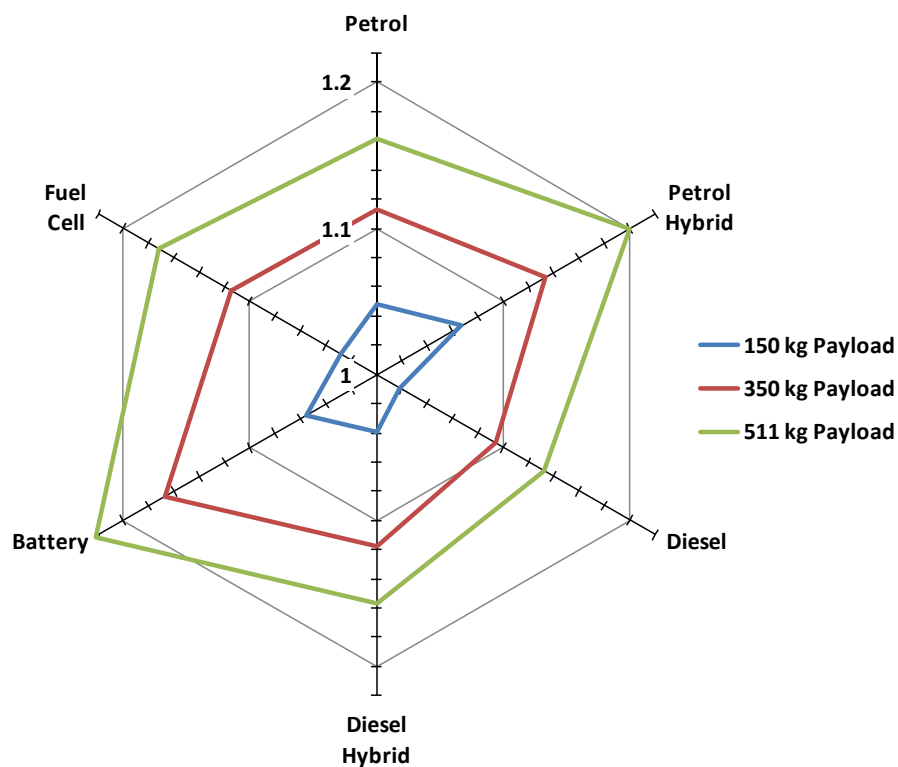


Figure 8.8 Power train fuel consumption sensitivity ratio for 150 kg, 350 kg and 511 kg payload.

8.4 Conclusions

A model analysis has been used to compare different types of vehicle drive trains under various drive cycles. Although battery and fuel cell power trains are more sensitive to differences in drive cycle, battery power trains are also more sensitive to extra payload. However, due to the high TtW energy efficiency and low absolute fuel consumption figures, the energy efficiency of fuel cell and battery vehicle would still be superior to any IC engine based and IC engine hybrid vehicle, whatever the drive cycle and payload.

9. Chapter Nine

Upgraded Version of H4 Micro-Cab

9.1 Introduction

In response to the weaknesses of the Micro-cab prototypes described in chapters 6 and 7, H4 004 Micro-Cab has been re-designed in order to improve the performance and efficiency. In the new design, a larger fuel cell was used to increase efficiency. Also, higher energy density lithium ion phosphate batteries replaced lead acid batteries; they were composite structures with 3kW PEMFC without DC-DC converter to prevent the energy being lost via power converters, as discussed in Chapter 5. Two individual Lynch pancake style permanent magnet DC motors powered each rear wheel through a high-efficiency belt & pulley mechanism, controlled by 2 separate Kelly motor controllers. Most of the components were rated at 48V DC to eliminate energy loss during voltage conversions. In addition regenerative braking was now possible.

9.2 Experimental Method

Since the upgrade was based on the original Micro-cab chassis, the best layout of component was not always possible. For instance, although front wheel drive configuration presented better motor cooling and more effective re-generative braking [185], the original Micro-cab was rear-wheel drive and the upgrade had to be designed based on it.

The original vehicle was designed for low speed (30mph) duty cycles, such as driving on campus, in which the aerodynamic drag can be negligible [186], safety crash rating is less critical. Bearing in mind that the stability and braking distance at higher speed are unknown, extra considerations and calculations must be taken to prevent potential failures and dangers at higher speed.

9.3 Upgrades

9.3.1 Individual Electric Motors and Controllers

Conventional vehicles' drive train is often equipped with a differential mechanism to allow the driving wheels to rotate at different speed when turning. The helical gears inside of differential mechanism and gearbox normally have a combined efficiency of 93% [155, 187]. Electric drive trains could employ separate motors for each drive wheel to eliminate the requirement for differential mechanism and gearbox, therefore improving the drive train efficiency by 7%.

The dual-motor and controller electric drive system is not only able to improve the efficiency, but could also enhance the handling and performance. Given the 'steer by wire' system will be installed in future vehicles, the motor controllers can communicate with the electric steering system while cornering. The speed of each wheel can increase or decrease according to the steering signal, limiting the potential under steering or over steering that a vehicle may suffer while turning. Alternatively, the dual motor systems can function as steering system themselves by continuously and individually adjusting the torque and speed of separate wheels according to the steering angle. In addition, since each electric motor achieves its maximum efficiency at higher load, the vehicle could be powered by a single motor where possible (i.e. in a low speed straight line).

In this new design, two Agni Lynch pancake shape light weight permanent magnet DC motors have been used; the specifications are listed in Table 9.1. These high power motors

provide up to 93% efficiency, and could maintain high efficiency over a wide range of loads and speeds as shown clearly in Figure 9.1.

Make	Model	Cont. I at 48V	Max rpm	Cont. kW at 48V	rpm/V	Efficiency	Weight
Agni	95-R	220	6000	9.5	71	Up to 93%	11Kg

Table 9.1 The specifications of Agni Lynch pancake shape light weight permanent magnet DC motors

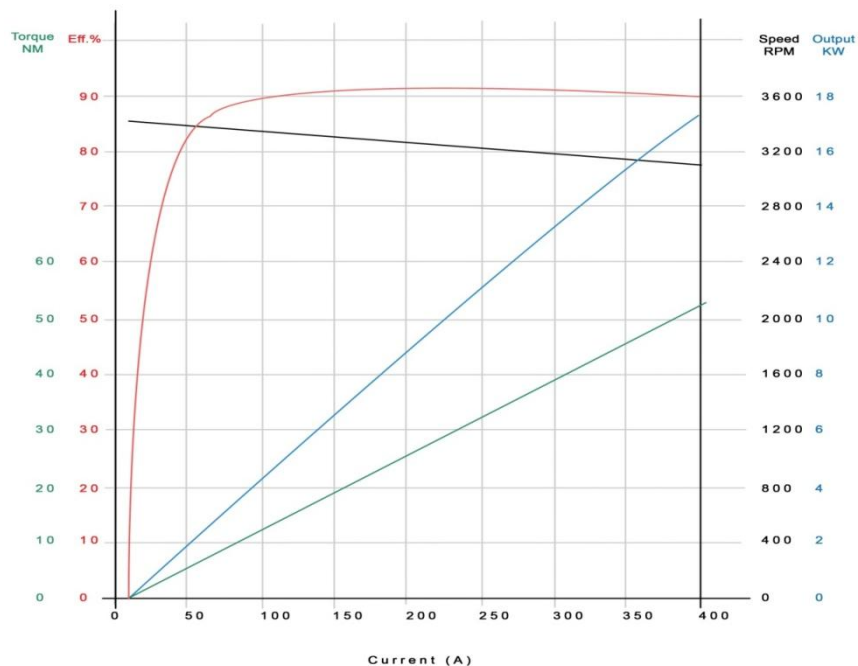


Figure 9.1 The performance of Agni 95-R motor at 48V[188]

9.3.2 Drive the Wheels via Belt & Pulley

There are few options to drive the wheels by individual electric motors. One novel approach is to use in-wheel hub motors which could eliminate the mechanical transmissions such as using reduction gear, drive shaft and axles, presenting a significant weight reduction and manufacturing/assembly saving [189]. But the hub motor has to be insulated from water, mud and impact to which a vehicle wheel normally is subjected. On the other hand, it has to be integrated with a thermal braking system and able to dissipate the heat effectively.

Therefore in-wheel hub motors are normally designed for large OEM production specifically. The key disadvantage of in-wheel hub motors is that the weight of the system, increasing the vehicle un-sprung weight which may reduce vehicle handling and ride [190]. So, the upgrade project chose to use the motors to power individual wheels through separate axles, as illustrated in Figure 9.2:

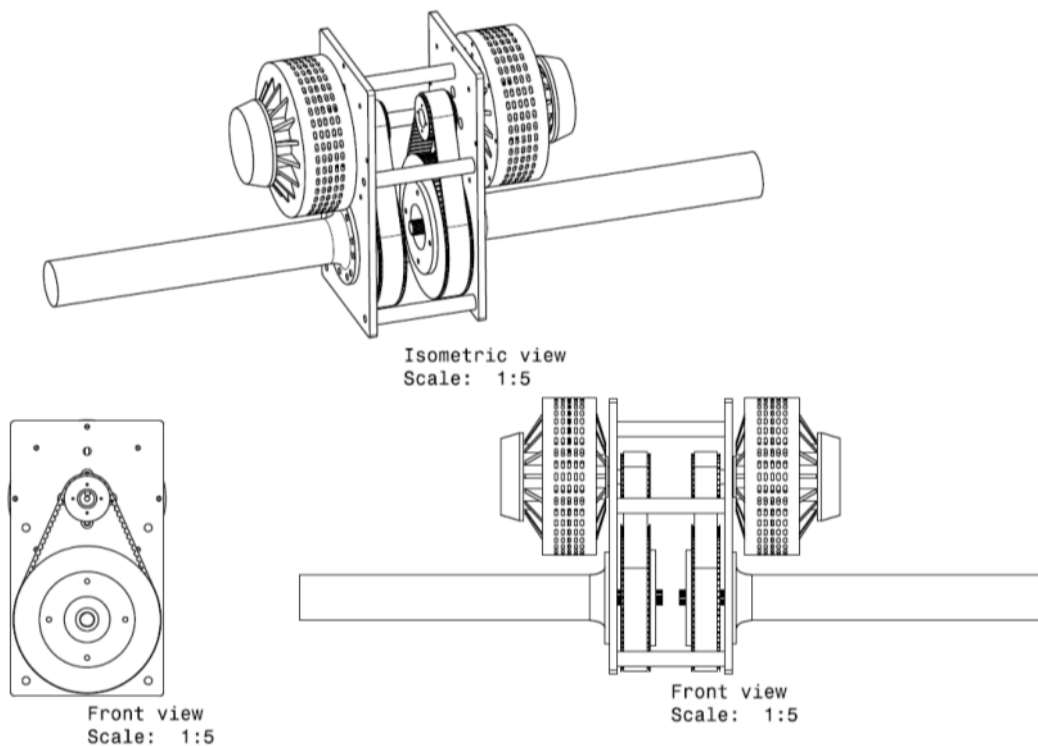


Figure 9.2 Illustration of in-wheel hub motors

The motor drove the wheel axle via a synchronous belt and pulley mechanism, as this is the lightest and most efficient options among spur gears, chain and shaft drive [191]. It also offered quiet, lubricant free and maintenance free operation. In order to increase the torque of the drive wheel and to reduce the top speed of the vehicle (with respect to safety), a 3.2:1 gear ratio was used. Two Kelly PM48501B motor controllers with re-generative braking

function were used on each motor, allowing the user to programme parameters such as current limit and torque control.

9.3.2 Additional PEM Fuel Cell Stack

In order to achieve a Charge Sustaining (CS) drive, the fuel cell should be able to supply the average power to complying with the requirement of the given drive cycle. The 1.2kW Ballard Nexa fuel cell was not sufficient to provide the sustainable power required for the ECE15 drive cycle, hence an additional 3kW PEM fuel cell manufactured by Horizon was installed in the front of the vehicle, as shown in Figure 9.3.



Figure 9.3 Horizon 3 kW PEM fuel cell at front to supply the traction power

This fuel cell could be considered either as a charger to charge the battery pack, or the source to supply traction power to the electric motors directly along with the 1.2kW Ballard

Nexa stack, when the motor needs to reach the maximum power, especially when quick acceleration and higher power for climbing hills are needed.

From the results achieved in Chapter 7, the DC-DC converter between fuel cell and batteries dissipated more than 20% of the fuel cell power, and the combined battery/fuel cell without DC-DC converter proved to be workable in Chapter 5. This concept has been adopted in this new design. Therefore the fuel cell has been carefully selected with respect to its I-V curve, in order to match the traction motor and batteries. Table 9.2 gives the specifications of the fuel cell.

Number of Cells	72
Rated Power	3kW
Operating Point	70A @43.2V
H₂ Pressure	0.45-0.55 bar
Size (with fan & casing)	51 cm x 16 cm x 35.5 cm
Flow rate at max output	42 l/min @SLPM
Start-up time	≤30S at ambient temperature 20°C
Efficiency of stack	40% @ 43.2V
Low voltage shut down	36V
Over current shut down	90A
External power supply	13V(±1V), 5A~8A

Table 9.2 Specifications of Horizon 3kW PEM fuel cell

9.3.3 9 kWh LiFePO₄ Battery

The battery in a fuel cell hybrid vehicle has to undertake three functions:

- Firstly, it is the energy source for fuel cell's start-up and pre-heating and provides energy to the motor.
- Secondly, it acts as the Peak Power Source (PPS) to assist in acceleration.
- Thirdly, it captures braking energy during deceleration.

The lithium ion phosphate battery (LiFePO₄) is seen as the most suitable lithium based battery for automobile use, owing to its high energy density, specific power and safety features [192, 193].

16 units of 3.4V 180Ah LiFePO₄ batteries that were connected in series configuration (54.4V) have been used in the system, storing up to 9.8kWh of energy, which was 6 times more capacity than that of the original lead acid battery pack, however with only 30kg addition in weight. The large capacity battery pack could enable the vehicle to use plug-in features, as well as to capture braking energy effectively during vehicle deceleration. For a fuel cell and battery hybrid vehicle, this larger battery pack could be hybridised with a relatively smaller fuel cell stack running at the most efficient point, allowing the fuel cell life to be prolonged.

9.3.4 System Configuration

Figure 9.4 illustrates the configuration of the revised system. As it shows, two fuel cell stacks were connected in parallel to provide electronic power to battery and motor controllers, and they shared the same hydrogen supply with different pressure regulators.

It can be seen that Fuel Cell 2 (Horizon 3kW) provides all its power directly to the battery, without powering conversion or auxiliaries load; Fuel Cell 1 (Nexa 1.2kW), however, only provides traction power when the vehicle needs extra power, but continuously supplies power to auxiliaries via the 24-12V converter, while also powering both the fuel cell controllers.

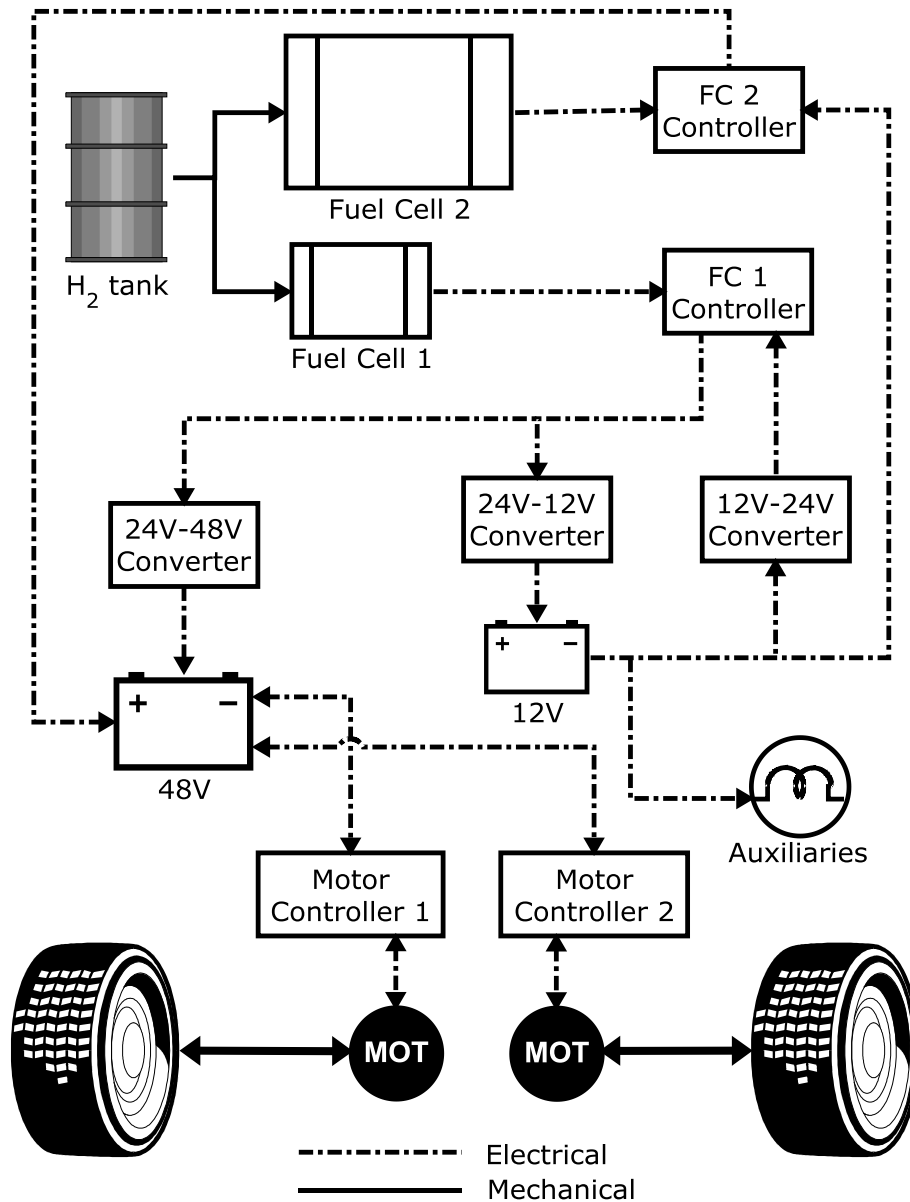


Figure 9.4 Upgraded power train configuration

9.3.5 Data Collection

A customised data logging system has been designed and installed in-house. The off-shelf Squirrel 2010 data logger has been used to collect 8 different currents and voltages across fuel cells, batteries, motor and motor controller, with a frequency of 1Hz, as listed in Table

9.3. The current sensors were adopted from the previous Tempus data logging system, re-arranged and programmed to suit the new power train.

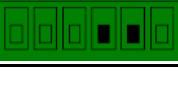
Component	Sensor Type	Connection
Battery Voltage ²⁵	Voltage - Single ended (-18.129 to 75.538V)	3x resistors 
Ballard FC Current	Voltage - Single ended (-847.5 to 352.5A)	LEM current clamp 
Horizon FC Current	Voltage - Single ended (-848.6 to 351.4A)	LEM current clamp 
Motor controller Current ²⁶	Voltage - Single ended (-844.59 to 355.41A)	LEM current clamp 
Motor Voltage+	Voltage - Single ended (-18.129 to 75.538V)	3x resistors 
Motor Voltage-	Voltage - Single ended (-18.129 to 75.538V)	3x resistors 
Ballard Voltage	Voltage - Single ended (-18.129 to 75.538V)	3x resistors 
Motor Current ²⁷	Voltage - Single ended (-845.08 to 352.38V)	LEM current clamp 

Table 9.3 Data logger settings

Due to the limited inputs of the data logger, not all of the data could be collected at the same time. In order to get the most of the important ones, a ‘shared collection’ strategy was used. For example, only one motor’s current and voltage were collected, assuming the other one was the same all the time in straight line driving. To check this, an initial test for both motors was carried out. Figure 9.5 shows the motor current of each wheel when driving in campus, the blue line represents the driver side motor, and the red line represents the

²⁵ LiFePO4 traction Battery’s voltage will be same as Horizon fuel cell when fuel cell is running.

²⁶ The motor controller current is the total current going in for both motor controllers.

²⁷ Only one motor current has been recorded, assume these two motors have same current all the times, because the test track is straight line.

passenger side motor, this test drive contained both forward driving and reverses driving, with different speeds and lots of turnings. It shows the currents from both motors were matched 99% of the time. In straight line testing, both motors output the same amount of power, hence data collected from one motor also can be used on the other one. However, attention needs to be paid at higher current output because at this point the driver side current output was slightly higher than the passenger side, this can be caused by road conditions, tyre pressure and measurement tolerance.

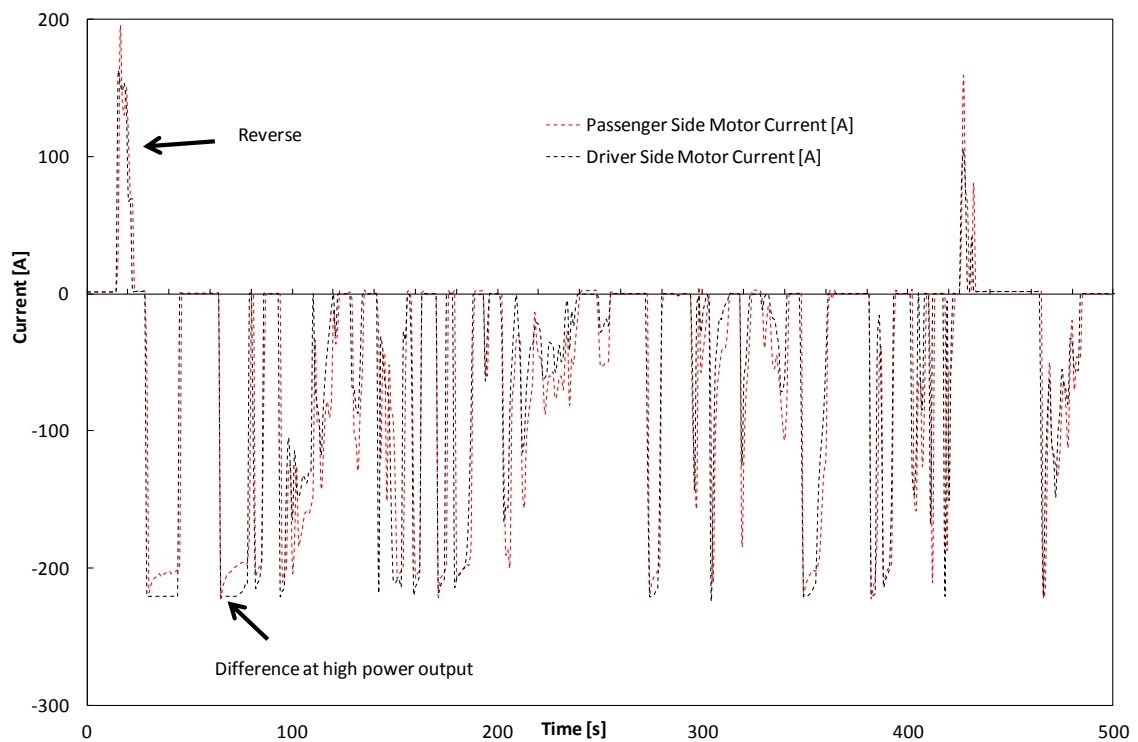


Figure 9.5 Comparisons of passenger/driver side motor current output

The RACE TECHNOLOGY DL1 data logger was used to collect the speed, distance and acceleration data. This high performance data logger can collect data at frequency of 100 Hz, with the speed error below 1% under typical condition. However, to match the Squirrel data logger results, data resolution of 1 Hz has been used in this study [194].

9.3.6 Testing Procedures

The ECE 15 drive cycle was used in these experiments; this cycle is an urban drive cycle (also known as UDC and MVEG-A cycle) used for emission certification of light duty vehicles in Europe and designed to represent European urban driving conditions with low vehicle speed, low engine load, such as in London and Paris. Figure 9.6 illustrates the characteristics of this cycle [195] and Table 9.4 lists the specific figures. This cycle is designed to perform on a chassis dynamometer rather than on the realistic road for tailpipe emission certification purpose. Although the Micro-cab vehicle has no tailpipe emission, this is the standard cycle which well suited the comparison with conventional vehicles.

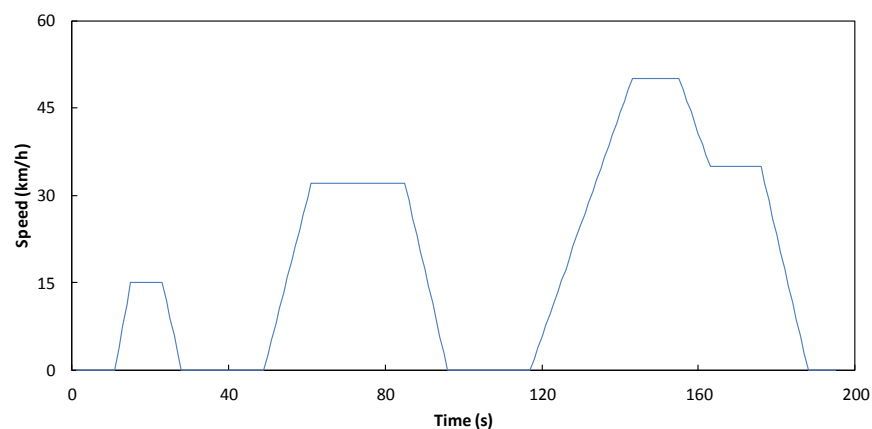


Figure 9.6 Characteristics of ECE 15 drive cycle

Time	195 seconds x 4 = 780 seconds
Distance	1.013 km x 4 = 4.052 km
Max speed	50 km/h
Average speed	18.7 km/h(with idling)
Max acceleration	1.06 m/s ²
Max deceleration	-0.83 m/s ²
Average acceleration	0.64 m/s ²
Average deceleration	-0.75 m/s ²
Idle time	64 seconds per run
Number of stops	3 times per run

Table 9.4 Preference of ECE 15 drive cycle

9.3.7 Test Track

The vehicle has been tested on Shakespeare County Raceway, an airfield style track which is good to test the top speed, acceleration and the ECE 15 drive cycle, as pictured in Figure 9.7. The ambient temperature on the test day was 20°C and wind speed was 9mph. Both batteries and fuel cells performed well under this condition. However, the rolling resistance was much higher than on a standard road, as this track is in general used for drag racing and is covered with rubber, as illustrated in Figure 9.7.



Figure 9.7 Testing track with speed indication of ECE drive cycle

9.4 Results

9.4.1 ECE15 Test without Passenger

First, the vehicle was tested according to the ECE 15 drive cycle with the driver only. The total weight of the vehicle including driver and testing equipment was 750kg \pm 10kg. In order to calculate the energy consumption, hydrogen pressure was recorded before and after the test, the 12V auxiliary lead acid battery voltage was observed and recorded manually, while the traction LiFePO₄ batteries were measured via Grant data logger. Raw results from both the Grant data logger and the Race-Tech data logger have been filtered after test, since the

data loggers were normally turned on a few minutes before the test and turned off a few minutes later after the test. For example, the useful data were effectively collected only within 195s for the ECE 15 drive cycle test as listed in Table 9.5.

	Before	After
Hydrogen Pressure	170	161
Traction Battery voltage	54.003 V	53.799 V
12V battery voltage	13.1 V	13.0 V
Grant Data Logger Clock time	17:17:40	17:20:55
GPS vector time	23	218

Table 9.5 Readings difference before and after ECE 15 testing without passenger

Figure 9.8 has combined both GPS data and electronic data, both horizontal axes represent the time consumed; with different vertical axes representing the speed, currents and voltages. In the upper part of diagram, the GPS speed against time is presented by the blue line; from the shape it can be observed that the figure is fairly close to the ECE 15 drive cycle as illustrated by the black dash line, bearing in mind the human errors; it shows the top speed and acceleration were slightly higher than the standard ECE 15 drive cycle. The red line is the motor voltage, which follows the trend of the GPS speed perfectly, as expected. The green line shows the cumulative distance travelled. The distance travelled was relatively longer than the standard because of the slight errors in acceleration and speed.

The lower part of Figure 9.8 shows the current and voltage characteristics of the major components during the test. These included:

9.4.1.1 Fuel Cell Stacks

As soon as the test started, the 3KW Horizon fuel cell began to charge the traction battery at a rate of 34.3-38.9A, represented by the green line; the voltage (the dark olive line) was

hovering around 54V, which means that at the beginning of the ECE 15 drive cycle idle period, the Horizon charged the battery at the rate of 2kW for 10 seconds. As soon as the

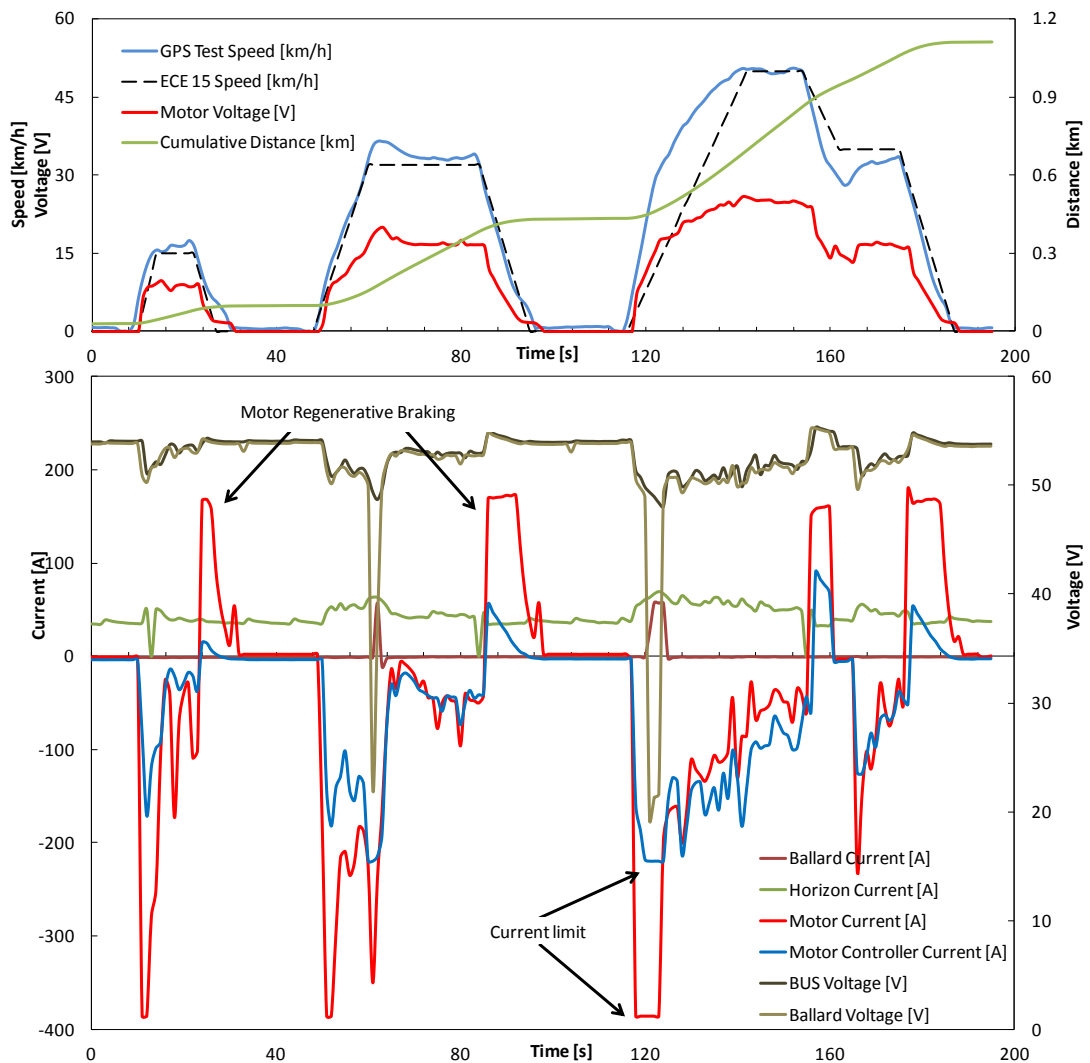


Figure 9.8 ECE 15 drive cycle test without passenger

motor controller commenced drawing power from the battery, the Horizon fuel cell started to react and the output increased to 50.1A at 51.1V, creating an output power of more than 2.5kW. Meanwhile, the Ballard fuel cell only supplied auxiliary power to the 48-12 V DC-DC converter which was continuously charging the 12V batteries which supplied power to the Horizon fuel cell controller. This is because the 24V Ballard has to supply traction power via the 24-48V step-up DC-DC converters which is voltage regulated rather than current

regulated, and the output could only be selected with 10V increments, therefore 50V output has been selected in order to protect both batteries and the fuel cell itself. This setting only allowed the 1.2kW Ballard fuel cell to be engaged when the traction battery voltage was lower than 50V, in another words, at a high power demand point.

The test proved that this concept worked, as reflected in the last section of ECE 15 testing (at reading 120s), when extra power was needed to complete this section. The Ballard fuel cell then engaged and provided a short period of boost to attain the harsh acceleration as shown in the GPS speed curve. The maximum output of the Ballard fuel cell was 57.2A at 21.7V, working at its rated full power. At the same time, a peak output of 69 A at 48.4V was captured from the Horizon. It is evident that both fuel cell stacks could work together very well to output maximum power when required, up to 4.6kW in total (1241.2 W from Ballard and 3339.6W from Horizon).

During the whole ECE 15 drive cycle, a total of 101Wh electronic energy was produced by the Horizon fuel cell stack, and only a fraction was supplied by the Ballard fuel cell which counted 1.8 Wh.

9.4.1.2 Electric Motors

The red line in the lower part of Figure 9.9 represents the individual motor current and the red line in the upper part represents its voltage. It is noticeable that the motor voltage purely corresponds to the vehicle speed, which clearly depicts the 3 sections of the ECE 15 drive cycle. According to the motor RPM and reduction gear ratio, 1V approximately equals

to 2km/h, therefore at the highest speed of this drive cycle, the motor voltage achieved the maximum of 25.9V.

The motor current curve corresponds to the power requirement of the vehicle. It can be seen that for all acceleration sections during the ECE 15 drive cycle, the motor current increased dramatically within few seconds. This is because these accelerations start from 0km/h, therefore the motor voltage started from 0V too. In order to provide the enough power to accelerate the vehicle, a great amount of current needs to be provided. When the speed increased, the current as seen started to decrease. The maximum single motor output recorded in the final ECE drive cycle section was 386.2²⁸ A at 25.2V, giving a total power from the single motor of 9.7kW which was the motor rated power output. At this peak point, other data were as listed in Table 9.6:

Bus Voltage	Ballard Current	Horizon Current	Motor Controller Current	Ballard Voltage
48.4 V	57.2 A	69 A	-219.8 ¹⁹ A	21.7

Table 9.6 Performance of other components at motor peak power output

It can be identified that more than half or the power is drawn from the fuel cell directly when the motor is in full demand, and the battery provides the rest. Despite this heavy load condition only lasted for 2-3 seconds during this test, for most of the time, both fuel cells were able to provide sufficient power to the motors.

²⁸ The figure mechanically limited by the current clamp, the actual figure may be higher.

9.4.1.3 Re-generative Braking

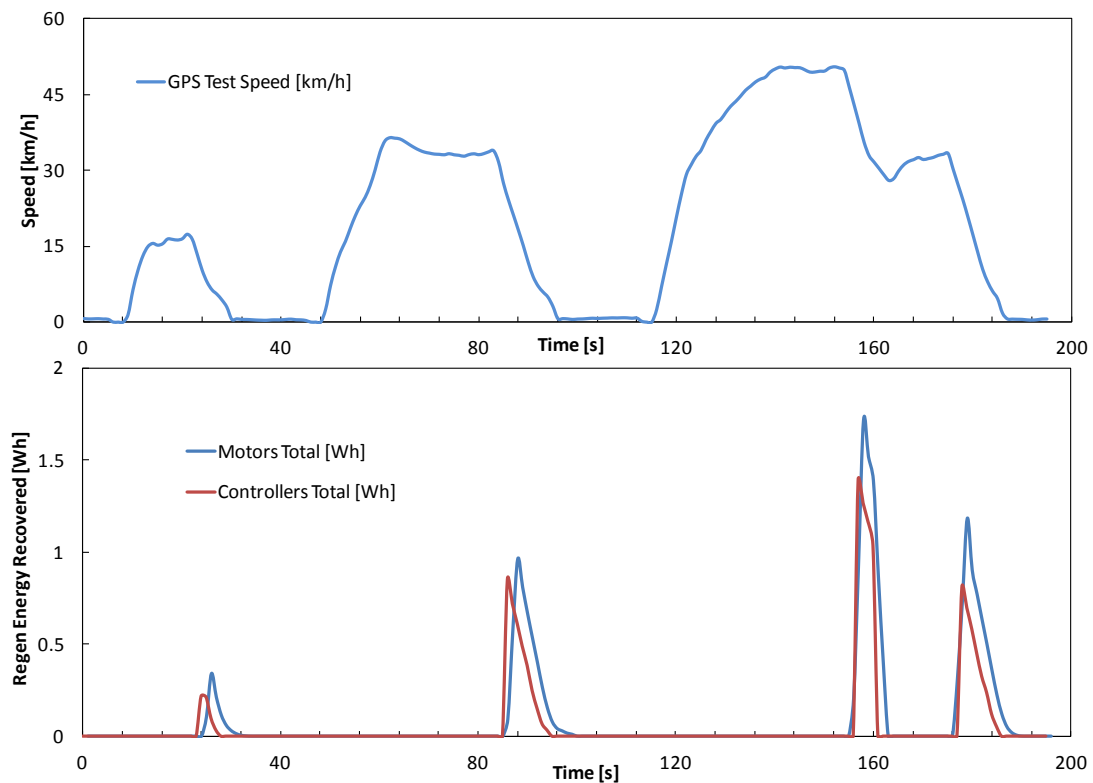


Figure 9.9 Details of energy recovery during the test

The motor controllers have enabled the re-generative braking function during the test, which could then capture the braking energy and replenish the battery in all deceleration cycles. In the whole drive cycle, electric motors totally acquired 18.3Wh braking energy, where 12.2Wh were replenished back to battery through motor controllers. Figure 9.10 shows the details of energy recovery during the test. The energy replenished to the battery contributed 8% of total energy used during the test. Because of the slow deceleration rate of ECE 15 drive cycle, during the deceleration process, the friction brake is only needed at the end of deceleration procedures to stop the vehicle completely.

9.4.1.4 Power Contribution

The battery SoC was floating at 54.003V before the test begins, and dropped down to 53.799V after the test, with only 0.2V decrease. The calculated fuel cells output 123.4Wh during the cycle, whereas the two motor controllers withdrew 144.3Wh, and the regenerative braking gained 12.2Wh, therefore totally 6.5Wh net energy were provided by the battery, which was merely trace amount of its energy capacity. Figures 9.10 illustrated the power split between each power resource. It shows 86% of energy came from the Horizon fuel cell; the battery contributed 4%, which was only half of that provided by the regenerative braking. Ballard fuel cell single engagement accounted for 2%.

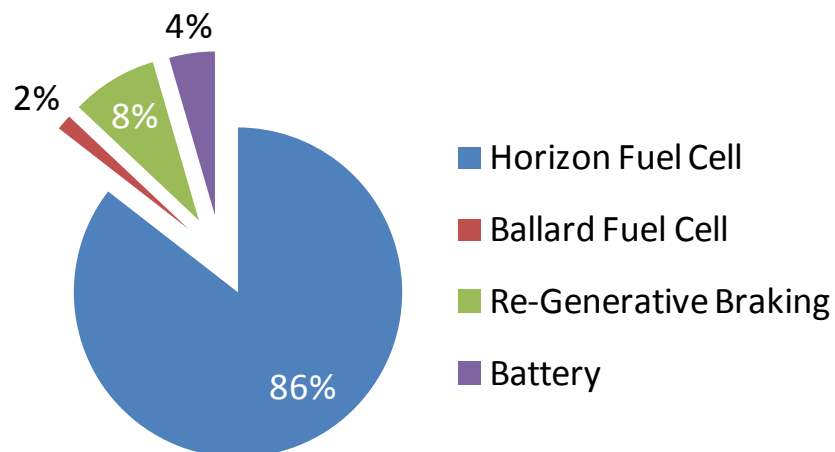


Figure 9.10 Energy split between each power sources of ECE 15 drive cycle test without passenger.

9.4.2 ECE 15 Test with Passenger

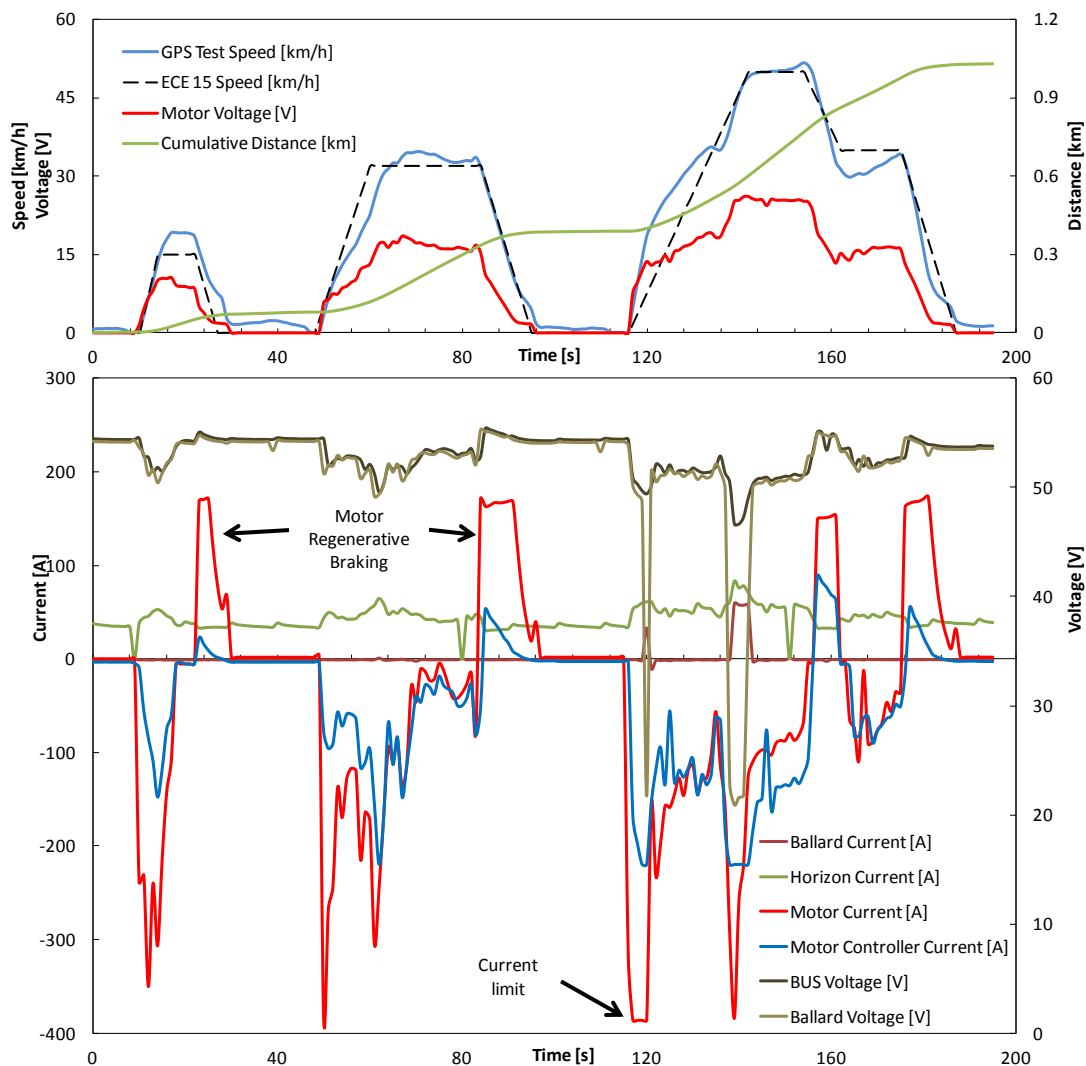


Figure 9.11 ECE 15 drive cycle test with 1 passenger

In order to find out how the weight could affect the fuel consumption, another ECE 15 test has been carried out with one passenger on-board who weighed 55Kg. This brought up the total vehicle weight to $805\text{kg} \pm 10\text{kg}$. Same analysis of vehicle performance has been done, as displayed in Figure 9.11, the result tends to be greatly similar to that of the previous study without passenger. It is worthy to point out that the weight effect may be interfered by human error in precisely following the driving cycle, therefore influencing the results.

	Before	After
Hydrogen Pressure	185 bar	174 bar
Traction Battery voltage	54.029V	53.959 bar
12V battery voltage	13.2V	13.2V
Grant Data Logger Clock time	17:11:40	17:14:55
GPS vector time	100	295

Table 9.7 Readings difference before and after ECE 15 testing with 1 passenger

Further study shows that almost all figures are comparable with the result gained from the ‘without passenger’ test, where Horizon fuel cell provided most of the power, and around 9% was generated from re-generative braking, as Figure 9.12 illustrated. This might be attributed to below facts:

- The interference caused by human error in precisely following the driving cycle may be greater than the impact of adding 55kg weight; heavier weight needs to be added and tested in order to distinct the results.
- The current sensor was restricted to collect the data that are beyond its designed testing range. The limitation points are marked by arrows in Figure 9.9 and Figure 9.12.

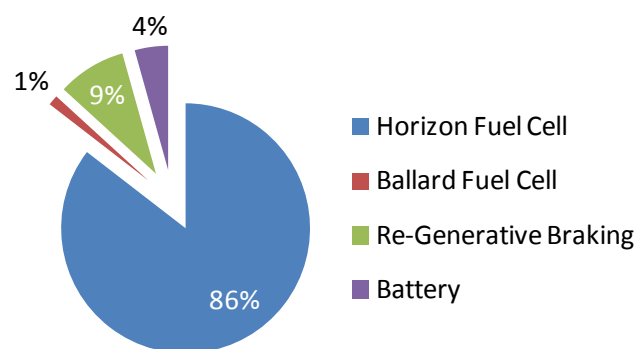


Figure 9.12 Energy split between each power sources of ECE 15 drive cycle tests with 1 passenger.

- Data resolution is only 1 Hz, within which a specific figure can change remarkably; meanwhile the Grant data logger collects data in sequence, which means the current and voltage may not perfectly match each other, however this issue existed among all of the data collections in this study.

9.4.3 Top Speed Test

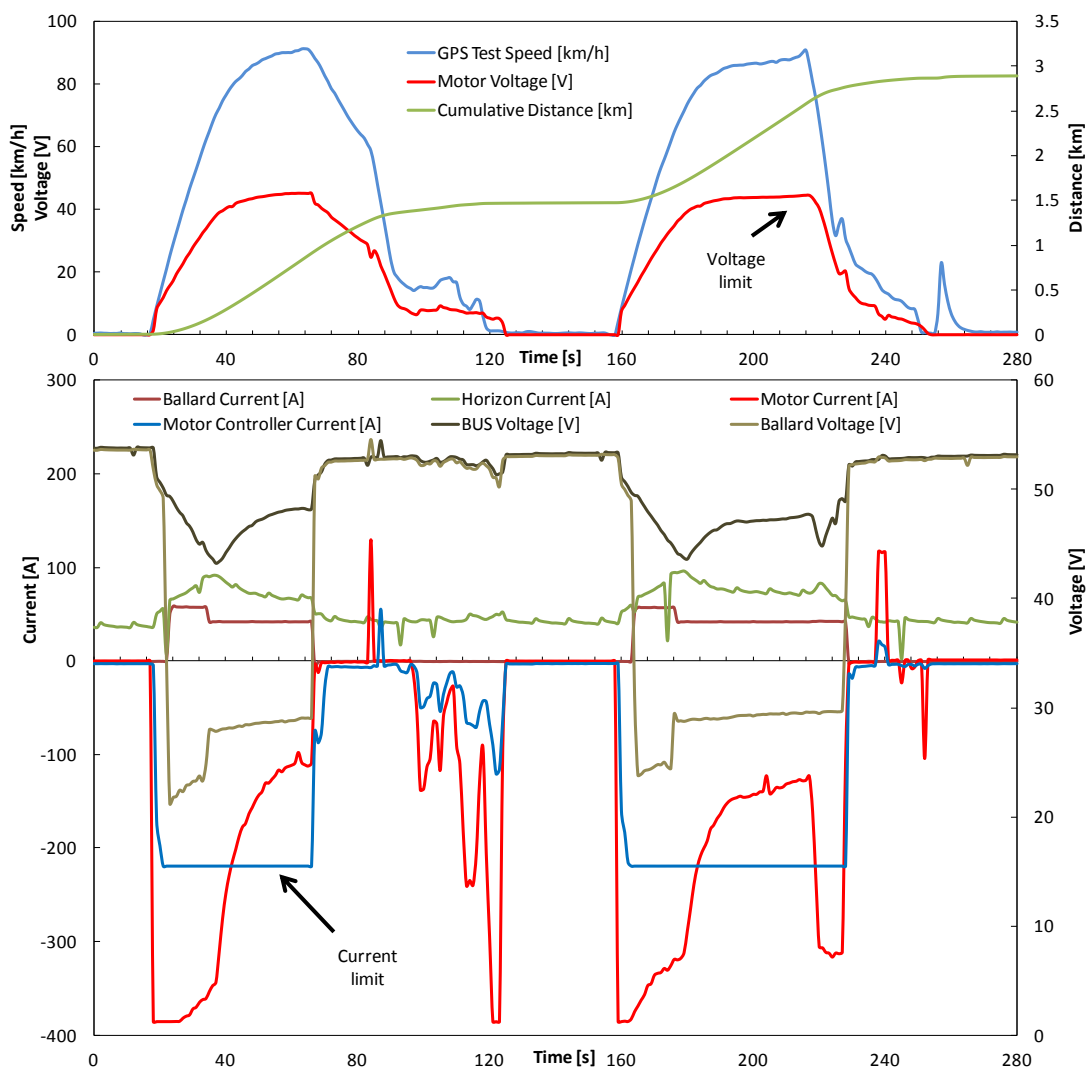


Figure 9.13 Vehicle top speed test

Calculated from the Excel mathematical model, this upgraded vehicle should be capable to cruise at a max speed of 90km/h, which effectively achieves the designed top speed for

NEDC low powered vehicle test. The modelling was based on the 48V systems, and 3.2 : 1 gear ratio, although the vehicle eventually hit the top speed of 91.3km/h, the acceleration rate turned to be extremely low when the speed was above 80km/h, which could hardly match the NEDC low powered vehicle test requirement. In addition, to carry out the NEDC test properly, a straight-line style track of 7km long is necessary, which was proved to be difficult to meet in this test due to the restrained length of the test track selected. Therefore, a top speed test has been undertaken instead of a comprehensive drive cycle testing to investigate the performance of each component, as shown in Figure 9.13.

As to this test, the results show that both fuel cell stacks operated at peak power output point in order to provide sufficient power to motors (see Table 9.8), with the li-ion batteries providing the rest power needed. Each motor provided 8.44kW traction power, which is close to the maximum rated power when the speed reached 80km/h, the reading of the current sensors on the motor controller was limited on 220A at this point of time. According to the efficiency behaviour of the controller manufacturer, the estimated input current should be 378.2A. This means 17,216.7W power was obtained from the battery and fuel cells, where the Horizon fuel cell contributed 3,729W and Ballard contributed 1,169.2W, along with the battery pack which provided the rest, see Figure 9.14:

Battery voltage	Ballard Current	Horizon Current	Motor Controller Current	Motor Voltage	Ballard Voltage	Motor Current
45.52 V	41.47 A	81.92 A	-219.78 A	41.78 V	28.194 A	-202 A

Table 9.8 Performance of other components at vehicle speed of 80 km/h

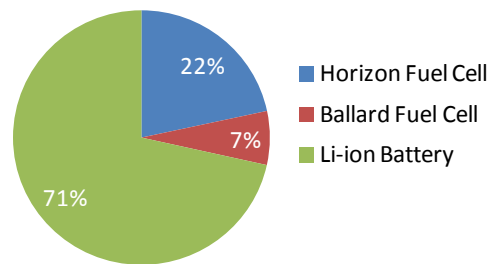


Figure 9.14 Power split between each power sources at vehicle speed of 80 km/h

The overall energy distribution is significantly different with the instant power distribution, as illustrated in Figure 9.15, the Horizon fuel cell still contributed most of the power consumed, however, reduced from 86% to 59% compared to the performance in ECE 15 test. But due to the demand of high power in the top speed test, Ballard fuel cell spontaneously contributed much more power, which was up to 10%. With the continuous acceleration in the test, energy recovered from braking became less, with the power drawn from the battery increased to 30%, equalling to 110.7Wh of energy.

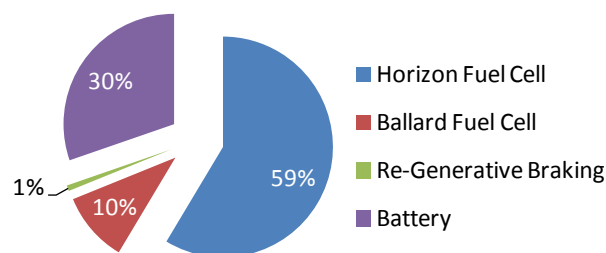


Figure 9.15 Energy split between each power sources of top speed test

The peak motor voltage as recorded was 45V during the test, as the top speed was limited by motor voltage, given the character of those motors are 71RPM per volt, the motor speed should be 3195RPM, and this corresponds to the modelling speed of 91.3km/h. At this point,

the motor voltage was very close to bus voltage. Therefore, it could be deduced that higher speed and acceleration can be achieved with higher voltage supplied, or with greater gear ratio, in order to carry out tests like NEDC or ARTEMIS.

9.4.4 Energy Consumption

The vehicle was upgraded with deliberate consideration of energy efficiency improvement, as expected, the overall results proved that great improvement has been achieved, with totally 23 miles have been done during the test day, combined with different drive cycles tests and load conditions. The hydrogen tank pressure dropped from 299 to 112 bar, as listed in Table 9.9, this equals 35.07MJ LHV, resulting in a hydrogen consumption of 0.98MJ/km which is equivalent to 99.7mpg (imperial), the efficiency was doubled compared to the original Micro-Cab H4 (with average 2.21MJ/km across all 4 vehicles, in Chapter 7), that means with a 2kg pressurised hydrogen store at 350bar (240MJ), such a vehicle had good urban performance and a range of 152miles. The overall battery voltage only increased negligible by 0.1V, and all aspects of the results obtained from both 2 ECE 15 tests were similar, hence the Charge Sustainable (CS) drive has been achieved overall.

Reading	Start pressure	Finish pressure	Temperature	Hydrogen in kg	Energy consumed	Start Voltage of Battery	Finish Voltage of Battery
Overall	299 bar	112 bar	15 °C	0.292 kg	35.07 MJ LHV	52.688 V	52.771 V
ECE 15 Without Passenger	170 bar	161 bar	16 °C	0.016 kg	1.88 MJ LHV	54.003 V	53.799 V
ECE 15 With 1 Passenger	185 bar	174 bar	14 °C	0.019 kg	2.25 MJ LHV	54.029 V	53.859 V
Top Speed	152 bar	136 bar	14 °C	0.029 kg	3.42 MJ LHV	53.842 V	53.164 V

Table 9.9 Parameters change between testing.

However, after the top speed testing, the battery voltage decreased by 0.7V, with the capacity dropped by 110Wh. It can be seen that under this drive condition, the battery cannot sustain its SoC, hence Charge Depleting (CD) drive has been identified. This can be further explained by Figure 9.16, which shows the differences of energy consumption between the ECE 15 and the top speed test. During the ECE 15 test, the fuel cell and regenerative braking provided the most of energy demand, whereas in the top speed test, the regenerative braking barely contributed anything. The power demand was insufficient even both fuel cells output their maximum power. The battery therefore needed to provide extra power. In addition, the continuous high power demand didn't give fuel cell an opportunity to replenish the battery. In other words, the upgraded vehicle is more suitable for urban driving condition.

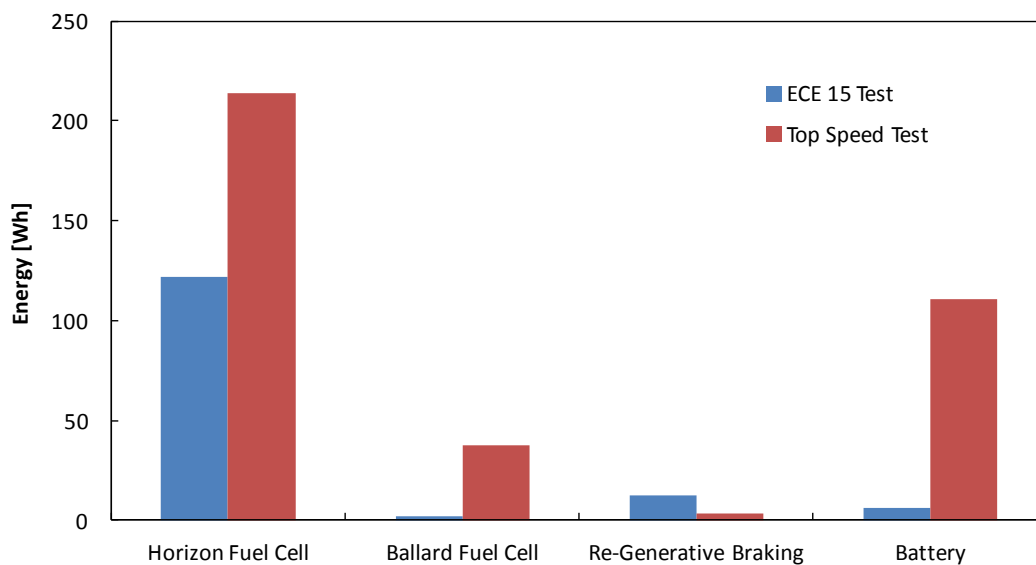


Figure 9.16 Comparisons of energy contribution from different power source between ECE 15 test and Top Speed test

9.5 Conclusions

The improvement on efficiency was obvious, average energy consumption of 100MPG equivalent goal has been achieved, the concept of hybrid fuel cell without DC converter was

proved to work well in practice. However, it is worth pointing out that the fuel cell operated over the rated power output occasionally, therefore further regulating of the fuel cell output could be carried out in future development, such as by regulating the hydrogen flow rate, or by optimising the battery voltage and capacity.

The study shows the Ballard fuel cell only engaged when large power is demanded, however, despite of the high speed test, this fuel cell stack only contributed a trace amount of energy overall. In order to maximise the function of Ballard fuel cell, the controlling strategy could be upgraded, such as introducing an appropriate high efficient DC converter, which could assist the power demand consistently, therefore enhancing its efficiency. Alternatively, it could be excluded when using in low power demand drive cycle, such as in campus and urban.

The regenerative braking could recover 8 -9% energy as demonstrated in ECE 15 test. This figure may be lower in the actual campus and urban drive, as mechanical brakes have to be involved most of the time. The large current generated by sudden deceleration in short period may damage the battery, therefore a super-capacitor would be suggested to be applied for re-generative braking.

Further studies should also investigate the plug-in range, the performance and the running cost, assisting by a data collecting system with higher accuracy.

10. Chapter Ten

Conclusions and Future Works

10.1 Overview

This research has fulfilled the original PhD proposed objectives. The model theory and experimental results were satisfactorily matched, proving that hydrogen fuel cell hybrid technology is superior to other competitive technologies in many aspects, possessing the potential to be the most important power-train in the future automotive market. The detailed conclusions are below.

10.2 Summary of Conclusions

10.2.1 Position of HFCV in Automotive Revolution

The fuels selected by the future automotive market will certainly have a much more diversified portfolio in the coming decade; the electric-drive vehicles powered by a fuel cell, battery, or a hybrid drive train are expected to increase noticeably. Although it is unlikely that any single type of power train would potentially be the 'silver bullet' at the moment, it has become increasingly clear from this study that fuel cell hybrid vehicles have greater possibility over other drive trains in order to achieve the 80% CO₂ reduction target by 2050. However, technology breakthroughs for both hydrogen and fuel cells are essential for the successful take-off of the HFCV.

10.2.2 Barriers for HFCV Penetration

The widespread introduction of hydrogen fuel cell vehicles faces three major technical challenges: improving cost competitiveness and the durability of fuel cells, innovating safer and lighter-weight tanks to store enough hydrogen on-board for acceptable driving range, and developing the infrastructure for hydrogen production, distribution and refuelling. However, shifting from conventional vehicles to hydrogen fuel cell vehicles is not only a technical issue. Even if the technologies can achieve a breakthrough, the hydrogen fuel cell

vehicles will still face great difficulties to emerge in the future automotive market without extensive governmental support and incentives. In addition, the consumer acceptance and awareness of hydrogen vehicles needs to be corrected and stimulated.

10.2.3 Hydrogen as Fuel

Hydrogen is recognised as a long-term sustainable fuel, because it can be used in both IC engines vehicles and fuel cells vehicles. From this study, H₂ICE can be more efficient than conventional petrol-fuelled engines while generating much less toxic and GHG emissions. However, the improvement is not sufficient to offset the limitation of hydrogen storage systems. Consequently, H₂ICE was considered as a bridging technology at the current stage, helping to build up the hydrogen infrastructure. And the experience gained from it can be directly transferred to fuel cells vehicles in the future. Fuel cells vehicles use hydrogen more efficiently, but the limitations are still awaiting technology breakthroughs as discussed.

10.2.4 Fuel Cell Vehicles for Niche Market

While the cost of fuel cells and hydrogen is still high, fuel cells vehicles designed for niche markets would be suggested, such as the hydrogen fuel cells scooter and the Micro-cab H4 urban fuel cells vehicles. The scooter is more affordable and can maneuver around traffic more easily in congestion. The hydrogen fuel cells hybrid scooter showed the extended range and top speed. With the plug-in feature, it has more advantages over conventional scooters in terms of mpg equivalent, energy efficiency, tail-pipe emissions and running costs. Micro-cab proved that it can function better than a standard diesel postal van vehicle under low speed duty cycle. Owing to the small size of those vehicles, smaller fuel cells and hydrogen storage are required, hence reducing overall cost, which is the key factor for early market penetration.

10.2.5 Hybridisation

PEM fuel cells are best operated at a constant load in order to achieve peak efficiency and maximum lifespan, whereas the power required for the automobile varies substantially, because of the variety of accelerations and decelerations under real-life driving conditions. However, the battery can accommodate these dynamic power changes perfectly, while also capturing the braking energy using electromagnetic deceleration, as this study demonstrated with PEM fuel cells and battery hybridization. Hybridisation offered the following benefits:

- Smaller fuel cells stack can be used (500W used in scooter, and 1.2kW and 3kW used in Micro-cabs), therefore to lower cost.
- Fuel cells stack can operate at higher efficiency point at certain times; better control strategies need to be engaged in order to optimise.
- Fuel cells stack lifetime is extended; it has been proved to operate longer than Ballard suggested life-time 1000 hours.
- Deep discharging from the battery is eliminated, therefore improving the batteries' lifetime.
- Fast start-up of the fuel cells stack; the vehicle is able to be operated on battery before fuel cells fully started.
- Improve power train efficiency through capturing of regeneration energy, up to 8% has been achieved.

10.2.6 Simulations and Tests

Computer simulation have demonstrated that battery and fuel cells vehicles are more sensitive towards different drive cycles, and payloads. Especially with battery vehicles.

However, due to the high TtW energy efficiency and low absolute fuel consumption figures, the energy efficiency of fuel cell and battery vehicle would still be superior to any IC engine and IC engine hybrid vehicle, regardless of the drive cycle and payloads.

10.2.7 Upgraded Micro-cab H4

This project combined both engineering and scientific research. A large amount of design, manufacture and installation process were involved, in return, the improvement on overall efficiency was more than double, average energy consumption of 100mpg equivalent goal has been achieved. The concept of hybrid fuel cell without DC converter was proved went well in practice, saving up to 20% energy generated from fuel cell. The regenerative braking could recover 8 to 9 % energy (12.2W) as demonstrated in ECE 15 tests, this figure may be lower in the actual campus and urban drive, as mechanical brakes have to be involved most of the time. The 1.2kW Ballard and 3kW Horizon fuel cell hybrid concept worked well to power the vehicle up to the top speed of 91.3km/h, however the acceleration rate proved to be extremely low when the speed was above 80km/h.

10.3 Future Works

10.3.1 Use of Ultracapacitors

According to the study in Chapter 9, the energy used to stop the vehicle during the ECE 15 drive cycle test mainly came from motor regenerative braking, and the battery recovered 66.7% of it; contributing up to 8% of total energy consumption. However, the deceleration during ECE 15 was gentle and less incentive than real life urban driving, hence more energy can be recovered in real life urban driving. However, the larger current during regenerative braking can degrade and even damage the battery pack, and only a limited amount of energy can be recovered. Ultra capacitors allow higher decelerations of the vehicle with

minimum loss of energy, and least degradation of the main battery pack, presenting better performance in specific power than battery, and can be charged and discharged thousands of times without performance reduction. These pose a valuable characteristic and can be used in combination with normal batteries, to improve the transient performance of an electric vehicle with the help of ultracapacitors. Besides, ultracapacitors allow regenerative braking even when the batteries are fully charged. Therefore further research of implementation ultracapacitors in future is suggested, however, 'tribrid' the fuel cell, battery and ultracapacitors will lead higher cost on top of the already expensive hybrid system, and make the control system more complex.

10.3.2 Heat Management

Although fuel cells and battery electric vehicles are highly energy efficient, there is still considerable amount of energy wasted via heat in the system, mainly from electric motors, power inverters and fuel cells (if applicable). This heat must be removed in order to prevent damage and allow proper function. On the other hand, heating the cabin of electric vehicles in cold weather consumes large amounts of energy, and significantly reduces the vehicle range. Therefore, a heat management system which can either dissipate or re-use to heat the cabin would be suggested for further study.

10.3.3 Electric Motor

In theory, the electric motor can achieve its maximum torque at zero RPM; hence a gear box is not required. From the experience of Lynch designed DC motor, the author found these motor's acceleration from stop was poor, but getting better along with the speed increasing. This was because although the motor can produce sufficient torque, it would require great amount of current to cope with. When the speed starts from zero, it would need infinite

large amount of current. In practice, if the motor controllers were limited to 500A, according to the motor RPM and reduction gear ratio, 1V approximately equals to 2km/h as found in Chapter 9, therefore at 10km/h, only 2.5kW power is provided by one motor. This could be improved in future by:

- Engaging a Continuously Variable Transmission (CVT) gearbox to maximum the motor performance and efficiency.
- Optimising the reduction gear ratio.
- Using higher voltage motor.

10.3.4 Continuing Research on Ultra Low Carbon Vehicles

After four years study and research on hydrogen fuel cell hybrid vehicles and related technologies, specifically on Micro-cab HFCVs, the author will continue to model and implement practical electrical and electronic control systems into low carbon vehicles, as well as develop the optimised electro-mechanical systems for overall efficiency, based on the vehicle shown in Figure 10.1.



Figure 10.1 New Micro-cab H₂EV (courtesy Coventry University)

References

1. Pollet, B.G., Staffell Iain, Shang Jin Lei, *Current status of hybrid, battery and fuel cell electric vehicles: From electrochemistry to market prospects*. *Electrochimica Acta*, 2012. **84**: p. 235-249.
2. Shang, J.L. and B.G. Pollet, *Hydrogen fuel cell hybrid scooter (HFCHS) with plug-in features on Birmingham campus*. *International Journal of Hydrogen Energy*, 2010. **35**(23): p. 12709-12715.
3. Shang, J.L., Kendall Kevin, Pollet Bruno G., *Hybrid Hydrogen PEM Fuel Cell and Batteries without DC Converter*. *International Journal of Low-Carbon Technologies*, 2013. DOI:10.1093/ijlct/ctt070.
4. Staffell, I., Shang Jin Lei, Kendall Kevin, *Atomic Models of Strong Solids Interfaces Viewed as Composite Structures*. *Applied Composite Materials*, 2013. **20**(3): p. DOI 10.1007/s10443-013-9330-y.
5. Pollet, B.G., Shang Jinlei, Staffell Iain, Molkovd Vladimir, *Fuel Cell (Hydrogen) Electric Hybrid Vehicles, in Alternative fuels and advanced vehicle technologies: Towards zero carbon transportation*, R. Folkson, Editor. 2013, Woodhead Publishing, ISBN: 0 85709 522 6: Cambridge.
6. Ali Emadi, Y.G., Mehrdad Ehsan, *Modern Electric, Hybrid Electric, and Fuel Cell Vehicles: Fundamentals, Theory, and Design, Second Edition*. 2009. ISSN 978-1-4200-5398-2(CRC Press).
7. Alizon, F., Shooter Steven B., Simpson Timothy W., *Henry Ford and the Model T: lessons for product platforming and mass customization*. *Design Studies*, 2009. **30**(5): p. 588-605.
8. Constable, G. and B. Somerville, *A century of innovation: twenty engineering achievements that transformed our lives*, 2003: Joseph Henry Press.
9. Sousanis, J., *World Vehicle Population Tops 1 Billion Units*, 2011; Available from: <http://tinyurl.com/ckd5dsb>.
10. McKinsey Company, *The role of Battery Electric Vehicles, Plug-in Hybrids and Fuel Cell Electric Vehicles in A portfolio of power-trains for Europe: a fact-based analysis*, 2011.
11. Hirose, K., *The future of polymer fuel cells and potential transport applications*. in *The Polymer Fuel Cells Challenge Launch Event*. 2009. London: The Carbon Trust.

12. World Bank Database, *GDP of United Kingdom Report 2011*. 2011; Available from: <http://data.worldbank.org/country/united-kingdom>.
13. Neeft, J., Makkee M. and J.A. Moulijn, *Diesel particulate emission control. Fuel processing technology*, 1996. **47**(1): p. 1-69.
14. Buckeridge, D.L., et al., *Effect of motor vehicle emissions on respiratory health in an urban area*. Environmental health perspectives, 2002. **110**(3): p. 293-293.
15. Westerholm, R. and K.E. Egeback, *Exhaust emissions from light-and heavy-duty vehicles: chemical composition, impact of exhaust after treatment, and fuel parameters*. Environmental health perspectives, 1994. **102**(Suppl 4): p. 13-13.
16. Künzli, N., Kaiser R., Medina S., et al., *Public-health impact of outdoor and traffic-related air pollution: a European assessment*. The Lancet, 2000. **356**(9232): p. 795-801.
17. Brunekreef, B. and S.T. Holgate, *Air pollution and health*. The Lancet, 2002. **360**: p. 1233-1242.
18. Maggetto, G. and J. Van Mierlo, *Electric vehicles, hybrid electric vehicles and fuel cell electric vehicles: state of the art and perspectives*. Annales de Chimie Science des Matériaux, 2001. **26**(4): p. 9-26.
19. Chan, C.C., *The state of the art of electric, hybrid, and fuel cell vehicles*. Proceedings of the IEEE, 2007. **95**(4): p. 704-718.
20. Turton, H., *Sustainable global automobile transport in the 21st century: An integrated scenario analysis*. Technological Forecasting and Social Change, 2006. **73**(6): p. 607-629.
21. Nikolas, H., Charlotte Brannigan, David Wynn, et al., *The role of GHG emissions from infrastructure construction, vehicle manufacturing, and ELVs in overall transport sector emissions*. 2011, European Commission Directorate-General Climate Action and AEA Technology plc.
22. Charlotte, B., Gena Gibson, Nikolas Hill, et al., *Development of a better understanding of the scale of co-benefits associated with transport sector GHG reduction policies, in EU Transport GHG: Routes to 2050?*, 2012, European Commission Directorate-General Climate Action and AEA Technology plc.

23. Saldiva, P., King M., Delmonte C., et al., *Respiratory alterations due to urban air pollution: An experimental study in rats*. Environmental Research, 1992. **57**(1): p. 19-33.
24. Contestabile, M., et al., *Battery electric vehicles, hydrogen fuel cells and biofuels. Which will be the winner?* Energy Environ. Sci., 2011. **4**(10): p. 3754-3772.
25. Pulles, T., Denier van der Gon, Hugo Appelman and M. Wilfred Verheul, *Emission factors for heavy metals from diesel and petrol used in European vehicles*. Atmospheric Environment, 2012. **61**: p. 641-651.
26. Lyons, T.J., Kenworthy, J. R., Moy, C. and F. dos Santos, *An international urban air pollution model for the transportation sector*. Transportation Research Part D: Transport and Environment, 2003. **8**(3): p. 159-167.
27. Owen, N.A., Inderwildi Oliver R. and D.A. King, *The status of conventional world oil reserves—Hype or cause for concern?* Energy Policy, 2010. **38**(8): p. 4743-4749.
28. Transport & Environment, *CO₂ Emissions from New Cars - Position paper in response to the European Commission proposal*. 2008, European Federation for Transport and Environment.
29. Erceg, C., Guerrieri L., Kamin S. B., *Did Easy Money in the Dollar Bloc Fuel the Oil Price Run-Up?* International Journal of Central Banking, 2011. **7**(1): p. 131-160.
30. Aydın, L. and M. Acar, *Economic impact of oil price shocks on the Turkish economy in the coming decades: A dynamic CGE analysis*. Energy Policy, 2011. **39**(3): p. 1722-1731.
31. Frenette, G. and D. Forthoffer, *Economic and commercial viability of hydrogen fuel cell vehicles from an automotive manufacturer perspective*. International Journal of Hydrogen Energy, 2009. **34**(9): p. 3578-3588.
32. Delucchi, M.A. and T.E. Lipman, *Chapter Two - Lifetime Cost of Battery, Fuel-Cell, and Plug-in Hybrid Electric Vehicles*, in *Electric and Hybrid Vehicles*. 2010, Elsevier: Amsterdam. p. 19-60.
33. Andrews, M.R., *A Fuel-cell/lead-acid-battery Hybrid Car*. Society of Automotive Engineers, 1972. ASIN: B00072RGAS.
34. Davis, B.P., *One Million Electric Drive Vehicles by 2015*. 2011(United States Department of Energy).

35. Andress, D., Das Sujit, Joseck, Fred and T. Dean Nguyen, *Status of advanced light-duty transportation technologies in the US*. Energy Policy, 2012. **41**(0): p. 348-364.
36. Meeus, L., Azevedo Isabel, Marcantonini Claudio, J.-M. Glachant, and M. Hafner, *EU 2050 Low-Carbon Energy Future: Visions and Strategies*. The Electricity Journal, 2012. **25**(5): p. 57-63.
37. Julia King, *The King Review of low-carbon cars*. 2007; Available from: www.lowcvp.org.uk/assets/presentations/Julia%20King.pdf.
38. Brand, C. and B. Boardman, *Taming of the few—The unequal distribution of greenhouse gas emissions from personal travel in the UK*. Energy Policy, 2008. **36**(1): p. 224-238.
39. Will Frank, *Fuel conservation and emission reduction through novel waste heat recovery for internal combustion engines*. Fuel, 2012. **102**(0): p. 247-255.
40. Berggren, C. and T. Magnusson, *Reducing automotive emissions—The potentials of combustion engine technologies and the power of policy*. Energy Policy, 2012. **41**(0): p. 636-643.
41. Environmental Protection Agency, *Light-Duty Vehicle Greenhouse Gas Emission Standards and Corporate Average Fuel Economy Standards for Model Years 2017–2025*. 2010.
42. European Commission, *Setting Emission Performance Standards for New Passenger Cars as Part of the Community's Integrated Approach to Reduce CO₂ Emissions From Light-duty Vehicles*, European Union Editor. 2009.
43. European Commission, *Progress Report of the Energy Efficiency Action Plan 2006*. 2011.
44. Transport & Environment, *Have existing fuel efficiency standards worked?* 2011; Available from: <http://tinyurl.com/9krz52k>.
45. Lettice, J. *Tough on e-vehicles, tough on the causes of e-vehicles*. Science 2009; Available from: http://www.theregister.co.uk/2009/04/17/dft_ev_analysis/.
46. Chan, C.C., A. Bouscayrol, and K. Chen, *Electric, hybrid, and fuel-cell vehicles: Architectures and modeling*. Vehicular Technology, IEEE Transactions on, 2010. **59**(2): p. 589-598.
47. Hudson, P., *£5,000 grant to buy plug-in electric cars in Telegraph.co.uk* 2010.

48. European Automobile Manufacturers' Association, *Overview of Tax Incentives for Electric Vehicles in the EU 2010*, ACEA: Belgium.
49. Jim, M., *China to Subsidize Electric Cars and Hybrids* in *Wheels Blog* 2010.
50. Mike King, *Global Automotive Manufacturing - Market Report 2010, 2011*; Available from: <http://tinyurl.com/8njjejv>.
51. Jostins, J., *Exhibition of Prototype Microcab*, in *United Nations 2nd World Urban Forum*. 2004: Barcelona, Spain.
52. Microcab Industries Limited, *Microcab's all new H2EV*. 2011; Available from: <http://www.microcab.co.uk/h2ev.html>.
53. B. Metz, O., Davidson, P. Bosch, R. Dave, and L.A. Meyer, *Contribution of Working Group III to the Fourth Assessment Report of the Intergovernmental Panel on Climate Change*, in *IPCC Fourth Assessment Report (AR4)*. 2007: Cambridge, United Kingdom and New York, NY, USA.
54. Bettina, K., Huib van Essen, Willem Braat, et al., *Impact analysis for market uptake scenarios and policy implications*, in *Impacts of Electric Vehicles - Deliverable 5*. 2011.
55. Genevieve Cullen, *Advancing the Deployment of Electric Vehicles: Market and Policy outlook for Electrifying Transportation*. 2011.
56. Chan, C.C. and Y.S. Wong, *The state of the art of electric vehicles technology*. 2004, IEEE. p. 46-57.
57. European Commission, *Monitoring the CO₂ emissions from new passenger cars in the EU: data for 2009*. 2010.
58. Health and Safety Executive, *Diesel Engine Exhaust Emissions*. 2012.
59. David Sheppard, *Europe's diesel imports to soar, fuelling pump prices*. Reuters (U.S.) 2008. Available from: <http://www.reuters.com/article/2008/09/30/us-energy-diesel-idUSTRE48T2ZV20080930>.
60. Kristian, B., John Heywood, *Europe's Evolving Passenger Vehicle Fleet: Fuel Use and GHG Emissions Scenarios through 2035*. 2008, Laboratory for Energy and Environment, MIT.

61. About Website, *The History of the Automobile - Gas Engines*. 2009; Available from: <http://inventors.about.com/library/weekly/aacarsgas.htm?rd=1>.
62. Korzeniewski, J., *Toyota explains Atkinson cycle*. 2008; Available from: <http://green.autoblog.com/2008/09/10/toyota-gets-all-techy-on-us-explains-atkinson-cycle/>.
63. Lynette, C., Christopher Evans, Anup Bandivadekar and J. Heywood, *Factor of Two: Halving the Fuel Consumption of New U.S. Automobiles by 2035*. 2007, Laboratory for Energy and Environment, Massachusetts Institute of Technology. Cambridge.
64. U.S. Department of Energy, *Fuel Cell Technology Challenges*. 2008; Available from: http://www1.eere.energy.gov/hydrogenandfuelcells/fuelcells/fc_challenges.html.
65. Fernando, J.d., Sisternes, *Plug-In Electric Vehicle Introduction in the EU*, in *Engineering Systems Division*. 2010, Massachusetts Institute of Technology.
66. Csaba Csere, *The Future of the Internal-Combustion Engine Car* and Driver magazine, 2010.
67. Matthew Beecham, *Research Analysis: Review of stop-start systems*. 2009; Available from: http://www.just-auto.com/analysis/review-of-stop-start-systems_id101657.aspx.
68. Mehrdad Ehsani and A.E. Yimin Gao, *Modern Electric, Hybrid Electric, and Fuel Cell Vehicles: Fundamentals, Theory, and Design*. Second ed. 2009: CRC Press.
69. Toyota Motor Corporation, *Worldwide Sales of TMC Hybrids Top 4 Million Units*. 2012; Available from: <http://www2.toyota.co.jp/en/news/12/05/0522.html>.
70. Honda, *Honda's Cumulative Worldwide Hybrid Vehicle Sales Reaches 800,000 Units*. 2012; Available from: <http://world.honda.com/news/2012/c120120Hybrid-Vehicle-Sales-800000-Units/index.html>.
71. Mehrdad Ehsani, Y.G., Ali Emadi, *Modern Electric, Hybrid Electric, and Fuel Cell Vehicles Fundamentals, Theory, and Design*. Second Edition ed. 2010: CRE Press.
72. Voelcker, J., *Lithium Batteries for Hybrid Cars*, in *IEEE Spectrum magazine* 2007, IEEE Spectrum
73. Hybridcenter org, *Hybrids Under the Hood*. 2010; Available from: <http://www.hybridcenter.org/hybrid-center-how-hybrid-cars-work-under-the-hood.html>.

74. The North Carolina Solar Center, *Hybrid Electric Vehicles*. 2012; Available from: <http://ncsc.ncsu.edu/wp-content/uploads/Hybrid-Electric-Vehicles-Overview-2-12.pdf>.
75. Matthew, Z., Ahmad A. Pesaran, Mark Mihalic, *Thermal Evaluation of Toyota Prius Battery Pack*. 2002, National Renewable Energy Laboratory.
76. Howell, D., *Plug-in Hybrid Electric Vehicle Battery research and Development Activities* 2007, FreedomCar and Vehicle Technologies Program
77. Encyclopædia Britannica, *Thomas Davenport*. 2012; Available from: <http://www.britannica.com/EBchecked/topic/152489/Thomas-Davenport>.
78. Chau, K.T. and Y.S. Wong, *Overview of power management in hybrid electric vehicles*. *Energy Conversion and Management*, 2002. **43**(15): p. 1953-1968.
79. Fuhs Allen E., *Hybrid Vehicles and The Future Of Personal Transportation*. 2009: CRC.
80. Globle Data, *Citizens Remain Critical of Battery Electric Vehicles*. 2012; Available from: <http://www.globaldata.com/PressReleaseDetails.aspx?PRID=297&Type=Industry&Title=Smart+Grid>.
81. Electric Power Research Institute, Natural Resources Defense Council, and Charles Clark Group, *Environmental assessment of plug-in hybrid electric vehicles; vol. 1: Nationwide greenhouse gas emissions, final report 1015325*, 2007.
82. Srinivasan, S., *Fuel cells: from fundamentals to applications*. 2006, New York: Springer.
83. BERR & DfT, *Investigation into the Scope for the Transport Sector to Switch to Electric Vehicles and Plugin Hybrid Vehicles*. 2008.
84. Mumu Moorthi, *Lithium Titanate Based Batteries for High Applications High Rate and High Cycle Life Applications*. 2010, NEI Corporation.
85. Murray, J., *Car CO₂ taxation and it's impact on the British car fleet*, in *Vehicle Fuel Consumption Regulation and Fiscal Policy Workshop*. 2011, Low Carbon Vehicle Partnership.
86. Andújar, J.M. and F. Segura, *Fuel cells: History and updating. A walk along two centuries*. *Renewable and Sustainable Energy Reviews*, 2009. **13**(9): p. 2309-2322.

87. Sequeira, C., Brito P., Mota A., et al., *Fermentation, gasification and pyrolysis of carbonaceous residues towards usage in fuel cells*. Energy Conversion and Management, 2007. **48**(7): p. 2203-2220.
88. Fuel Cell Markets, *What is a Fuel Cell?* 2012; Available from: http://www.fuelcellmarkets.com/fuel_cell_markets/fuel_cells/4,1,1,2114.html.
89. U.S. Department of Energy, *Types of Fuel Cells - Polymer Electrolyte Membrane (PEM) Fuel Cells*. 2011; Available from: http://www1.eere.energy.gov/hydrogenandfuelcells/fuelcells/fc_types.html#pem.
90. U.S. Department of Energy, *Fuel Cell Technologies Program - Fuel Cell Basics* 2012; Available from: <http://www1.eere.energy.gov/hydrogenandfuelcells/fuelcells/basics.html>.
91. Chalk, S.G. and J.F. Miller, *Key challenges and recent progress in batteries, fuel cells, and hydrogen storage for clean energy systems*. Journal of Power Sources, 2006. **159**(1): p. 73-80.
92. U.S. Department of Energy, *Hydrogen and Fuel Cell Activities, Progress, and Plans: Report to Congress*. 2009.
93. Syed, N.H., *Fuel Cell Hybrid Vehicles*. 2011, Syed Najam Haider, Automotive Technology, Dept. of Mechanical Engineering, NUST College of E&ME.
94. Volkswagen, *Volkswagen Golf Price List*. 2012; Available from: <http://www.volkswagen.co.uk/#/new/golf-vi/which-model/brochures/>.
95. Silicon Valley Bank Cleantech Practice, *The Advanced Biofuel and Biochemical Overview*. 2012.
96. HMRC UK, *Fuel Duty Rates*, Her Majesty's Revenue and Customs. 2011.
97. Fuel Economy, *Electric Vehicles: Compare Side-by-Side*. 2012; Available from: <http://www.fueleconomy.gov/feg/evsbs.shtml>.
98. Washington state Department of Transportation, *The Fuel and Vehicle Trends Report*. 2012; Available from: <http://www.wsdot.wa.gov/NR/rdonlyres/72BFCA39-700B-4D4E-AE8C-9AFEACF9E5DC/0/FuelandVehicletrends.pdf>.
99. Paul Bolton, *Petrol and diesel prices*, Department of Energy and Climate Change. 2012.

100. Myers, B., Ariff D., B.D. James, and R.C. Kuhn, *Hydrogen from renewable energy sources: Pathway to 10 quads for transportation uses in 2030 to 2050*. US Department of Energy Consultant's Report, Directed Technologies Inc., Arlington, VA, 2003.
101. Muradov, N.Z. and T.N. Veziroğlu, *From hydrocarbon to hydrogen-carbon to hydrogen economy*. International Journal of Hydrogen Energy, 2005. **30**(3): p. 225-237.
102. European Commission, *European CO₂ Capture and storage projects*. Brussels, Directorate-General for Research, Directorate J-Energy, Unit J2-Energy production and distribution systems, 2007. **1018-5593**.
103. International Energy Agency, *CO₂ Emissions From Fuel Combustion Highlights (2011 Edition)*. 2011, IEA.
104. Consumer Energy, Center *Energy Losses in a Vehicle*. 2008; Available from: http://www.consumerenergycenter.org/transportation/consumer_tips/vehicle_energy_losses.html.
105. Thomas, C.E., *Fuel cell and battery electric vehicles compared*. International Journal of Hydrogen Energy, 2009. **34**(15): p. 6005-6020.
106. Car History Organization, *First internal combustion engine*. 2010; Available from: <http://www.car-history.org/>.
107. Lanz, A., *Hydrogen fuel cell engines and related technologies*. 2001: College of the Desert, Energy Technology Training Center.
108. Barton, J. and R. Gammon, *The production of hydrogen fuel from renewable sources and its role in grid operations*. Journal of Power Sources, 2010. **195**(24): p. 8222-8235.
109. Watkiss, P. and N. Hill, *The Feasibility, Costs and Markets for Hydrogen Production*. A study for British Energy Undertaken by AEA Technology Environment, Abingdon, Oxfordshire, 2002.
110. Hoffmann, P. *Forever fuel: the story of hydrogen*. 1981; Available from: http://www.osti.gov/energycitations/product.biblio.jsp?osti_id=6744880.
111. Armaroli, N. and V. Balzani, *The hydrogen issue*. ChemSusChem, 2011. **4**(1): p. 21-36.
112. Nieminen, J. and I. Dincer, *Comparative exergy analyses of gasoline and hydrogen fuelled ICEs*. International Journal of Hydrogen Energy, 2010. **35**(10): p. 5124-5132.

113. U.S. Department of Energy, *Single-Cylinder Hydrogen, Spark Ignition Engine*. 2011; Available from: http://www.transportation.anl.gov/engines/spark_ignition_h2_engines.html.
114. Schlapbach, L. and A. Züttel, *Hydrogen-storage materials for mobile applications*. *Nature*, 2001. **414-6861**: p. 353-358.
115. Centre of Excellence for Low Carbon and Fuel Cell Technologies, *Hydrogen Van Trials*. 2010; Available from: <http://www.cenex.co.uk/research/hydrogen/hydrogen-van-trials>.
116. Verhelst, S. and T. Wallner, *Hydrogen-fueled internal combustion engines*. *Progress in Energy and Combustion Science*, 2009. **35**(6): p. 490-527.
117. Fayaz, H., Saidur R., Razali, N., et al., *An overview of hydrogen as a vehicle fuel*. *Renewable and Sustainable Energy Reviews*, 2012. **16**(8): p. 5511-5528.
118. Ji, C. and S. Wang, *Experimental study on combustion and emissions performance of a hybrid hydrogen-gasoline engine at lean burn limits*. *International Journal of Hydrogen Energy*, 2010. **35**(3): p. 1453-1462.
119. Revolve Company, *Bi-fuel conversion brings hydrogen fuel to existing ICE technology*. 2010; Available from: <http://www.revolve.co.uk/Projects/Bi-fuel-conversion>.
120. Van Blarigan, P. and J.O. Keller, *A hydrogen fuelled internal combustion engine designed for single speed/power operation*. *International Journal of Hydrogen Energy*, 1998. **23**(7): p. 603-609.
121. Adrian Cho, *Fire and ICE: Revving up for H2*. *Science*, 2004. **Vol. 305, No. 5686** p. Page 964-965
122. Green Motion, *Fuel Cell - Hydrogen Car Rental*. 2012; Available from: http://www.greenmotion.co.uk/fleet_hydrogentechnology.php.
123. Environment News Service, *Fuel Cell Electric Vehicles Demonstrate 'Rapid' Advance*. 2012; Available from: <http://ens-newswire.com/2012/08/15/fuel-cell-electric-vehicles-demonstrate-rapid-advance/>.
124. Honda Worldwide, *Home Energy Station*. 2013 ; Available from: <http://world.honda.com/FuelCell/FCX/station/>.

125. Satyapal, S., Petrovic John , Read Carole, G. Thomas, and G. Ordaz, *The U.S. Department of Energy's National Hydrogen Storage Project: Progress towards meeting hydrogen-powered vehicle requirements*. Catalysis Today, 2007. **120**(3–4): p. 246-256.
126. European Commission, *European fuel cell and hydrogen projects 1999-2002*. 2003, Office for Official Publications of the European Communities.
127. Ogden, J.M., *Prospects for Building a Hydrogen Energy Infrastructure*. Annual Review of Energy and the Environment, 1999. **24**(1): p. 227-279.
128. Jeanne Ryba, *Liquid Oxygen and Liquid Hydrogen Storage*. NASA John F Kennedy Space Center. 2007; Available from: http://www.nasa.gov/mission_pages/shuttle/launch/LOX-LH2-storage.html.
129. Wasz, M.L., Schwarz, R. B., Srinivasan, S. and M.P. Sridhar Kumar, *Sn-Substituted LaNi₅ Alloys for Metal Hydride Electrodes*. MRS Proceedings, 1995. **393**: p. 237-242.
130. Laura Becker, *Hydrogen Storage*. 2001; Available from: <http://www.csa.com/discoveryguides/hydrogen/overview.php>.
131. French Alternative Energies and Atomic Energy Commission, *On-board hydrogen storage*. 2004. p. 2.
132. F. Brown, L., *A comparative study of fuels for on-board hydrogen production for fuel-cell-powered automobiles*. International Journal of Hydrogen Energy, 2001. **26**(4): p. 381-397.
133. Gu, W., Shen J. P., Song C., *Hydrogen Production From Intergrated Methenol Reforming Over Cu-ZnO/Al₂O₃ AND Pt/Al₂O₃ Catalysts For PEM Fell Cells*. Preprints of Papers- American Chemical Society, Division of Fuel Chemistry, 2003. **48**(2): p. 804-804.
134. Office of Energy Efficiency & Renewable Energy, *Infrastructure Technologies Program Multi-Year Research*. Development and Demonstration Plan, 2012.
135. Nancy Garland, *US Department of Energy Fuel Cell Technologies Program. 18th World Hydrogen Energy Conference 2010–WHEC 2010 Proceedings Speeches and Plenary Talks*. 2010. Forschungszentrum Jülich.
136. Simbeck, D. and E. Chang, *Hydrogen supply: cost estimate for hydrogen pathways–scoping analysis*. NREL, Bolden, Colorado, 2002.

137. Rosenberg, J. *Hindenburg Disaster - The tragedy that ended lighter-than-air passenger travel in rigid dirigibles*. 1994; Available from: <http://history1900s.about.com/cs/disasters/a/hindenburgcrash.htm>.
138. Bain, A. and Van Vorst, *The Hindenburg tragedy revisited: the fatal flaw found*. International Journal of Hydrogen Energy, 1999. **24**(5): p. 399-403.
139. Cadwallader Herring Engineering Laboratory, *Safety issues with hydrogen as a vehicle fuel*. 1999, Idaho National Engineering and Environmental Laboratory.
140. Gilbert, S. and S. Colt, *Village Wind Diesel Hydrogen Report*. 2006: University of Alaska Anchorage, Institute of Social and Economic Research.
141. Hydrogen Association org, *Hydrogen safety - Fact sheet*. 2011; Available from: http://arhab.org/pdfs/h2_safety_fsheets.pdf.
142. Office of Energy Efficiency & Renewable Energy, *High-Pressure Hydrogen Tank Testing*. 2011; Available from: http://www1.eere.energy.gov/hydrogenandfuelcells/storage/hydrogen_storage_testing.html.
143. Flynn, R., Bellaby P., Ricci M. *Risk perception of an emergent technology: the case of hydrogen energy*. 2006.
144. Tromp, T.K., et al., *Potential environmental impact of a hydrogen economy on the stratosphere*. Science, 2003. **300**(5626): p. 1740-1742.
145. Prather, M.J., *An Environmental Experiment with H₂?* Science, 2003. **302**(5645): p. 581-582.
146. Miriam, R., Bellaby P., Flynn R., and P. Ekins, *Hydrogen risks: A critical analysis of expert knowledge and expectations*. Hydrogen energy: Economic and social challenges, 2010: p. 217-240.
147. Miriam, R., *Experts' assessments and representations of risks associated with hydrogen*. Institute for Social, Cultural and Policy Research, University of Salford, 2005.
148. Tso, C. and S. Chang, *A viable niche market-fuel cell scooters in Taiwan*. International Journal of Hydrogen Energy, 2003. **28**(7): p. 757-762.
149. Colella, W.G., *Market prospects, design features, and performance of a fuel cell-powered scooter*. Journal of Power Sources, 2000. **86**(1-2): p. 255-260.

150. Sripakagorn, A. and N. Limwuthigraijirat, *Experimental assessment of fuel cell/supercapacitor hybrid system for scooters*. International Journal of Hydrogen Energy, 2009. **34**(15): p. 6036-6044.
151. Go-Ped Group of Companies, *ESR750H Hoverboard*. 2009; Available from: <http://www.goped.com/Products/ESR750Hover/Default.asp>.
152. Ubertini, S., and Desideri, U., *Aerodynamic Investigation of a Scooter in the University of Perugia Wind Tunnel Facility*. SAE Technical Paper, 2002. **2002-01-0254**.
153. Horizon Fuel Cell Technologies, *Horizon H-Series Stack*. 2013; Available from: <http://www.horizonfuelcell.com/#!h-series-stacks/c52t>.
154. Tianjin Highland Energy Technology Development, *Hydrogen Storage Tank MH300-1*. 2010; Available from: http://www.tjhighland.com.cn/jianjie_en.asp.
155. Anup, B., Kristian Bodek, Lynette Cheah, et al., *On The Road in 2035: Reducing Transportation's Petroleum Consumption and GHG Emissions*, in Report No. LFEE 2008-05 RP. 2008, MIT Laboratory for Energy and the Environment: Cambridge, Massachusetts.
156. Skinner I., Smokers R and Hill N, *Towards the decarbonisation of EU's transport sector by 2050*. 2010: Final report produced under the contract ENV.C.3/SER/2008/0053 between European Commission Directorate-General Environment and AEA Technology plc; see www.eutransportghg2050.eu.
157. Edwards, P., et al., *Hydrogen and fuel cells: Towards a sustainable energy future*. Energy Policy, 2008. **36**(12): p. 4356-4362.
158. Ehsani, M., Gao Yimin, Emadi Ali, *Modern Electric, Hybrid Electric, and Fuel Cell Vehicles: Fundamentals, Theory, and Design, Second Edition* 2009: CRC Press
159. O'Hayre, P., Cha W., Colella W. and F. Prinz, *Fuel cell fundamentals*. 2006: John Wiley & Sons Hoboken, New Jersey.
160. Barbir, F. and T. Gomez, *Efficiency and economics of proton exchange membrane (PEM) fuel cells*. International Journal of Hydrogen Energy, 1996. **21**(10): p. 891-901.
161. Binggang, C., Zhifeng Bai, Wei Zhang, *Research on control for regenerative braking of electric vehicle*. 2005. DIO: 10.1109.

162. Staffell Iain, *Results from the Microcab fuel cell vehicle demonstration at the University of Birmingham*. International Journal of Electric and Hybrid Vehicles, 2011. **3**(1): p. 62-82.
163. Rand, D., *Valve-regulated lead-acid batteries*. 2004: Elsevier Science.
164. Wakihara, M., *Recent developments in lithium ion batteries*. Materials Science and Engineering: R: Reports, 2001. **33**(4): p. 109-134.
165. Ritchie, A. and W. Howard, *Recent developments and likely advances in lithium-ion batteries*. Journal of Power Sources, 2006. **162**(2): p. 809-812.
166. Ohzuku, T. and R.J. Brodd, *An overview of positive-electrode materials for advanced lithium-ion batteries*. Journal of Power Sources, 2007. **174**(2): p. 449-456.
167. Wagner, T., Lakshmanan B., Mathias M. F., *Electrochemistry and the Future of the Automobile*. Nature, 2010. **486**: p. 43-51.
168. Omar, N., Monem Mohamed Abdel, Firouz Yousef, et al., *Lithium iron phosphate based battery – Assessment of the aging parameters and development of cycle life model*. Applied Energy, 2004. **113**: p. 1575-1585.
169. Cooke, P., *The United Kingdom Automotive Industries - Status, Economic Recovery and Expectations*. 2009.
170. U.S. Department of Energy, *Fuel Economy vs. Weight and Performance*. 2010; Available from: http://www1.eere.energy.gov/vehiclesandfuels/facts/m/2010_fotw630.html.
171. Kendall, K., et al., *Hydrogen fuel cell hybrid vehicles (HFCHV) for Birmingham campus*. Journal of Power Sources, 2011. **196**(1): p. 325-330.
172. Gibson, C., *Nexa (310-0027) Power Module User's Manual*. 2004, Ballard Power Systems Inc.
173. Dynetek Industries Ltd, *Specification sheets of Model L026*. 2004; Available from: <http://www.dynetek.com/pdf/350.pdf>.
174. BBC News, *Hydrogen fuel station is unveiled in University of Birmingham*. 2008; Available from: http://news.bbc.co.uk/1/hi/england/west_midlands/7352195.stm.

175. Powervamp Racing, *ODYSSEY Extreme Series PC680 Batteries*. 2003; Available from: www.powervampracing.com/PC680.
176. Kendall, K., Pollet B. G. , Dhir, A., et al., *Hydrogen fuel cell hybrid vehicles (HFCHV) for Birmingham campus*. *Journal of Power Sources*, 2011. **196**(1): p. 325-330.
177. Electropaedia Woodbank Communications, *Battery and Energy Technologies: Battery Life (and Death)*. 2009; Available from: <http://www.mpoweruk.com/life.htm>.
178. Markel, T., Brooker A.,Hendricks T., et al., *ADVISOR: a systems analysis tool for advanced vehicle modeling*. *Journal of Power Sources*, 2002. **110**(2): p. 255-266.
179. Richard Stobart, R., Chen, *Duty Cycles, Standardisation and Validation of Low Carbon Power Systems*. 2008, Department of Aeronautical and Automotive Engineering, Loughborough University.
180. Peter Mock, J.G., Anup Bandivadekar,Iddo Riemersma, *Discrepancies between type-approval and "real-world" fuel-consumption and CO₂ values: Assessment for 2001-2011 European passenger cars*. 2012, International Council on Clean Transportation.
181. Michel André, *Real-world driving cycles for measuring cars pollutant emissions-Part A:The Artemis European driving cycles*. INRETS report, Bron, France, 2004. **411**: p. 97.
182. Michel André, *The ARTEMIS European driving cycles for measuring car pollutant emissions*. *Science of The Total Environment*, 2004. **334–335**: p. 73-84.
183. GRPE/WLTP informal group, *WLTC methodology*, United Nations Economic Commission for Europe Editor. 2011.
184. Bach, C., *World wide light duty vehicle test procedure WLTP*. 2012; Available from: http://www.strasseschweiz.ch/dcs/users/2/SSM_GV_2012_Referat_Bach.pdf.
185. Guoqing, X., Weimin Li, Kun Xu, Zhibin Song, *An Intelligent Regenerative Braking Strategy for Electric Vehicles*. *Energies*, 2011. **4**(9): p. 1461-1477.
186. Lum, D., *Aerodynamics and vehicle performance*. 2012; Available from: http://www.datsuns.com/Tech/tech_aero.htm.
187. Baglione, M., Duty, M., Pannone, G., *Vehicle System Energy Analysis Methodology and Tool for Determining Vehicle Subsystem Energy Supply and Demand*. SAE Technical Paper, 2007: p. 01-0398.

188. AGNI Motor, *95 Series Motor Performance Graphs*. 2009; Available from: http://agnimotors.com/95_Series_Performance_Graphs.pdf.
189. Protean Electric, *Protean's in-wheel motors benefit*. 2012. Available from: http://www.proteanelectric.com/?page_id=158&post=224.
190. Hrovat, D., *Influence of unsprung weight on vehicle ride quality*. Journal of Sound and Vibration, 1988. **124**(3): p. 497-516.
191. Sclater, N. and N.P. Chironis, *Mechanisms and mechanical devices sourcebook*. 2001: McGraw-Hill.
192. Huang, H., Faulkner T., Barker, J. and M.Y. Saidi, *Lithium metal phosphates, power and automotive applications*. Journal of Power Sources, 2009. **189**(1): p. 748-751.
193. Notter, D.A., Gauch Marcel, Widmer Rolf, et al., *Contribution of Li-Ion Batteries to the Environmental Impact of Electric Vehicles*. Environmental Science & Technology, 2010. **44**(17): p. 6550-6556.
194. Race Technology Ltd, *DL1 Data Logger - the UK's number one data logger*. 2012; Available from: http://www.race-technology.com/dl1_classic_mk2_2_27.html.
195. DieselNet, *Emission Test Cycles: ECE 15 + EUDC / NEDC*. 2000; Available from: http://www.dieselnet.com/standards/cycles/ece_eudc.php.